Conducting Organic Radical Cation Salts with Organic and Organometallic Anions

Urs Geiser* and John A. Schlueter

Materials Science Division, Argonne National Laboratory, 9700 South Cass Avenue Building 200, Argonne, Illinois 60439

Received March 24, 2004

Contents

1. Introduction and Scope

Since the discovery of high electrical conductivity in an organic complex in 1954,[1] the field of molecular conductors has stimulated a great deal of research. A large number of electron-donor and -acceptor molecules have been synthesized, and conducting salts thereof have been crystallized, and we are aware of well over 5000 publications in this subject area. Major milestones include the discovery of metallic conduction over a wide range of temperatures in TTF–TCNQ[2,3] (TTF = tetrathiafulvalene, TCNQ = tetracyanoquinodimethane), the prediction by Little[4] of high-temperature superconductivity in certain organic compounds (not yet realized in the way envisioned by Little), and the discovery of superconductivity in polymers,[5] crystalline electron-donor radical cation salts,[6] and fullerene electron-acceptor radical anion salts.[7] The field of radical cation salts has been driven to a large extent by the search for

10.1021/cr0306844 CCC: $48.50
Published on Web 10/19/2004

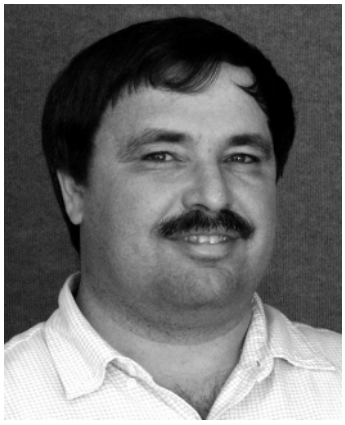

Urs Geiser was born in 1956 in Switzerland. He attended the University of Berne, Switzerland, where he graduated in 1980 with a Lic. Phil. degree in Chemistry and a diploma thesis in the area of single-crystal circular dichroism spectroscopy in trigonal chromium(III) complexes under the guidance of Professor H.-U. Güdel. From 1981 to 1985 he attended Washington State University to earn his Ph.D. degree in Chemistry with thesis work on the crystal structures and magnetic properties of low-dimensional copper(II) and nickel(II) systems in the group of Professor R. D. Willett. He then joined the group of Dr. Jack M. Williams at Argonne National Laboratory, first as a postdoctoral appointee and then in 1988 as staff scientist, to work on the structural and physical characterization of organic superconductors and related materials. He served as Acting Group Leader for the molecular conductors program from 1997 to 2000. He was a member of the team winning the Outstanding Scientific Accomplishment Award within the Materials Science Division of the U.S. Department of Energy, Office of Science, in 1990 and of the Decade of Discovery Award from the U.S. Department of Energy for sustained outstanding work in the area of organic superconductivity in 2001.

John A. Schlueter was born in 1965 near Chicago, IL. He attended Valparaiso University (Valparaiso, IN), where he graduated with high distinction in 1987 with his B.S. degree in Chemistry and Physics. His thesis project, under the guidance of Professor A. G. Cook, examined the extent of conjugation in aliphatic β-nitroenamines via dipole moment measurements. In 1992 he earned his Ph.D. degree in Chemistry from Northwestern University (Evanston, IL). His thesis work, under the direction of Professor Tobin Marks, involved the synthesis and characterization of molecular metals and charge-transfer salts derived from tetrachalcogenotetracene derivatives, diphenylglyoximates, and phthalocyanines. He then accepted a postdoctoral position in the research group of Dr. Jack Williams at Argonne National Laboratory, with research initially focused on superconducting fulleride salts. Since 1995, when he was promoted to staff scientist, his research has focused on BEDT-TTF-based salts, especially those with organometallic or organic anions. He was a member of the team winning the Decade of Discovery Award in 2001 from the U.S. Department of Energy for sustained outstanding work in the area of organic superconductivity. His current research interests include the design, synthesis, crystallization, and characterization of molecular-based solids with novel electronic or magnetic properties, including the development of structure/property relationships in molecular-based superconductors, molecular-based magnets, and nanostructured materials.

new superconductors (see, e.g., the books by Williams et al.[8] and Ishiguro et al.[9]), although other low-dimensional physics phenomena and the development (still in its infancy) of hybrid materials, where one component is an organic conductor, also occupy a good fraction of the literature. Review articles abound,[10−26] and the proceedings of the International Conference on Synthetic Metals (ICSM), published in numerous volumes of *Synthetic Metals*, provide a wealth of the primary literature. Finally, the review articles in this volume present a good cross-section over many aspects of this fascinating field.

Within this vast area this review attempts to summarize all the work that has been carried out on the conducting salts that are formed between molecular radical cations (generated by the oxidation of electron-donor molecules) and organic and organometallic anions (the latter defined as having covalent bonds between transition-metal cations and the carbon atoms of carbanion ligands). For the purpose of this review, we restrict ourselves to those anions that are introduced already in the form of anions with a well-defined charge state, while the radical cations (often with fractional average charge) are generated oxidatively during the crystallization process. This type of salts is usually referred to as cation radical salts. We therefore deliberately exclude the vast field of ionic donor−acceptor complexes (or charge-transfer salts sensu strictu), where a (fractional or complete) charge transfer between the electron-donor and -acceptor molecules takes place during the crystallization. We are also omitting the (much less numerous) radical anion salts between reduced electron-acceptor molecules and diamagnetic, well-defined organic cations (e.g., tetraalkylammonium). Both classes of salts have been reviewed elsewhere.[27−33]

The vast majority of the electron-donor molecules treated in this review are based on tetrathiafulvalene (TTF) and its homologues, although a few others are also included for the sake of completeness. These are summarized in Chart 1. Many of the organic anions described here are shown in Chart 2. Because of its propensity of yielding superconductors, the electron-donor molecule bis(ethylenedithio)tetrathiafulvalene (BEDT−TTF or ET) has attracted a disproportionally large share of attention. We therefore devote a major section of this review to the organic and organometallic anion salts of this molecule alone. The salts of the other TTF-related donor molecules are presented in section 3, while the relatively few salts of donor molecules that are not directly based on TTF or its homologues are described in section 4. All the compounds described through section 4 were obtained as crystalline products—most of them as single crystals and the remainder as polycrystalline samples. Section 5 deals with the salts prepared as thin films supported either by a liquid−air interface (Langmuir−Blodgett films) or on top of a solid substrate. Within this narrowly defined scope we attempted to include all known compounds and their literature through the earliest parts of 2004. However, we realize that inevitably some contributions are overlooked in a work of this sort, and we apologize upfront for any omissions—none are intended.

Chart 1. Electron-Donor Molecules

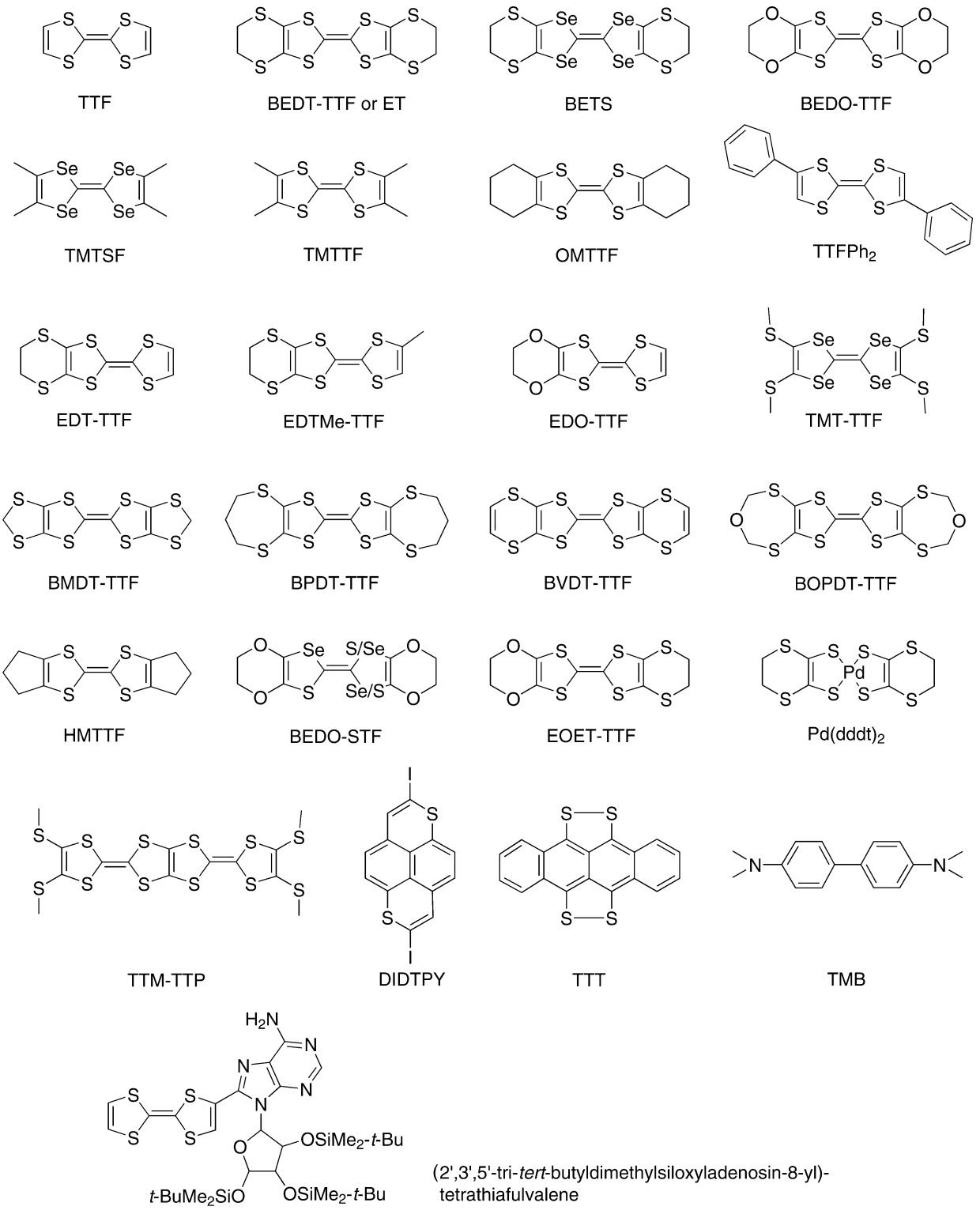

2. Salts of BEDT–TTF or ET, Bis(ethylenedithio)-tetrathiafulvalene

Within this major section we grouped the literature by anion type for convenience. A summary of basic crystallographic data is given in Table 1. The (*M*,*S*,*L*) scheme used in Table 1 is useful to classify the overall unit cell building principle in the case of layered salts.[69] The three letters denote the number of molecules (*M*) along the stack direction, the number of stacks (*S*) within one conducting layer, and the number of donor molecule layers (*L*) per unit cell. In some cases the unit cell parameters were transformed from those in the literature in order to facilitate comparisons or to present them in a standard setting.

2.1. Carboxylate Anions: R–CO_2^-

The carboxylate functional group is the quintessential anionic group of organic chemistry and biochemistry owing to the low pK_a (usually around 4.7)

Chart 2. Anions

Sulfonates

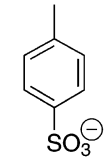
tosylate

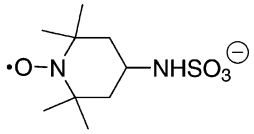
tsfa$^-$

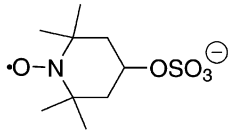
tosu$^-$

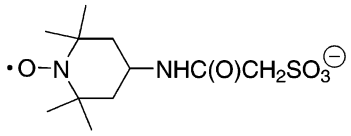
TEMPO-NHCOCH$_2$SO$_3^-$


pentafluorobenzene sulfonate

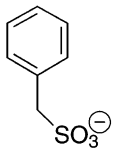
benzylsulfonate

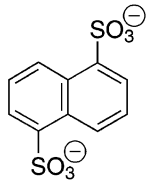
1,5-naphthalenedisulfonate

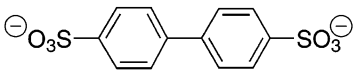
p-biphenyldisulfonate

Carboxylates

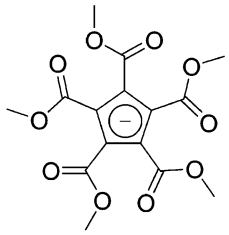
PMC$^-$

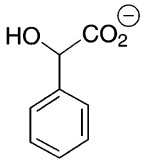
mandelate

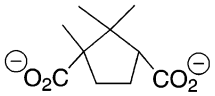
camphorate

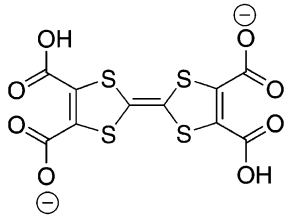
TTF(CO$_2$H)$_2$(CO$_2$)$_2^{2-}$

Tetraazofulvalenediides

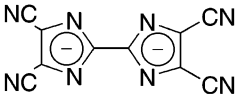
TCTAF^{2-}

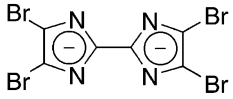
TBTAF^{2-}

Organometallic Anions

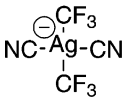

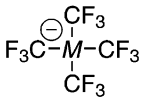
M = Cu, Ag, Au


R = CF$_2$H, CF$_2$CF$_3$, C$_6$Cl$_5$

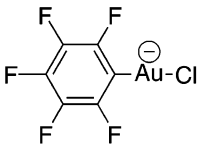

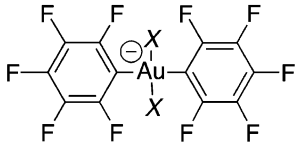
X = Cl, I

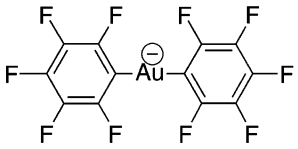

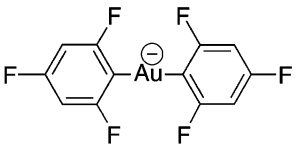

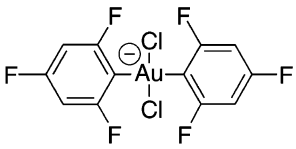

Chart 2 (Continued)

Polycyano Anions

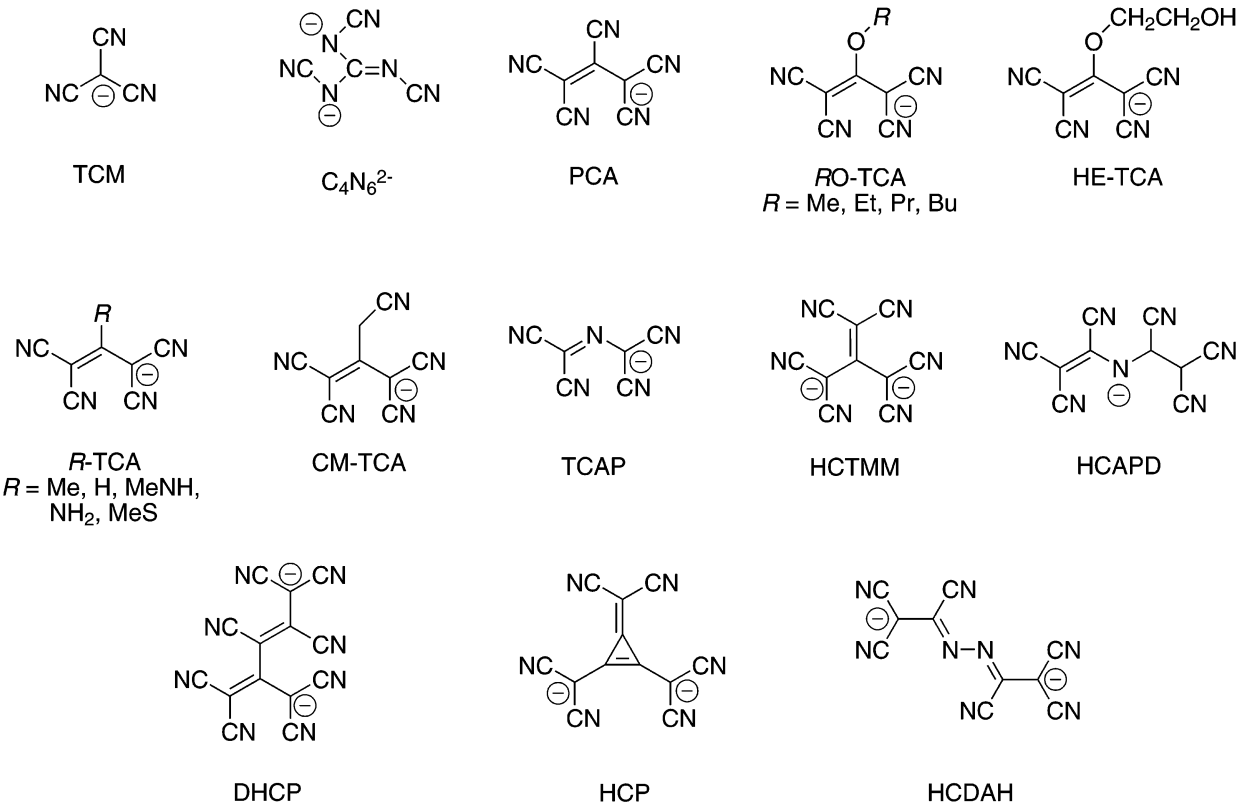

Phenolates

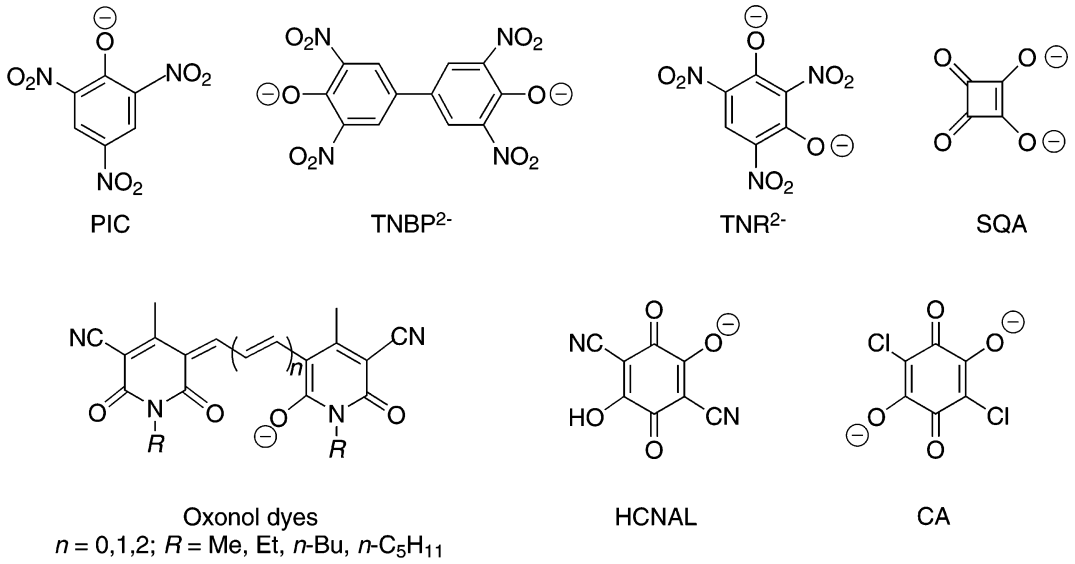

of the conjugate acid. It may seem therefore at first surprising that very few electron-donor cation salts with carboxylate anions have been reported. The reason for this dearth of salts may be found in the relative instability of the functional group, especially upon prolonged exposure to oxidating conditions, as typically found in the electrocrystallization procedure commonly employed in the synthesis of cation radical salts. Decarbonylation and decarboxylation are the two dominant decomposition pathways. In chlorinated solvents, it is furthermore observed that decomposition liberates chloride anion. ET forms a

Table 1. Summary of Room Temperature (unless otherwise indicated) Crystallographic Data for ET (BEDT-TTF) Salts

compound	space group	*a* (Å)	*b* (Å)	*c* (Å)	α (°)	*β* (°)	*γ* (°)	unit cell vol. (Å^3)	Z	(*M,S, L*)	ref
carboxylate and sulfonate anions											
β″-(ET)$_2$(fumarate)	$P\bar{1}$	6.135	8.107	16.981	79.98	79.68	81.88	812.9	1	(2,1, 1)	34
(ET)$_2$CF$_3$SO$_3$	$P2_1/n$	6.649	33.050	15.018	90	90.98	90	3300	4	(4,1, 2)	35
κ-(ET)$_2$CF$_3$SO$_3$	$C2/c$	34.171	8.239	11.623	90	99.74	90	3225	4	(-,-,2)[a]	36
(ET)$_2$CF$_3$SO$_3$	Cc	35.239	6.544	14.646	90	110.26	90	3168.5	4	(4,1, 2)	37
β″-(ET)$_2$SF$_5$CH$_2$SO$_3$	$P\bar{1}$	8.805	11.799	17.728	75.88	86.16	77.33	17424	2	(2,2, 1)	38
β″-(ET)$_2$SF$_5$CHFSO$_3$	$P\bar{1}$	8.796	11.726	17.576	95.89	90.18	102.29	1761.6	2	(2,2, 1)	38
β′-(ET)$_2$SF$_5$CF$_2$SO$_3$	$P\bar{1}$	7.699	13.151	17.642	81.32	87.42	74.99	1705.7[b]	2	(2,2, 1)	38
β″-(ET)$_2$SF$_5$CH$_2$CF$_2$SO$_3$	$P\bar{1}$	9.260	11.635	17.572	94.69	91.70	103.10	1835.5	2	(2,2, 1)	39
β″-(ET)$_2$SF$_5$CHFCF$_2$SO$_3$	$P\bar{1}$	9.223	11.593	17.809	93.86	94.54	103.07	1841.9	2	(2,2, 1)	40, 41
β″-(ET)$_2$CF$_3$CH$_2$SO$_3$	$P\bar{1}$	8.878	11.724	17.222	77.30	86.95	77.24	1705.5	2	(2,2, 1)	42
β″-(ET)$_2$Li(CF$_3$CHFSO$_3$)$_2$	$P\bar{1}$	8.640	11.498	20.344	82.01	80.06	80.64	1951.3[c]	2	(2,2, 1)	42
δ′-(ET)$_4$Li(CF$_3$CHFSO$_3$)$_3$(H$_2$O)$_2$	$P\bar{1}$	13.325	15.546	18.658	85.173	78.856	86.968	3776.2[c]	2	(4,2, 1)	43
δ′-(ET)$_2$CF$_3$CF$_2$SO$_3$	$Pca2_1$	14.497	6.609	35.169	90	90	90	3369.8[c]	4	(4,1, 2)	42
δ′-(ET)$_2$(CH$_2$:CHCH$_2$SO$_3$)(H$_2$O)	$Pma2$	32.772	7.960	6.687	90	90	90	1744.5	2	(2,1, 2)	44
(ET)$_3$[SO$_3$C$_2$H$_2$CF(CF$_3$)$_2$]$_4$(H$_5$O$_2$)$_2$	$C2/c$	60.454	11.213	12.764	90	99.14	90	8539	4	(3,2, 2)	45
(ET)$_3$(TEMPO-NHCOSO$_3$)$_2$(H$_2$O)$_6$[d]	$P2_1/c$	26.467	11.625	12.491	90	94.18	90	3833.0	2	(3,2, 1)	46
α′/*τ*-(ET)$_2$(*p*-CH$_3$-Ø-SO$_3$)	$P2$	7.785	6.697	34.402	90	91.10	90	1793.2	2	(2,1, 2)	35
(ET)$_2$[(C$_6$F$_5$)SO$_3$](TCE)[e]	$P\bar{1}$	6.741	15.893	19.140	89.81	94.28	93.20	2095	2	(4,1, 1)	40
β-(ET)$_2$[(C$_6$H$_5$)CH$_2$SO$_3$](H$_2$O)	$P\bar{1}$	9.931	12.367	16.982	71.04	82.46	67.58	1823.4	2	(2,2, 1)	47
κ$_{4\times4}$-(ET)$_2$[(C$_6$H$_5$)CH$_2$SO$_3$](H$_2$O)	$P2_1/c$	16.576	21.706	10.174	90	95.00	90	3646	4	(-,-,1)[a]	40
β″-(ET)$_4$[O$_3$S(C$_{10}$H$_6$)SO$_3$]	$P\bar{1}$	7.761	12.890	18.415	73.14	78.67	73.38	1676.2	1	(2,2, 1)	40
polycyano anions											
δ′-(ET)$_2$[C(CN)$_3$]	$P2/a$	14.979	6.700	16.395	90	94.80	90	1639.7	2	(4,1, 1)	48
β″-(ET)$_2${C$_3$H$_7$OC[C(CN)$_2$]$_2$}	$P\bar{1}$	9.584	11.184	20.73	78.23	85.90	65.4 2	1977	2	(4,1, 1)	49
(ET)$_x${C$_3$H$_7$OC[C(CN)$_2$]$_2$}$_y$	triclinic	6.78	7.8	31.4	34.8?[f]	90.1	96.0	923		g	49
(ET)$_2$[C$_4$(CN)$_6$]	$P2/a$	34.212	6.725	7.958	90	94.1 8	90	1825.9	2	(2,1, 2)	50
(ET)$_2$[C$_4$(CN)$_6$](BzN)[h]	$P\bar{1}$	12.919	18.643	7.855	93.63	107.81	91.43	1795.5		g	50
δ′-(ET)$_2$[C$_5$(CN)$_5$](TCE)$_x$[e]	$Pncm$	6.774	14.657	41.471	90	90	90	4075	4	(4,1, 2)	51
"*β*"-(ET)$_4$[*cis*-C$_6$(CN)$_8$](THF)$_{\sim2}$[i]	$P\bar{1}$	9.523	11.666	19.620	89.35	96.38	112.72	2001.1	1	(4,1, 1)	52
(ET)$_4$[*trans*-C$_6$(CN)$_8$](THF)$_{\sim2}$[i]	$P\bar{1}$	12.96	15.365	21.369	77.02	99.92	105.22	4946	2	(4,1, 2)	52
δ′-(ET)$_2$[N(CN)$_2$]	$Pcca$	14.744	6.676	32.151	90	90	90	3165	4	(4,1, 2)	53
α″-(ET)$_2$[N(CN)$_2$](H$_2$O)	$P2_1/c$	17.145	4.333	22.928	90	99.92	90	1678.0	2	(1,4, 1)	54
(ET)$_x$[N(CN)$_2$]$_y$(H$_2$O)$_z$	monoclinic	7.943	6.685	30.328	90	97.04	90	1598.2		*j*	54
(ET){N[C$_2$(CN)$_3$]$_2$}	$P2_1/c$	6.839	16.308	22.255	90	96.54	90	2466.0	4	*k*	55
sulfonyl-stabilized methanide and amide anions											
β″-(ET)$_2$[N(SO$_2$CF$_3$)$_2$]	$P\bar{1}$	6.639	8.656	17.349	94.70	97.21	68.95	922.7	1	(2,1, 1)	56
β″-(ET)$_2$[CH(SO$_2$CF$_3$)$_2$]	$P\bar{1}$	6.596	9.137	33.038	83.72	89.00	69.73	1856.1	2	(2,1, 2)	57
β′,*θ*-(ET)$_2$[C(SO$_2$CF$_3$)$_3$]	$P\bar{1}$	6.269	8.422	40.249	94.566	90.949	106.73	2026.9	2	(2,1, 2)	57
(ET)[C(SO$_2$CF$_3$)$_3$]	$P\bar{1}$	8.641	11.591	13.658	85.97	88.18	86.56	1361.5	2	*k*	57
phenolate anions											
α′-(ET)$_2$HCNAL[l]	$P2/c$	7.606	6.773	34.53	90	93.12	90	1776	2	(2,1, 2)	58
β″$_{432}$-(ET)$_4$HTNBP[m]	$P\bar{1}$	8.691	12.936	16.208	97.38	96.23	103.89	1735.9	1	(2,2, 1)	59
α″-(ET)$_2$(C$_6$H$_2$N$_3$O$_8$)	$P\bar{1}$	8.422	21.761	23.331	80.96	84.44	89.99	4202.5	4	(2,4, 1)	61
α″-(ET)$_2$(C$_6$H$_2$N$_3$O$_7$)(THF)[i]	$C2/c$	43.152	4.216	23.256	90	99.29	90	4175.4	4	(1,4, 2)	61
organometallic anions											
(ET)$_2$Cu(CF$_3$)$_4$	monoclinic	4.997	10.577	35.471	90	93.78	90	1870.7	2	*j*	62
(ET)$_2$Ag(CF$_3$)$_4$	$P2_1/n$	5.004	10.594	35.728	90	93.6 9	90	1890.0	2	(1,2, 2)	63
(ET)$_2$Au(CF$_3$)$_4$	$P2_1/n$	5.020	10.557	35.734	90	93.9 7	90	1889.4	2	(1,2, 2)	62
κ$_L$-(ET)$_2$[Ag(CF$_3$)$_2$(CN)$_2$]	$P2_1/n$	4.966	9.336	38.772	90	91.5 6	90	1796.9	2	(1,2, 2)	62
κ$_L$-(ET)$_2$Cu(CF$_3$)$_4$(TCE)[e]	$Pnma$	13.169	38.031	8.539	90	90	90	4276.4	4	(-,-,2)[a]	64
κ$_L$-(ET)$_2$Cu(CF$_3$)$_4$(2DBCE)[n]	$Pnma$	13.204	38.104	8.528	90	90	90	4290	4	(-,-,2)[a,j]	62
κ$_L$-(ET)$_2$Cu(CF$_3$)$_4$(DBCE)[o]	$Pnma$	13.169	38.031	8.539	90	90	90	4276.4	4	(-,-,2)[a,j]	62
κ$_L$-(ET)$_2$Ag(CF$_3$)$_4$(TCE)[e]	$Pnma$	13.175	38.174	8.595	90	90	90	4322.8	4	(-,-,2)[a]	65
κ$_L$-(ET)$_2$Ag(CF$_3$)$_4$(2DBCE)[n]	$Pnma$	13.209	38.123	8.602	90	90	90	4332	4	(-,-,2)[a,j]	62
κ$_L$-(ET)$_2$Ag(CF$_3$)$_4$(DBCE)[o]	$Pnma$	13.228	38.227	8.579	90	90	90	4338	4	(-,-,2)[a,j]	62
κ$_L$-(ET)$_2$Ag(CF$_3$)$_4$(TBE)[p]	$Pnma$	13.270	38.284	8.588	90	90	90	4363	4	(-,-,2)[a,j]	62
κ$_L$-(ET)$_2$Au(CF$_3$)$_4$(1BDCE)[q]	$Pnma$	13.262	38.071	8.592	90	90	90	4338	4	(-,-,2)[a,j]	62
κ$_L$-(ET)$_2$Au(CF$_3$)$_4$(TCE)[d]	$Pnma$	13.221	38.057	8.590	90	90	90	4322.1	4	(-,-,2)[a,j]	66
κ$_L$′-(ET)$_2$Cu(CF$_3$)$_4$(DBCE)[o]	$C2/c$	39.235	8.5512	13.193	90	102.99	90	4312.9	4	(-,-,2)[a]	67
κ$_L$-(ET)$_2$[Ag(CF$_3$)$_3$Cl](TCE)[e]	$Pnma$	12.850	37.614	8.471	90	90	90	4094[r]	4	(-,-,2)[a]	62
(ET)Au(C$_6$Cl$_5$)$_4$	$P2_1/c$	14.784	20.227	16.730	90	101.40	90	4904.2	4	*k*	68

[a] No stacks in layer. [b] Unit cell at 120 K. [c] Unit cell at 150 K. [d] TEMPO = 2,2,6,6-Tetramethylpiperidin-*N*-oxyl. [e] TCE = 1,1,2-Trichloroethane. [f] Certainly a typographic error in the original. [g] No details given. [h] BzN = Benzonitrile. [i] THF = Tetrahydrofuran. [j] Unit cell only. [k] Not a layered structure. [l] HCNAL = Cyanilic acid monoanion, (CN)$_2$C$_6$(O)$_3$(OH)$^-$. [m] HTNBP$^-$ = 3,3′,5,5′-Tetranitro-4,4′-biphenyldiol monoanion. [n] 2DBCE = 2-Bromo-1,1-dichloroethane. [o] DBCE = 1,2-Bibromo-1-chloroethane. [p] TBE = 1,1,2-Tribromoethane. [q] 1BDCE = 1-Bromo-1,2-dichloroethane. [r] Unit cell at 123 K

series of very stable chloride−hydrate salts, $(ET)_3Cl_2(H_2O)_2$ being the best known,[70−72] that have been found as unwanted side products by many research groups attempting to synthesize other salts of ET. This includes not only carboxylates but also a number of labile metal complex anions.

The only ET carboxylate salt that has been described in detail is the fumarate (monoanion), $(ET)_2$(*trans*-$HO_2CCH{=}CHCO_2$).[34,73] Given the above note on chlorinated solvents, it is somewhat surprising that the crystals of ET−fumarate were actually grown in a mixture of dichloromethane and ethanol. This could be due to extra stabilization against decomposition by formation of an extensive hydrogen-bonding network within the anion layer of the ET salt. The packing of the formally +1/2 charged ET cations is of the β''-type,[74] but with only weak interactions out of the plane of the ET molecule, semiconducting in-plane resistivity results. Unusually anisotropic atomic displacement parameters in the anion hint at some crystallographic complications that were not taken into account in the published structural analysis.[34]

2.2. Sulfonate Anions: $R–SO_3^-$

In contrast to the carboxylate anion, the sulfonate group has much greater stability toward oxidative decomposition, a fact that has been exploited in its use as an electrolyte in batteries and fuel cells.[75] Its greater stability is also reflected in the much lower pK_a of the conjugate acids, which rival or exceed the strongest mineral acids and have often been termed 'superacids'.[76] Further stabilization of the anion and increased strength of the conjugate acid is imparted by partial or complete fluorination of the adjacent carbon atoms. Correspondingly, there is a much larger body of work on cation radical salts with sulfonate-containing anions.

2.2.1. ET Salts with Trifluoromethylsulfonate

Salts of the trifluoromethylsulfonate ('triflate') anion are commercially available and frequently employed as a chemically inert counterion to crystallize cations of special interest. It is therefore not surprising that a triflate salt of ET was prepared some time ago by Chasseau et al.[35] It was electrocrystallized from tetrabutylammonium triflate and neutral ET in dichloromethane. The crystal structure of $(ET)_2CF_3SO_3$ contains alternating layers of ET and triflate, two layers each per unit cell. Within each donor layer there are stacks of four ET molecules per repeat, arranged into dimers that are twisted with respect to each other by 30°. The electrical resistivity along the most elongated crystal dimensions (assumed to be within the donor layer, transverse to the stacking axis) is that of a complex semiconductor: below 218 K and above 306 K it is simply activated, with gap energies of 0.1 and 0.07 eV, respectively, but between these temperatures convex curvature is observed in a plot of $\log(\rho)$ vs temperature (increasing gap $\partial \ln(\rho)/\partial(1/T)$ with increasing temperature). The discontinuity at 218 K was not observed in the spin susceptibility, which is characterized by a magnetic excitation of ca. 0.1 eV. It was discovered later[77] that the upper transition in the electrical transport measurements (including also thermopower) varied from crystal to crystal (type A ≈ 303 K, type B ≈ 277 K), although no differences were observed in the crystallographic lattice parameters. The application of pressure showed the most prominent (and most puzzling) difference between the two types: the upper transition in type B was reduced strongly with increasing pressure, coalescing with the rising lower transition at ca. 7 kbar, while in type A the upper transition remained essentially unchanged and the lower transition exhibited a small increase to ca. 240 K at 10 kbar.

Several additional phases containing ET and the triflate anion have been reported: In 1995, Fettouhi et al.[36] described the κ-phase of the 2:1 salt, and they also mentioned without details a 1:1 salt solvated with tetrahydrofuran (THF), $(ET)(CF_3SO_3)(THF)_{0.5}$. The structure of the former contains the orthogonal ET dimer arrangement typical of the κ-type packing motif, and the band electronic structure is said to be typical of other κ-phase salts.[78] The anions were found to be disordered, with superimposed trifluoromethyl and sulfonate groups. The salt is a semiconductor with an activation energy of 0.10 meV between 270 and 220 K. The ESR spectra show an unusual temperature dependence of the line width. Above ca. 200 K it is temperature independent (40−58 G, dependent on sample orientation) and then undergoes a broad maximum below 100 K, where it approximately doubles and finally becomes much narrower at liquid helium temperatures. The authors attribute this result to magnetic fluctuations and also imply an influence of the disordered dipoles of the anions, with the possibility of an anion ordering transition below room temperature not ruled out (although there is no experimental evidence for that at this time).

Yet another 2:1 salt was recently reported by Jia et al.[37] Its crystal structure is closely related to the first salt.[35] Both salts contain ET layers that are made up of stacks with two twisted donor molecule dimers per repeat unit and one stack per repeat in the in-plane direction. The two salts differ in the relative arrangement of successive layers: When projected along the shortest crystallographic axis, in the Chasseau salt,[35] adjacent layers have opposite tilt with respect to the anion layer (2-fold rotation relating the two layers), whereas in the Jia salt,[37] the sense of tilt remains the same (lattice centering operation). It may thus be appropriate to regard the two salts as polytypes. The conductivity of the Jia salt, 0.29 S cm^{-1} at 298 K, is nearly temperature independent above 150 K, but below that temperature it becomes gradually more insulating, approaching an activation energy of ca. 0.1 eV.

2.2.2. Superconductor $(ET)_2SF_5CH_2CF_2SO_3$

The study of ET salts with sulfonate anions was greatly stimulated by our discovery, in 1996, of superconductivity below 5 K in $(ET)_2SF_5CH_2CF_2SO_3$.[39,79] This salt represented the first truly organic superconductor among charge-transfer salts where both the cationic as well as the anionic component

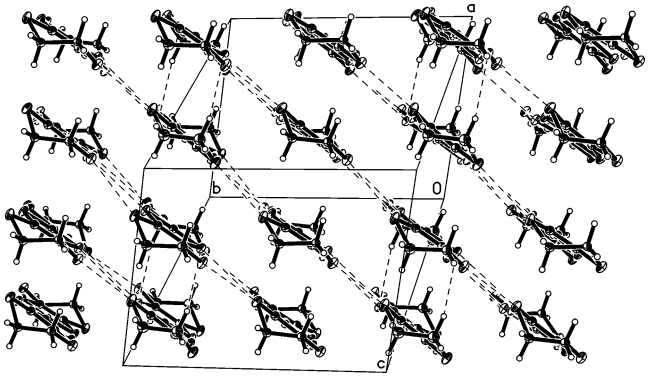

Figure 1. Packing of the electron-donor radical cations within the conducting layer of β''-$(ET)_2SF_5CH_2CF_2SO_3$ at 118 K. Intermolecular contacts shorter than the sum of the van der Waals radii are indicated by dashed lines.

was made up of an organic molecule. Much of our work since then has focused on finding (unsuccessfully) superconductors among the many salts with closely related anions. These will be described below, after the description of the superconductor, which has attracted a great number of physical studies.

$(ET)_2SF_5CH_2CF_2SO_3$ was prepared[39] by electrocrystallization in 1,1,2-trichloroethane (TCE). The anion source was the lithium salt, solubilized by the addition of 12-crown-4 (1,4,7,10-tetraoxacyclododecane). Its layered crystal structure[39] contains tilted stacks of formally +1/2-charged cations of the electron donor in typical β''-type packing,[74] except for a doubling of the transverse axis due to the space requirements of the large anion, see Figure 1. The band electronic structure calculated from the crystal structure exhibits shallow hole-like pockets of two-dimensional Fermi surface in addition to warped 1D segments. The band electronic structure was later revised,[80] but the salient features remained the same.

$(ET)_2SF_5CH_2CF_2SO_3$ is a semiconductor at room temperature. Upon cooling, the resistivity undergoes a broad maximum centered around 100−140 K. Below that temperature range, the in-plane conductivity becomes metallic, with a sharp drop at the superconducting onset temperature (around 5 K). The low-temperature resistivity was studied in detail by F. Zuo and co-workers.[81−83] They determined the upper critical field by measuring the interplane resistance as a function of strength and orientation of an external magnetic field.[83] H_{c2} was found to exhibit a sharp cusp of almost 12 T when the field was applied parallel to the conducting layers, thus well beyond the BCS Pauli limit of 9.6 T (calculated for a superconducting critical temperature, T_c, of 5 K). A very pronounced peak in the interlayer magnetoresistance with the magnetic field applied perpendicular to the conducting layers was observed when the field strength was just above that required to suppress superconductivity.[81,82] The peak was most prominent at the lowest temperature studied (1.82 K), and it vanished when the temperature exceeded T_c in zero field (~5 K), where $\partial\rho/\partial H$ remained positive at all fields. The peak maximum was fitted to a form $H_{max} = H_0(1 - T/T_c)^n$, with $H_0 = 1.5 \pm 0.2$ T, $n = 2.1 \pm 0.1$, and $T_c = 5.4 \pm 0.2$ K. The origin of the peak and the large negative magnetoresistance at fields above the peak remains unclear. A model of stacked Josephson junctions was unable to account quantitatively for the observed data. No peak was found when the field was applied parallel to the conducting layers.

The suppression of T_c with external hydrostatic pressure (as measured with ac susceptibility in a helium-filled pressure cell) was found to be essentially linear up to the maximum measured pressure of 2.4 kbar, with a slope of $\partial T_c/\partial p$ of -1.34 ± 0.1 K/kbar.[84] This slope is comparable to that found in β-phase organic superconductors but somewhat smaller than the higher T_c in κ-phase salts. The magnetic zero-pressure value was determined to be 4.45 ± 0.05 K, slightly smaller than the 4.8−5.2 K onset T_c found in electrical transport measurements, but this discrepancy, plus sample-to-sample variation, is commonly found in organic superconductors. It was later found[85] that the derivative $\partial T_c/\partial p$ decreases from the above value at pressures above ca. 3 kbar, and hints of superconductivity could be observed up to 11.7 kbar at 0.4 K.

The specific heat of $(ET)_2SF_5CH_2CF_2SO_3$ was studied by Wanka et al.[86] A small anomaly due to the superconducting transition was observed on top of a large phonon background (Debye temperature, $\Theta_D = 221 \pm 7$ K), which also contained a contribution linear in temperature due to the conduction electrons. The latter was approximately 3.5 larger than the Sommerfeld constant estimated for a two-dimensional metal from the band electronic structure. It was found to be necessary to include two Einstein modes of energies 16 and 31 cm^{-1} in the fit of the phonon background, in rough agreement with observed Raman modes between 20 and 50 cm^{-1} (see below). The magnetic field (perpendicular to the conducting planes) dependence of the specific heat anomaly allowed for extrapolation of the upper critical field to $T = 0$ K, $B_{c2}(0) = 3.4 \pm 0.4$ T, corresponding to an in-plane coherence length of ca. 10 nm. The magnitude of the specific heat jump was interpreted with an enhanced gap ratio compared to simple BCS theory and a strong-coupling limit. This assumption allowed extraction of the electron−phonon coupling parameter, $\lambda = 1.1 \pm 0.1$. Comparison with other organic superconductors whose specific heat has been measured indicated that the coupling parameter in these salts increases systematically with T_c. Together with the mass enhancement of the Sommerfeld constant, the magnitude of the electron−phonon coupling parameter gives strong evidence for large many-body effects in $(ET)_2SF_5CH_2CF_2SO_3$.

The same paper[86] also reported the temperature dependence of the irreversibility field from ac susceptibility and of the lower critical field from magnetization measurements. With the field applied perpendicular to the conducting layers, extrapolation of the lower critical field to $T = 0$ K was determined to be $B_{c1}(0) = 2 \pm 0.5$ mT, while in the parallel direction B_{c1} was found to be smaller than 6 μT down to 2 K. The thermodynamical critical field calculated from $B_{c1}(0)$, 37 mT, agrees almost perfectly with that obtained from extrapolation of the specific heat anomaly, 40 mT. On the basis of the large reversible

range of the phase diagram and the large Ginzburg–Landau parameter, $\kappa \approx 59$, $(ET)_2SF_5CH_2CF_2SO_3$ exhibits strong type II behavior.

The London penetration depth (λ) of $(ET)_2SF_5CH_2CF_2SO_3$ was measured by Prozorov et al.[87] with the external rf field applied both parallel and perpendicular to the conducting planes. For the parallel orientation, they extrapolated a value of 1−2 μm for T = 0 K, while in the perpendicular direction, it was estimated to be several hundred times as large, i.e., ~800 μm, which is larger than the sample dimensions. The temperature dependence of $\Delta\lambda = \lambda_{||}(T) - \lambda_{||}(0)$ was found to follow a T^3 law up to $T/T_c \approx 0.5$. A superconductivity mechanism based on *p*-wave pairing was suggested, but it was conceded that strong coupling with a realistic phonon spectrum in the more conventional *s*-wave pairing model could also account for this temperature dependence.

The Fermi surface of $(ET)_2SF_5CH_2CF_2SO_3$ was probed in a number of experiments by the groups of J. Wosnitza, J. Singleton, F. Zuo, and J. S. Brooks. Shubnikov-de Haas (SdH) and angle-dependent magnetoresistance (AMRO) oscillations were first reported by the former group.[88,89] At fields above 7 T and with the field normal to the conducting planes, SdH oscillations with a principal frequency of 200 T (and minor harmonics) were observed at 0.44 K. Oscillations were observed as long as the field angle (θ) remained less than 62°, but the SdH frequency increased with increasing angle, following a 1/cos θ law. The frequency at $\theta = 0$ corresponds to ~5% of the first Brillouin zone. The absence of a beat pattern indicates extremely small warping of the Fermi surface cylinder, i.e., extreme two-dimensional behavior. The effective cyclotron mass ($\sim 2m_e$ at $\theta = 0$) was deduced from the temperature dependence of the SdH amplitude. Its angle dependence is consistent with the 1/cos θ law of the oscillation frequency. The presence of AMROs indicates that there is some warping of the Fermi cylinder, but the warping must be extremely small because of the absence of a beat pattern in the SdH oscillations. The angle dependence of the amplitude of the quantum oscillations was analyzed in more detail by Symington et al.,[90,91] who concluded that a damping term proportional to exp(−α tan θ) (θ = angle of the field with respect to the normal to the conducting planes; α = a fitting constant) had to be present at least in $(ET)_2SF_5CH_2CF_2SO_3$ and $(ET)_2(NH_4)Hg(SCN)_4$ but quite possibly in quasi-2D organic conductors in general.

The investigation of AMROs was extended to higher fields and more azimuthal rotation angles within the conducting plane, which allowed mapping in detail the in-plane Fermi surface.[92,93] A strongly elongated (1:9) elliptical pocket with an area of ~5% of the first Brillouin zone (compared to band electronic structure calculations, which estimate 14%) is deduced from the magnetoresistance data. A similar result was obtained by Hayes et al.[94] The size of the Fermi surface was also deduced from de Haas–van Alphen (dHvA) oscillations.[92] Additional evidence for the elongated Fermi surface pocket comes from observation of cyclotron resonances in millimeter wave absorption in a varying magnetic field.[95,96] The

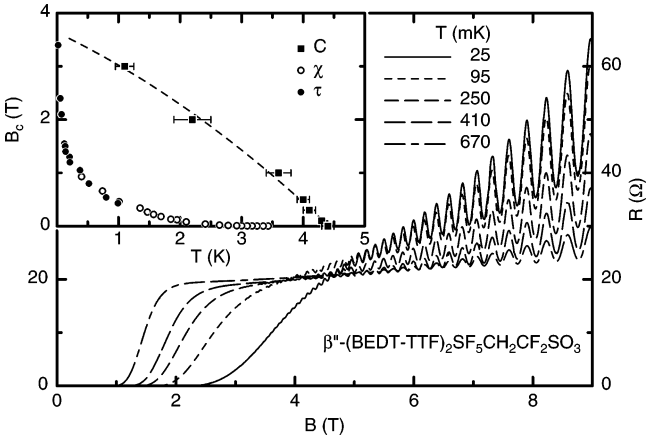

Figure 2. Field dependence of the resistance perpendicular to the conducting planes of β''-$(ET)_2SF_5CH_2CF_2SO_3$ at several temperatures. (inset) Temperature dependence of the upper critical field (■) and the irreversibility field (circles). (Reprinted with permission from ref 100. Copyright 2000 American Physical Society.)

dHvA signal exhibited an almost ideal inverse saw tooth shape, which was very well reproduced with the assumption of a perfectly two-dimensional metal with a charge-carrier reservoir.[97,98] This explanation implies the presence of a fixed chemical potential, presumably due to the presence of localized electron states at the Fermi surface. It furthermore requires the existence of a quasi-1D band (in agreement with the calculated band electronic structure) and an exceptionally large density of states of this band (in contradiction to the band electronic structure). This view was contradicted by Nam et al.,[99] who favor an explanation based on thermal activation between Landau levels based on a fit of the magnetoresistance maxima to a Landau-level fan diagram. It is further supported by the observation of bistability in the zero-field resistance perpendicular to the conducting layers between 35 and 140 K. Such bistability is indicative of a density wave, presumably due to nesting of the quasi-1D band, which is therefore effectively removed from the electron transport at low temperature.

SdH oscillations were observed even in the superconducting, mixed state at very low temperatures (25 mK), i.e., well below the upper critical field of ~3.6 T and not much above the field below which the resistivity vanishes (see Figure 2).[100] The fundamental frequency of the oscillations in the mixed state, 199 ± 1 T, is exactly the same as in the normal state. Moreover, no attenuation of the SdH (or the dHvA) was observed upon crossing B_{c2}. One possible explanation, that of a gapless superconductor (i.e., nodes in the gap function), was discounted because the specific heat data[86] clearly proved the existence of a gap, at least at $B = 0$. The observation of finite resistance in this extremely two-dimensional material therefore requires a dissipative mechanism within the superconducting regime, not only in the vortex cores.[100] In a later paper Wosnitza et al.[101] reported dHvA oscillations in the mixed state at very low temperatures (30 mK) and applied magnetic field (as low as 1.4 T). A field-modulation technique was employed in order to gain higher field resolution and

sensitivity. The most important result of these measurement was the reduced attenuation of the oscillation amplitude upon entering the superconducting state, indicating the importance of superconducting fluctuations. Possibilities for the diminished damping include a reduced quasiparticle scattering rate and an additional oscillatory contribution in the superconducting state.

Early on[102] it was already recognized that the background magnetoresistance underlying the SdH oscillations was anomalous in that its temperature and field dependence was more characteristic of a nonmetal, unlike all other organic conductors where oscillations had been observed. The dHvA and SdH measurements were extended[103,104] to higher fields in a special cantilever device that allowed the simultaneous recording of both magnetic torque (proportional to $B^2 dM/dB$) and magnetoresistance. The simultaneous measurement was essential to extract the correct background resistance in order to derive the anomalous SdH oscillations. It was found that the background magnetoresistance exhibits a field-induced metal-to-insulator (MI) transition at a critical field of ca. 3.5 T, which is near the upper critical field of the superconductor, and the curves obtained at different temperatures were scaled to a universal curve. Again, the model proposed by Nam et al.[99] based on the presence of a Landau gap and a chemical potential that resides within the gap provides an alternate explanation of the large magnetoresistance maxima near integer ratios of the oscillation frequency with the applied field without invoking a field-induced MI transition.

Hagel et al.[85] studied the pressure dependence of the magnetoresistance of $(ET)_2SF_5CH_2CF_2SO_3$. The SdH frequency increased by ca. 15% at 6 kbar from the ambient pressure value of 199 T. This increase is much larger than would be expected for a closed orbit from the growth of the Brillouin zone due to the compressed crystal volume. It is speculated that the open (1D-like) bands contribute to this rapid increase. The AMRO maxima measured at several pressure values remained essentially constant, further indicating that the elliptical closed portion of the Fermi surface retains its shape and size under applied pressure. By comparison of both the SdH and AMRO signal, it was possible to extract the pressure dependence of the effective mass and the spin *g*-factor. The former was found to decrease much more strongly than expected within an independent electron picture, thus indicating the presence of strong many-body (electron−electron or electron−phonon) effects. Simultaneously, the *g*-factor increases by about 20% at 10 kbar, indicative of strong electron−electron correlations.

The application of higher pressure led to observation of a first-order phase transition to an insulating below 153 K state around 10 kbar.[105] This transition, which has a hysteresis of ca. 4 kbar, was observed in the c^*-resistance upon both varying the pressure at constant temperature and changing the temperature at various constant pressures. This transition must be due to a subtle structural change, although unpublished preliminary neutron diffraction results indicate no gross change in the crystal structure. In the same paper[105] the dependence of the fundamental SdH frequency (at 0.44 K) on the angle of the magnetic field with the conducting plane normal at several pressure values was presented, which led to a more precise determination of the effective cyclotron mass and its approximately linear decrease from $2.0 \pm 0.1\ m_e$ at 0 kbar to $1.23 \pm 0.10\ m_e$ at 10 kbar. In the insulating state the temperature dependence of the second-harmonic SdH frequency indicates that the band structure is reconstructed at high pressure.[105]

The question of coherence in the interlayer transport in quasi-2D organic superconductors was probed by Wosnitza et al.[106] in two ET salts, κ-$(ET)_2I_3$ (T_c = 3.5 K) and $(ET)_2SF_5CH_2CF_2SO_3$. The measurement consisted of recording the resistance of the crystal perpendicular to the conducting layers and carefully rotating it in a magnetic field around an axis within the layers and perpendicular to the field at very low temperatures. For κ-$(ET)_2I_3$ it was observed that when a field sufficiently large to suppress superconductivity was applied exactly within the conducting plane, enhancement of the resistance occurred. The full angular width of this peak was only 0.34°, independent of field strength. This peak is indicative of coherent interlayer transport, albeit marginal as the interlayer overlap integral is only slightly smaller than the scattering rate. On the other hand, no such peak was observed in $(ET)_2SF_5CH_2CF_2SO_3$ even though it was looked for at a number of azimuthal angles of the rotation axis. The peak was not found even under an applied hydrostatic pressure of 6 kbar.[107] Therefore, no evidence exists for coherent transport in the latter material, probably due to a much smaller interlayer overlap integral; thus, it may be regarded as a most extremely two-dimensional metal among the organic conductors.

The uniaxial thermal expansion coefficients of $(ET)_2SF_5CH_2CF_2SO_3$ were measured as a function of temperature and in applied magnetic fields.[108] They were found to be highly anisotropic, even within the conducting planes. There is a pronounced sharp anomaly at the superconducting transition, but the sign of the anomaly varies with the crystallographic direction: it is negative perpendicular to the conducting planes, positive along the in-plane *b*-direction, and negligible along the in-plane *a*-axis. When combined with the specific heat anomaly at T_c,[86] the dependence of T_c with uniaxial pressure along the corresponding directions may be deduced via the Ehrenfest relationship. The value of $\partial T_c/\partial p_i$ averaged over the three directions, -1.6 ± 0.5 K/kbar, agrees well with the magnetic measurements under hydrostatic pressure (-1.34 ± 0.1 K/kbar).[84] The overall negative sign is dominated by the interlayer pressure dependence, which illustrates the importance of interlayer interactions for the onset of superconductivity. The same qualitative behavior is also reported in the same paper[108] for another organic superconductor, κ-$(ET)_2Cu(NCS)_2$.

The isotope effect on the superconducting transition temperature upon substitution of the electron-donor molecule hydrogen atoms with deuterium was

studied in our group.[109,110] We found that T_c increases with the ^2H substitution, as is the case for the majority of organic superconductors, e.g., κ-$(ET)_2Cu(NCS)_2$,[111−116] κ-$(ET)_2Cu[N(CN)_2]Cl$,[117] κ-$(ET)_2Ag(CN)_2(H_2O)$,[118] and κ-$(ET)_2Ag(CF_3)_4(C_2H_3Cl_2Br)$.[119] In the classical Bardeen−Cooper−Schrieffer model of superconductivity[120,121] the superconducting transition temperature is proportional to the frequency of a phonon that is strongly coupled with the electronic system; thus, T_c is expected to be reduced with increasing isotopic mass. The "inverse" isotope effect observed in the organic superconductors for ^2H substitution indicates that the C−H intramolecular phonons are not essential to the electron-pairing mechanism. We speculated[110] that the shortening of the C−^{2}H bond length compared to C−^{1}H leads to a slight increase in the intermolecular distances, and from the point of rigid molecular assemblies, this corresponds to a reduction in lattice pressure and thus to an increased T_c considering the negative values of $\partial T_c/\partial p$ as illustrated above. This idea was further studied by Kawamoto et al.[122] in their study of the isotope effect in κ-$(ET)_2Cu[N(CN)_2]Br$, where the situation is complicated due to the vicinity of a magnetically ordered state.

The optical properties of $(ET)_2SF_5CH_2CF_2SO_3$ were studied in a series of papers by Musfeldt and coworkers.[80,123,124] Polarized reflectance spectra in the frequency range from 35 to 35 000 cm^{-1} were recorded between 10 and 300 K from the best-developed crystal face (*ab*-plane, parallel to the conducting layers). The spectra exhibit sharp molecular transitions superimposed over a broad background band due to the conduction electrons. As illustrated in Figure 3, the electronic spectrum is anisotropic within the plane, with considerably higher optical conductivity along the interstack (*b*) direction than along the stack at all frequencies up to 10 000 cm^{-1} (at 300 K). The anisotropy is consistent with the band electronic structure calculation by Koo et al.[80] The low-frequency behavior is weakly metallic, but the plasma edge is only visible in the interstack direction. The room-temperature electronic spectra are similar to several other β-type organic conductors[125,126] but not as extremely anisotropic as β''-$(ET)_4Fe(C_2O_4)_3(H_3O)(C_6H_5CN)$.[127] The spectra remain characteristic of a weak metal even at low temperatures (all spectra were taken at $T > T_c$), but the most surprising feature is the absence of a Drude response even at 14 K. Instead, localization is observed in the far-infrared. The broad electronic band in the mid-infrared becomes enhanced and red shifted at low temperature, possibly due to increased interdimer interactions. Most of the molecular vibrations superimposed over the electronic background are totally symmetric, because only these are enhanced due to vibronic coupling, although a few other modes are visible as well. They were assigned to either the known vibrations of the partially ET cation or the anion by Dong et al.[123]

The electron-spin resonance spectra of $(ET)_2SF_5CH_2CF_2SO_3$ were examined by Wang et al.[128,129] At room temperature the anisotropy of the signal was recorded in rotations about the crystallographic *b*- and *c**-axes. The former compares the in-plane with the out-of-plane response, while the latter probes the anisotropy within the conducting planes. In the *a***c**-plane the maximum *g*-value (2.012) and line width (34 G) occurred with the magnetic field near the *c**-axis. Minimum values were 2.004 and 23 G, respectively. Within the conducting plane, *g*-values ranged from 2.004 to 2.008 and line widths from 24 to 27 G. In both rotations the maxima of the *g*-values were observed at the same orientation as the maxima of the line width. Spectra with the magnetic field in the conducting plane were distinctly distorted by an admixture of dispersion in the absorption signal (Dysonian line shape).[130] This phase shift is indicative of electrical conduction in the planes, and the amount of distortion is directly related to the conductivity (the exact relationship depends on the sample shape), although absolute scaling is difficult. From a fit of the Dysonian distortion at various rotation angles, the anisotropy ratio of the in-plane microwave conductivity was therefore estimated to be ca. 1.35 between the maximum (approximately along the *b*-direction) and the minimum (approximately along the *a*-direction) at room temperature. The observation of a conductivity maximum along the interstack (*b*) direction is consistent with the band electronic structure and the optical spectra.[80] The temperature dependence of the ESR spectrum with the magnetic field along *c** was examined in the range 4−410 K. At the lowest temperatures, the signal vanishes due to the onset of superconductivity. The line width

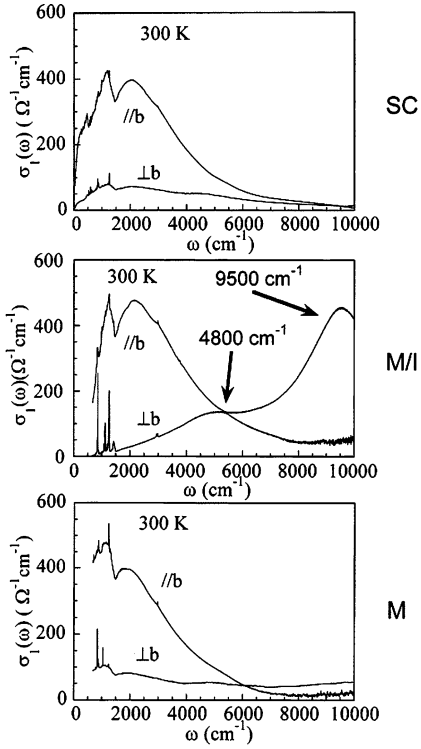

Figure 3. Frequency-dependent conductivity of β''-$(ET)_2SF_5CH_2CF_2SO_3$ (SC), β''-$(ET)_2SF_5CHFCF_2SO_3$ (M/I), and β''-$(ET)_2SF_5CHFSO_3$ (M) at room temperature, illustrating the higher ac conductivity along the interstack direction. Electronic excitations at 4800 and 9500 cm^{-1} are highlighted in the spectrum of the β''-$(ET)_2SF_5CHFCF_2SO_3$ salt. (Reprinted with permission from ref 132. Copyright 2000 American Chemical Society.)

decreases monotonically throughout the entire range, although the slope of the decrease changes gradually from ca. 0.035 G/K well above 150 K to 0.155 G/K between 20 and 150 K. The tiny residual line visible at 5 K had a width of only 0.26 G. The spin susceptibility (proportional to the integrated ESR signal) also decreased with decreasing temperature above ca. 120 K but remained approximately constant below 120 K until the onset of superconducting fluctuations below 10 K. The susceptibility is consistent with the observation of activated bulk electrical conductivity above 100−120 K and weakly metallic behavior below 100 K. No phase transition was observed in the ESR signal above room temperature up to 410 K, where the sample started to decompose.

2.2.3. Other Aliphatic Sulfonate Anions

Building on the success of finding superconductivity in $(ET)_2SF_5CH_2CF_2SO_3$, we quickly set out to explore chemically modified analogues of this salt. Four distinct modification routes may be envisaged: (1) replacement of the SO_3 anionic group, (2) replacement of the SF_5 end group, (3) modification of the fluorine/hydrogen substitution pattern on the carbon backbone, and (4) change in the length of the carbon backbone. Other than a few unrelated carboxylates, no cation radical salts with other organic oxoanion groups have been reported. Route 1 is therefore still open for future research. It is certainly conceivable that organic phosphonate or selenolates will yield novel molecular conductors, maybe even superconductors.

The first specifically targeted analogue was of the third category, i.e., replacement of one hydrogen atom by fluorine to form $(ET)_2SF_5CHFCF_2SO_3$.[40,41] Superficially, this salt is very similar to the superconductor in many respects. The ET donor molecule layers in the two salts are essentially the same, and the anions occupy the same general crystallographic location. However, the major structural difference is that in the $CHFCF_2$ salt the backbone of the anion is crystallographically disordered, consisting of a superposition of the *R*- and *S*-isomers of the racemic mixture (the anion contains one chiral carbon center). Note that this disorder is not dictated by symmetry as there are centers of inversion elsewhere in the structure, and distinct locations for the anions of opposite handedness are available. It is thought that the disorder maximizes the number of attractive H···F intermolecular attractions.[131] At lower temperature there are more pronounced structural differences between the two salts, i.e., the ethylene end groups of the ET molecules order in eclipsed fashion in the superconductor but in the staggered conformation in the $CHFCF_2$ salt. The anion disorder does not disappear, however, as it would require either the exchange of entire molecules between crystal sites or the breaking and forming of C−H and C−F bonds. The subtle structural differences manifest themselves in the band electronic structure:[41,132] In both salts the ET molecules are increasingly more dimerized at lower temperatures, with an alternation of the overlap orbitals along the stacking direction. In the $CHFCF_2$ salt, however, this dimerization is much more pronounced to the point where the interdimer overlap essentially vanishes and electron localization sets in. The localization is seen in the electrical resistivity, which is weakly metallic at room temperature ($\rho_{298} = 0.08\ \Omega$ cm within the conducting plane). Upon cooling below 190 K, the resistivity suddenly increases but then levels off to a value only slightly higher than the room-temperature value. The discontinuity around 190 K is also seen upon warming, but it does not retrace the cooling curve. The transition is accompanied with a rapid drop in the ESR spin susceptibility. At room temperature the in-plane conductivity anisotropy was estimated to be around 1.1 from orientation-dependent ESR spectra,[41] in a fashion similar to the superconducting salt (see above). The temperature dependence of the unit cell parameters within the conducting layer also exhibits a transition below 200 K, with the *a*-axis increasing slightly and the *b*-axis dropping by 1% in addition to the normal thermal contraction.[133]

However, the optical properties[131,132,134] of the $CHFCF_2$ salt are much more anisotropic than the CH_2CF_2 superconductor. In the polarization along the interstack (*b*) direction, the low-frequency reflectance is high with a pronounced drop in the mid-infrared quite similar to the superconductor, while in the interstack polarization, the reflectance is low and flat in the infrared but not overdamped as in the superconductor.[80] As shown in Figure 3, a low-lying electronic excitation around 2000 cm^{-1} is observed in the $\|b$ polarization, while in the $\perp b$ polarization strong absorptions near 9500 cm^{-1} and a shoulder around 4800 cm^{-1} are manifest. The former is split into a doublet at low temperature, indicating additional localization. Otherwise, the changes between 300 and 10 K are slight, consistent with the observation that the electrical resistivity remains within the same order of magnitude between the two temperatures. The low optical conductivity along the stack direction is consistent with the dimerization proposed by the band electronic structure.[41] The screened plasma frequency ($\|b$) of 4800 cm^{-1} is very similar to that in the superconductor (4700 cm^{-1}).

Solid solutions $(ET)_2(SF_5CH_2CF_2SO_3)_{1-x}(SF_5CHFCF_2SO_3)_x$ were studied for $x = 0.25$, 0.5, and 0.75.[133] Two types of disorder are present in these salts: (1) due to the distribution of the two constituents (spatial disorder) and (2) local disorder due to the presence of multiple configurations ($SF_5CHFCF_2SO_3^-$ anion) or conformations (ET ethylene end groups at room temperature). No superconductivity was observed in any of the mixed salts, but the metal-to-insulator transition was present only in the $x \geq 0.5$ samples. The lattice parameters showed a gradual change from $x = 0$ to 0.5 (increase in *b* and *c*, decrease in *a*), but at $x = 0.75$ they were essentially identical to the pure $x = 1$ salt, where *a* is larger and *b* smaller than in the superconductor ($x = 0$). The bulk of the paper,[133] however, deals with the optical spectra of the solid solutions and the influence of spatial vs local disorder on the low-lying electronic excitations. It was concluded that the local disorder is much more effective in creating oscillator strength for these excitations than spatial disorder.

We subsequently reported on the modifications with only one carbon atom in the anion backbone.[38,40] All three possible H/F substitution patterns were prepared, and three very different 2:1 salts resulted.[38] The ET molecular packing in $(ET)_2SF_5CH_2SO_3$ and $(ET)_2SF_5CHFSO_3$ is of the β''-type,[74] but the layers differ in detail. In the CHF salt, like in the CH_2CF_2 superconducting analogue, all molecules within a stack are crystallographically identical but two crystallographically distinct stacks exist. On the other hand, in the CH_2 salt, all stacks are identical with two alternating independent ET molecules per repeat unit. Thus, in the former type the inversion centers are located on the stacks, whereas in the latter they are located between stacks. From an analysis of the bond lengths[135] within the ET cation it is estimated that the +1/2 charge is approximately evenly distributed over the two cation sites in $(ET)_2SF_5CHFSO_3$, while uneven charges of +0.4 and +0.6 may be assigned to the two molecules in the case of $(ET)_2SF_5CH_2SO_3$. In both salts the anions are weakly dimerized via soft hydrogen bonds between the aliphatic hydrogen atoms and sulfonate oxygen atoms. No disorder of the type seen in the $SF_5CHFCF_2SO_3^-$ salt exists in the crystal structure of the chiral anion $SF_5CHFSO_3^-$, which is also present as a racemic mixture. $(ET)_2SF_5CF_2SO_3$ crystallizes in the β'-packing type, which is characterized by stacks of face-to-face dimers that are laterally offset from each other. Two crystallographically distinct stacks form one unit cell within the electron-donor molecular plane. No short intermolecular contacts are observed between anions, as there are no hydrogen atoms present to form hydrogen bonds.[38]

The resistivity of the CHF salt is similar to the superconductor, with a broad transition from semiconducting at high temperature to weakly metallic below ca. 100 K. However, it does not become a superconductor at ambient pressure and exhibits a turnover to semiconducting behavior below 10 K. The metallic nature of this salt is reflected in the band electronic structure, which is in most respects very similar to that of $(ET)_2SF_5CH_2CF_2SO_3$. The other two one-carbon analogues are less conducting ($\rho_{290} \approx 19$ and 1.3×10^3 Ω cm for the CH_2 and CF_2 salts, respectively), and both show activated conductivity ($E_a = 56$ and 110 meV, respectively). The activated behavior in $(ET)_2SF_5CH_2SO_3$ may be explained by the partial charge localization, which splits the HOMO energies of the two crystallographically distinct molecules by ca. 0.17 eV. The two charge states are also observed in the Raman spectrum of $(ET)_2SF_5CH_2SO_3$, where two separate ν_3 C−C stretching vibrations are observed at 1460.4 and 1476.8 cm^{-1}. These correspond to fractional charges +0.38 and +0.54 in the empirical relationship between frequency and charge in ET molecules,[136] in excellent agreement with those estimated from the bond lengths.[38]

Because of its similarity with $(ET)_2SF_5CH_2CF_2SO_3$ and $(ET)_2SF_5CHFCF_2SO_3$, the optical properties of $(ET)_2SF_5CHFSO_3$ were examined (see Figure 3).[132,134] The electronic excitation spectrum at room temperature was found to be more similar to the superconductor than to the second salt, again highlighting the role of anion disorder in the oscillator strength of the higher energy (~5000 and 9500 cm^{-1}) transitions. Garlach et al.[133] studied the solid solutions between $(ET)_2SF_5CH_2CF_2SO_3$ and $(ET)_2SF_5CHFSO_3$ in several ratios (0.25:0.75, 0.5:0.5, 0.75:0.25). Unlike the case of mixing the two 2-carbon chain salts (see above), the lattice constants vary almost linearly between the two end points (pure salts). The 50:50 salt exhibits an electrical resistivity that is almost identical to that of the pure CHF compound, and no superconductivity was observed in any mixing ratio. Interestingly, a significant enhancement of the conductivity peak at ~9500 cm^{-1} was observed, compared to the pure compounds, where it was barely or not at all visible. Again, these charge-transfer excitations are thought to be enhanced by the random potentials created by the spatial disorder.[133]

As mentioned before, β'-$(ET)_2SF_5CF_2SO_3$ is more unique compared to the β''-type salts described above. The different ET packing type naturally leads to a different band electronic structure,[38,137] which nevertheless predicts the possibility of metallic behavior in the one-electron representation, especially along the *b*- (intrastack) direction. However, both the optical conductivity within the *ab*-plane[137] and the magnetic properties[38,137] are indicative of a magnetic semiconductor. No crystals large enough to measure electrical properties have been obtained to date. The optical data exhibit pronounced anisotropy within the plane, with pronounced electronic excitations at 4000−6000 ($E||b$) and 3200 cm^{-1} ($E\perp b$). The former may be assigned to the $\psi_+ \rightarrow \psi_-$ interband transition, but the latter is not adequately explained by the band electronic structure. Rather, it may originate from the charge transfer from one singly charged dimer to a neighboring and thus provide a direct measure of the on-site Coulomb repulsion, *U*. As the latter is of similar size as the bandwidth, electron−electron correlations are important in this material. The vibrational transitions of symmetry type A_g are enhanced by electron−phonon coupling, and they dominate the reflection spectra.

The temperature dependence of the optical spectra of β'-$(ET)_2SF_5CF_2SO_3$ was analyzed by Pigos et al.[137] The broad charge-transfer band centered around 3200 cm^{-1} was modeled by the superposition of three oscillators whose characteristic parameters varied with temperature. The lowest frequency oscillator exhibited a significant weakening between 100 and 50 K, thus leading to a shift of the band envelope to higher frequency in this temperature range. On the other hand, the largest changes in the vibronic spectrum occurred around 200 K (for details, see the paper[137]), indicating a possible structural transition in that range.[38] However, there is no obvious change in the crystal structure obtained from X-ray diffraction, except for the typical thermal contraction (details of the room-temperature crystal structure are not published), although the variation of the lattice parameters with temperature exhibits a minute anomaly of $\Delta b = 0.010 \pm 0.002$ Å, $\Delta\alpha = 0.030 \pm 0.011°$, $\Delta\gamma = 0.066 \pm 0.014°$ around 160 K.[138] Future work is needed to clarify the nature of this transition. A much more pronounced transition is observed at

45 K, where the ESR spin susceptibility along all three crystal axes exhibits a sharp spike followed by a precipitous drop at low temperatures.[38,137] The temperature of the transition was later redetermined to be 33 K rather than 45 K.[139] Above the transition, the spin susceptibility follows approximately the one-dimensional $S = 1/2$ Heisenberg antiferromagnetic chain model. The transition was originally thought to be to a spin-Peierls transition, albeit at an extraordinarily high temperature, but more recent high-field ESR and NMR measurements[140] have cast doubt on this interpretation. Instead, below the transition (shifted to 20 K due to the presence of a large magnetic field of up to 24 T), three-dimensional antiferromagnetic order appears to prevail, presumably due to interchain magnetic interactions. Single crystals large enough to perform anisotropic static magnetic susceptibility measurements at lower applied fields will be required to fully clarify this transition.

The next type of modification possible in the search for superconducting analogues of $(ET)_2SF_5CH_2CF_2SO_3$ consists of replacement of the SF_5 headgroup with other fluorinated substituents, e.g., CF_3. We recently compared the crystal structures and some preliminary properties of the ET salts with fluorinated ethylsulfonate anions, i.e., $CF_3CH_2SO_3^-$, $CF_3CF_2SO_3^-$, and $CF_3CHFSO_3^-$.[42] The former two formed 2:1 salts with ET, but the CHF analogue formed a double salt $(ET)_2Li(CF_3CHFSO_3)_2$, where the lithium ion originated in the electrolyte. The CH_2 salt adopts the β'' packing and is in many respects very similar to $(ET)_2SF_5CH_2SO_3$. The packing of the ET molecules in $(ET)_2CF_3CF_2SO_3$ is made of stacks of ET dimers that are twisted with respect to each other around an axis perpendicular to the ET molecular plane. This packing motif is frequently designated as δ'.[141] The double salt $(ET)_2Li(CF_3CHFSO_3)_2$ contains strongly dimerized ET molecule in a packing that is reminiscent of the β'-type, but the lateral offset of the dimers is so pronounced that the structure hardly contains stacks anymore. More interesting in this structure is the anion layer, which is composed of ribbons of tetrahedrally coordinated Li^+ cations and bridged by the sulfonate groups of two anions. Both $(ET)_2SF_5CH_2SO_3$ and $(ET)_2Li(CF_3CHFSO_3)_2$ are semiconductors, the latter with an activation energy of 0.1 eV. No resistivity data are available for $(ET)_2CF_3CF_2SO_3$, but ESR spectroscopy reveals that the spin susceptibility drops substantially below 50 K, perhaps indicating antiferromagnetic long-range order. Since the publication of this paper[42] we identified at least three more phases in the ET^{x+}:(Li^+):$CF_3CHFSO_3^-$ system: a 2:1 β''-type salt without lithium similar to $(ET)_2SF_5CH_2SO_3$, another double salt, $(ET)_4Li(CF_3CHFSO_3)_3(H_2O)_2$, and an additional phase of a composition yet to be determined (preliminary results indicate that it, too, contains lithium).[43,142] In $(ET)_4Li(CF_3CHFSO_3)_3(H_2O)_2$ each lithium ion is complexed by two $CF_3CHFSO_3^-$ anions and two water molecules and a third $CF_3CHFSO_3^-$ anion bridges the complexes via hydrogen bonds and organizes them into ribbons within the anion layer. The ET molecule packing is a variant of the δ'-mode with twisted dimers.[43]

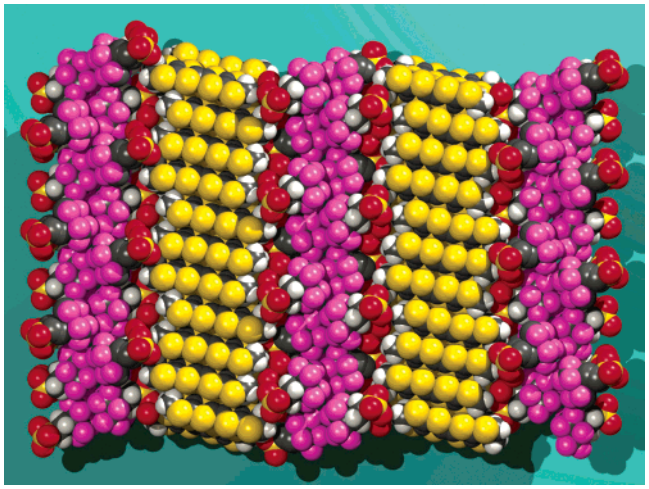

Figure 4. Space-filling rendering of the crystal structure of $(ET)_3[SO_3C_2H_4CF(CF_3)_2]_4(H_5O_2)_2$ illustrating the extreme thickness and the bilayered nature of the anion layer: gray, carbon; white, hydrogen; magenta, fluorine; red, oxygen; yellow, sulfur.

The synthesis (electrocrystallization from sodium allylsulfonate with 18-crown-6 in 1,2-dichloroethane) and crystal structure of $(ET)_2(CH_2{:}CHCH_2SO_3)(H_2O)$ was recently reported.[44] The ET molecules pack in the δ'-type twisted dimer mode. The allylsulfonate anions are located on mirror planes, where they are lined up by weak C−H···O hydrogen bonds. The water molecules are also hydrogen bound to the sulfonate end groups. The resistivity of this salt is activated, with a room-temperature resistivity of 0.049 Ω cm and an activation energy of 0.32 eV. A figure in the paper[44] shows a maximum of the resistivity at ca. 180 K, but as the text does not refer to it, it may reflect an experimental artifact.

We recently explored what would happen if a really bulky fluorinated organic substituent would be attached to the sulfonate anionic group and crystallized with ET. We succeeded in the growth of extremely thin crystals of the salt $(ET)_3[SO_3C_2H_4CF(CF_3)_2]_4(H_5O_2)_2$.[45] The crystal structure (shown in Figure 4) is layered, with the ET molecules arranged in stacks. The molecules in adjacent stacks are tilted in the opposite direction from the stack axis, similar to the α-packing type.[78] However, in contrast to most other α-phases, except for $(ET)_3(CuBr_2)_{0.5}(CuBr_4)_{0.5}$[143] and $(ET)_3(CoCl_4)(TCE)$,[144] the molecules within a stack are grouped into trimers, followed by a stack slip. The analysis of the bond lengths[135] indicates that the ET molecule at the center of the trimer has a charge approaching +1, while the outer molecules are less charged ($+0.6 \pm 0.1$). The anion layer is a most peculiar one for cation radical salts. It consists of a bilayer (similar to that formed by detergents and biological lipids) with the fluorocarbon end groups in the center and the anionic sulfonate groups, hydrogen-bound by water or hydronium molecules, on the outside. It is thus the sulfonate side of the anion that is in contact with the ethylene end groups of the ET molecules. The bilayer nature of the anion packing leads to one of the largest separations between ET

layers, i.e., the thickness of the anion layer up to the van der Waals radius is 17.8 Å. The extreme layered nature of the crystal structure is reflected in the flakelike morphology of the crystals. Unfortunately, insufficient material is available for physical properties measurements. However, the ET packing, together with the charge segregation, makes it unlikely that $(ET)_3[SO_3C_2H_4CF(CF_3)_2]_4(H_5O_2)_2$ is a good conductor.[45]

2.2.4. TEMPO Sulfonate Anions

The functional group 2,2,6,6-tetramethylpiperidin-*N*-oxyl (TEMPO) is a commonly used stable radical in the search for purely organic magnets as well as a paramagnetic marker in biological systems.[145−147] Derivatives of the radical have also been employed as electron donors in a number of charge-transfer salts.[148−152] In a series of papers Akutsu and coworkers described anions derived from TEMPO with sulfonate groups, where the anionic substituent is connected via a suitable spacer at the 4-position of the piperidine ring (para to the nitroxyl group). Anions containing the amido (−NH−),[153,154] oxo (−O−),[154] and acetylamido (−NHC(O)CH_2−)[46] spacers have been reported, and the ET salt of the last derivative is known, i.e., $(ET)_3(TEMPO{-}NHCOCH_2SO_3)_2(H_2O)_6$.[46] The packing of the ET molecules in this salt is quite similar to that in $(ET)_3[SO_3C_2H_2CF(CF_3)_2]_4(H_5O_2)_2$,[45] with α-type[78] stacks of trimers and a thick anion layer with hydrogen-bonded water−sulfonate entities on the outside. However, here the charges of the ET molecules are estimated to be approximately equal (+2/3), irrespective of their position within the trimer. The salt should therefore be a band insulator, although the resistivity is that of a semiconductor with activation energy 0.05 eV and $\rho_{RT} = 5.1$ Ω cm. The magnetic susceptibility shows weak ferromagnetic interactions between the TEMPO spins. A fit to the 1D Heisenberg model indicates an exchange parameter $J/k_B = +0.42$ K.

2.2.5. Aromatic Sulfonate Anions

The ET salt with *p*-toluenesulfonate (tosylate), $(ET)_2$(*p*-CH_3-Ø-SO_3), was first synthesized in polycrystalline form by use of (hydroxytosyloxyiodo)-benzene as a chemical oxidant.[155] Little information about its properties were given until Chasseau et al.[35] obtained the salt by traditional electrochemical means and reported its crystal structure. The ET donor molecule packing is of the type referred to variously as α′ and τ,[141] i.e., it contains stacks of coplanar ET molecules that are twisted with respect to each other around the normal to the molecular plane. A slight dimerization is observed along the stacks. The tosylate anion appears to be disordered with overlapping positions of the sulfonate and the methyl substituents. As is common to the ET salts of most aromatic sulfonate anions described here, the plane of the aromatic rings lies approximately within the anion plane. The conductivity measurements indicate that $(ET)_2$(*p*-CH_3-Ø-SO_3) is a semiconductor with an activation energy of 0.13 eV between 150 and 300 K. The spin susceptibility is reminiscent of other α′-salts where the static susceptibility followed the 1D Heisenberg antiferromagnetic model.

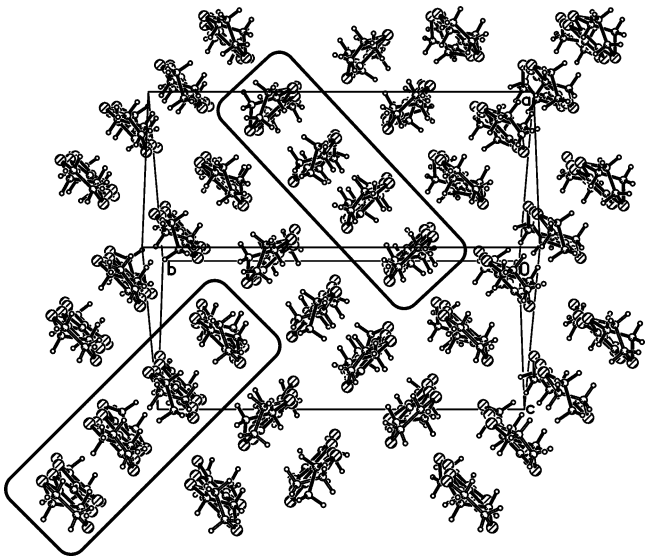

Figure 5. κ(4 × 4)-packing of the ET molecules in $(ET)_2$(benzylsulfonate)(H_2O). Two of the tetrameric units characteristic of this packing type are outlined by black ovals.

We recently reported several new ET salts with aromatic sulfonate anions.[40] The crystal structure of $(ET)_2[(C_6F_5)SO_3]$(1,1,2-trichloroethane) contains stacks of ET molecules that are twisted with respect to each other. Four ET molecules are present per repeat distance along the stack, two of which are located on inversion centers. Significant intermolecular interactions are primarily in the transverse direction. The plane of the anion phenyl group is perpendicular to the anion plane but also approximately perpendicular to the ET molecular planes. This arrangement leads to the maximal number of C−F···H interactions. The salt is a semiconductor with an activation energy of 0.22 eV.

Two phases were found in the system ET:benzylsulfonate. The published salt[40] has the composition $(ET)_2[(C_6H_5)CH_2SO_3](H_2O)$. Its crystal structure (shown in Figure 5) contains ET tetramers that are rotated by ca. 90° with respect to each other, in analogy to the well-known κ-phases, which contain rotated dimers.[78] This so-called κ(4 × 4) packing was first seen in $(BETS)_2ClO_4$(1,1,2-trichloroethane)$_{0.5}$,[156] but the present salt is the first example of an ET compound with this packing motif. The anion layer is composed of hydrogen-bonded $(BzSO_3)(H_2O)_2(O_3SR)$ dimers that are tilted in the *bc*-plane in the same orthogonal fashion as the ET tetramers. According to preliminary results, $(ET)_2[(C_6H_5)CH_2SO_3](H_2O)$ is metallic above 200 K, where a metal-to-insulator transition occurs. We also found a second phase of the same composition.[47] In this second phase the same hydrogen-bonded anion dimers are arranged all in parallel with each other, and the ET molecules follow this structure-directing motif to pack in a β-type.

We also investigated several aromatic disulfonate anions. The 4:1 salt with centrosymmetric 1,5-naphthyldisulfonate[40] belongs to the β″-family of ET salts. Its conductivity between room temperature and 210 K was weakly semiconducting, but below that temperature the salt was metallic to the lowest temperature that it was measured (1.2 K). However, no

superconductivity was found at ambient pressure.[40] Other ET disulfonate salts prepared in our group include the salts with indigo carmine disulfonate and *p*-biphenyldisulfonate, although they have not been published to date.

2.3. Methanides (R_3C^-), Amides (R_2N^-), Extended Polycyano Anions ($C_x(CN)_y^{z-}$)

Carbanions normally are among the strongest Brønsted bases that will abstract protons from a vast number of sources. Thus, they are not very stable under the conditions that are employed to synthesize cation radical salts. Even if they could be synthesized, the salts would decompose under all but the most rigorously controlled environments of physical measurement. However, two factors can stabilize these anions (i.e., reduce the pK_a of the conjugate acid into the single digits): conjugation and electron-withdrawing substituents, such as cyano (−CN) and sulfonyl ($-SO_2R$) (especially when R is perfluoroalkyl) groups. Although secondary amines are considerably more acidic than hydrocarbons, their conjugate bases are still stabilized by the same substituents. Salts of ET as well as other electron-donor molecules with a number of these stabilized anions have been synthesized.

2.3.1. With Cyano Groups

The simplest of the polycyano anions is tricyanomethanide, $C(CN)_3^-$ (tcm, also known as cyanoform), and its 2:1 ET salt was reported by Beno et al.[48] and independently also found by Yamochi et al.[50] The crystal structure was determined at both room temperature and 125 K. Except for a contraction of the unit cell parameters and a reduction of the atomic displacement parameters at the lower temperature, the two structures were reported as being identical, ignoring the observation of extremely weak Bragg reflections with half-integer k-index on long-time photographic exposures at 125 K (doubling of the *b*-axis). The donor molecule layers contain stacks of face-to-face ET dimers that are twisted with respect to each other, according to the δ' packing type.[141] The tcm anion plane is parallel to the conducting (ab) planes, and the anion is placed on the 2-fold rotation axis of the space group. A sharp metal-to-insulator transition around 180 K was observed in the electrical resistivity (along the *a*-axis), ESR spectrum, and bulk magnetic susceptibility.[48] Above the transition, the conductivity is approximately constant and weakly metallic (ca. 1[48] or 6 S cm^{-1},[50] at room temperature), and it drops by 3 orders of magnitude within 5 degrees of 180 K.[48] Similarly, the magnetic susceptibility (both in ESR and in the bulk) exhibits a sharp transition from constant Pauli paramagnetism at the higher temperatures to diamagnetism at low temperature. The ESR signals also become much sharper at the transition (25−27 G above 185 K, 10 G and less, but with vanishing intensity, below 180 K). The band electronic structure calculation[48] revealed the possibility of one-dimensional metallic conduction (along *a*, transverse to the stack direction) with strong warping of the Fermi surface and the presence of a nesting vector $a^* + b^*/2$. It is therefore reasonable to interpret the 180 K transition as a Peierls distortion of the electronically one-dimensional system.

The room-temperature-polarized infrared reflectance spectrum[157] (ab-plane) of $(ET)_2C(CN)_3$ exhibited anisotropic charge-transfer bands at 2000 cm^{-1} ($||b$) and broad transitions 1400 ($||a$) and around 1200 cm^{-1} ($||b$). The 1400 cm^{-1} band was ascribed to the vibronically enhanced ν_{27} (b_{1u}, antisymmetric ring C=C stretching) mode, which is strongly coupled to the electronic system. The anion C≡N stretching mode at 2350 cm^{-1} was observed in both polarizations, and a few additional vibrational features are visible in the $||a$-polarization below 1000 cm^{-1}. The temperature dependence of the vibrational features was determined in the infrared spectrum of polycrystalline $(ET)_2C(CN)_3$ in KBr pellets.[157] The $\nu_{27}(b_{1u})$ mode shows a dramatic change at the 180 K phase transition, shifting from 1410 cm^{-1} just above the transition to 1425 cm^{-1}. In addition, because of its strong vibronic coupling it becomes much sharper and more intense below the transition, in agreement with the pronounced changes in the electronic system, as seen in the other physical properties (see above).[48]

ET salts based on the polycyano-allyl (or -propenide) anion include the pentacyanoallyl[50] and various tetracyanoallyl anions where the central backbone carbon atom contains another substituent such as $C_nH_{2n+1}O-$ ($n = 1-4$),[49,158] $C_nH_{2n+1}NH-$ ($n = 0, 1$),[55] and CH_3S-.[55] $(ET)_2[C_3(CN)_5](solvent)_{0.5}$ (where solvent is THF, tetrahydrofuran, or TCE, 1,1,2-trichloroethane) was obtained only in polycrystalline form, but the semiconducting electrical resistivity of compressed pellets was remarkably low ($\rho_{298} = 17$ Ω cm, $E_a = 0.11$ eV for the THF solvate; $\rho_{298} = 1.0$ Ω cm, $E_a = 0.01$ eV above 270 K, 0.07 eV below 238 K for the THF solvate).[50]

Yamochi et al.[49] reported the synthesis of ET salts with $C_3H_7O[C(CN)_2]_2^-$ and $C_4H_9O[C(CN)_2]_2^-$, although only the former was described in any detail. $(ET)_2\{C_3H_7O[C(CN)_2]_2\}$ occurs in two triclinic modifications, i.e., needles and plates; only the structure of the needle form was determined fully, but a unit cell was reported for the plate form (its stoichiometry is not known with certainty, but a 2:1 composition may be assumed from the unit cell volume). The ET donor layer of the needle phase is a variation of the β''-packing type with slanted stacks (along $a + c$) of approximately parallel ET molecules. In contrast to other β''-phases, the ET molecules are grouped into tetrameric units that are offset from their neighbors along the stack by a slip along the long molecular axis. The anions are loosely stacked along the *a*-axis. The band electronic structure indicates a complete gap between the occupied and unoccupied states, consistent with the activated behavior of the conductivity ($\sigma_{298} = 3-42$ S cm^{-1}, $E_a = 0.06$ eV; later revised[158] to $\sigma_{298} = 25$ S cm^{-1}, $E_a = 0.09$ eV). The plate modification is also a semiconductor with $\sigma_{298} \approx 0.01$ S cm^{-1} and $E_a \approx 0.12$ eV.[49] A few more salts of general composition $(ET)_2\{C_nH_{2n+1}OC[C(CN)_2]_2\}(solvent)_x$ ($x = 0-1$) were mentioned in a subsequent conference proceedings paper[158] without much detail.

The methoxy derivative occurs in three monoclinic salts, a metallic needle phase without solvent (σ_{298} = 120 S cm^{-1}) with the β''-structure (space group $P2_1/n$, no unit cell parameters given) and two semiconducting solvated platelike α′-phases (space group $P2_1/n$, no unit cell parameters given), one with 1,1,2-trichloroethane and the other with tetrahydrofuran in the structure ($\sigma_{298} \approx 0.001$ S cm^{-1}, $E_a = 0.1$ eV for both). The salt with the ethoxy derivative is also solvated with THF, adopts the α′-packing (space group $P2_1/n$, no unit cell parameters given), and is a semiconductor ($\sigma_{298} \approx 0.0026$ S cm^{-1}, $E_a = 0.18$ eV). (ET)$_2${C$_4$H$_9$OC[C(CN)$_2$]$_2$} adopts the α′-packing in a different space group (*C*2/*c*, no unit cell parameters given) and is a semiconductor with $\sigma_{298} \approx 0.0028$ S cm^{-1}, $E_a = 0.11$ eV. The magnetic susceptibility of the α′-phases was fitted to a quasi-1D Heisenberg antiferromagnetic model with $|J|/k_B \approx 60-80$ K. Single crystals of the solvated methoxy salts were converted to the metallic nonsolvated phase upon heating at 332 K for 24 h. The samples retained their original shapes but were polycrystalline after heat treatment.[158]

The needlelike salts (ET)$_2${CH$_3$SC[C(CN)$_2$]$_2$}, (ET)$_2$-{CH$_3$NHC[C(CN)$_2$]$_2$}, and (ET)$_2${NH$_2$C[C(CN)$_2$]$_2$} were recently reported without much detail.[55] The first two are metallic down to at least 2.5 K with a T^2 dependence of the resistivity (at room temperature, 0.010 and 0.013 Ω cm, respectively). The amino derivative is a semiconductor ($\rho_{298} \approx 1.1 \times 10^3$ Ω cm) with a magnetic susceptibility indicative of a Mott insulator with antiferromagnetic interactions (fit to a 1D Heisenberg model with $|J|/k_B \approx 65$ K). The crystal structures of these salts were reported to be under investigation.[55]

Only one polycyano anion with a four-carbon backbone has been reported to form a salt with ET, i.e., the branched dianion C[C(CN)$_2$]$_3^{2-}$ (hexacyanotrimethylene methanediide, HCTMM^{2-}). Two modifications that are not distinguishable by sight were obtained by electrocrystallization from benzonitrile: a monoclinic 2:1 salt without solvent and a triclinic 4:1 salt with cocrystallized benzonitrile.[50] The structure of the former contains ET molecule layers that are composed of twisted dimers with short S···S contacts within the dimer as well as in the direction perpendicular to the stack. The HCTMM^{2-} anions are disordered across an inversion center, and there are some short N···S contacts between the anions and the outer sulfur atoms of the ET molecules. The electrical resistivity of this salt is semiconducting but very anisotropic, i.e., $\rho_{298} \approx 59$ Ω cm, $E_a = 0.19$ eV along the *c*-axis (stacking direction) and $\rho_{298} \approx 3.1 \times 10^4$ Ω cm, $E_a = 0.10$ eV along the *a**-direction. Thus, the short contacts between the anion and cation layers do not facilitate electrical transport significantly. No structure was reported for (ET)$_4${C[C-(CN)$_2$]$_3$}(C$_6$H$_5$CN). It is also a semiconductor but with a smaller room-temperature resistivity of 2.6 Ω cm (along an unspecified direction), probably due to the nominally partial charge on the ET molecule in this salt.

The ET salt of the pentacyanocyclopentadienide, (ET)$_2$[C$_5$(CN)$_5$](TCE)$_x$ (TCE = 1,1,2-trichloroethane), was reported by Watson et al.[51] Its crystal structure contains ET layers with a δ'-type packing,[141] i.e., stacks of face-to-face dimers that are twisted with each other along the *b*-axis and major S···S interactions transverse to the stacking direction. The mixed anion/solvent layer contains "pancake" stacks of C$_5$(CN)$_5^-$ anions along the 2_1 screw axis of the *a*-direction interspersed with channels of disordered 1,1,2-trichloroethane solvent molecules along the same direction. The structure of a solvate with tetrahydrofuran (THF) is assumed to be isostructural based on geometrical X-ray data. Both TCE and THF solvate are semiconductors with an activation energy of ∼0.12 eV and room-temperature conductivities along the needle (*a*) axis of 0.32 and 0.45 S cm^{-1}, respectively. ESR spectra with the magnetic field along the *c*-axis were recorded as a function of temperature. The line width was approximately constant (∼18−20 G) from room temperature to 90 K, below which it increased rapidly to become too broad to be measured below 30 K. The relative spin susceptibility exhibited a broad maximum with a flat top between 200 and 100 K and slowly falling values below 90 K. Antiferromagnetic interactions in a Mott insulator are implied.[51]

Several isomers of octacyano-hexadienediide anion are possible, but only two, the *cis*- and *trans*-isomers of 2-dicyanomethylene-1,1,3,4,5,5-hexacyanopentenediide (DCHP^{2-}), have afforded salts with ET so far.[52] Both are of the composition (ET)$_4$[C$_6$(CN)$_8$](THF)$_{\sim 2}$, and both adopt packing types with coplanar ET molecules in the electron-donor layer. In both cases the layers are separated by bulky anion/solvent layers that lead to extremely anisotropic electronic properties. The *cis*-salt, labeled ET1 by Saito et al.,[52] contains stacks of dimers in a fashion intermediate between the β, β', and β'' packing types.[74] The band electronic structure places ET1 at the border between a narrow-gap semiconductor and a semimetal, although the in-plane conductivity at room temperature is rather high, $\sigma_{RT} = 10-100$ S cm^{-1}. Its temperature dependence in some of the samples (others remained semiconducting in the entire temperature range) is weakly metallic to about 180 K, below which the resistivity increases rapidly. The transition to insulating behavior is accompanied by a gradual decrease and narrowing of the ESR signal. The *trans*-salt, ET2, contains tilted stacks of tetrameric ET units with short intermolecular S···S contacts only along the transverse direction, similar to those seen in (ET)$_2$ClO$_4$(TCE)$_{0.5}$.[159] The band electronic structure[52] exhibits small hole and electron pockets, consistent with the observation of metallic in-plane conduction ($\sigma_{RT} \approx 10-100$ S cm^{-1}, $\sigma_{1.3K} = 5\sigma_{RT}$) in most samples. The ESR signal in ET2 shows a weak decrease with falling temperature above 150 K, below which the decrease becomes much more pronounced. The spin susceptibility shows a gradual decrease to ∼30% of its room-temperature value at 50 K, but below that temperature it increases again, probably due to Curie impurity. The sample-to-sample differences may be attributed to partial loss of solvent, which may create inhomogeneities in the crystals of both types.[52]

The crystal structure of one phase of $(ET)_2[N(CN)_2]$ has been published,[53] but we have unpublished, preliminary evidence of at least two others, i.e., a hydrate $(ET)_2[N(CN)_2](H_2O)$ and a monoclinic phase of unknown stoichiometry.[54] The published phase, apparently obtained as a side product in the attempted synthesis of an ET:Ag:I:$N(CN)_2$ salt, as AgI was present during the electrocrystallization process, contains dimers of parallel ET molecules that are twisted with the neighboring dimers along the stacking direction, i.e., δ'-packing.[53] The hydrate, which has only been found in twinned crystals, contains layers of ET molecules that may be described as a combination of β''- and α-type packing: two adjacent stacks are arranged with ET molecules of one tilting direction, whereas the next two stacks have opposite tilt.[54] The same rare packing type was previously found in $(ET)_2CsHg(SCN)_4$, where it was denoted the α''-packing motif.[160] The other ET:dicyanamide phase, also heavily twinned and weakly diffracting, has only yielded a set of preliminary lattice parameters so far.[54]

$HCAPD^-$ (1,1,2,4,5,5-hexacyano-3-azapentadienide[161]) may be regarded as an extended dicyanamide where the −CN groups are replaced by tricyanoethenyl substituents. Two salts with ET were crystallized, a rod-shaped 1:1 phase and needle-shaped crystals of composition $(ET)_2(HCAPD)(THF)_{0.5}$.[55] Unlike most ET salts, the structure of (ET)(HCAPD) does not exhibit segregated cation and anion layers; rather, it forms side-by-side ribbons of facing $(ET)_2$ dimers that are surrounded by anion stacks. Due to the strong dimerization, the electrons of the $ET^{\bullet+}$ radical cations are paired, and the electrical conductivity is poor ($\rho_{RT} \approx 10^7$ Ω cm, $E_a = 0.5$ eV). The crystal structure of $(ET)_2(HCAPD)(THF)_{0.5}$ has not yet been reported because of poor crystal quality, and its composition was deduced from elemental analysis only. The resistivity ($\rho_{RT} = 1.9$ Ω cm), measured on a bundle of needles, shows three regimes with different activation energies. The transition at 200 K ($E_a = 0.027$ eV above 200 K, $E_a = 0.220$ eV below 200 K) is fairly sharp, but the turnover to a low-temperature activation energy of 0.082 eV happens much more gradually around 140 K. A transition in the form of a decrease of ca. 30% around 200 K is also seen in the ESR spin susceptibility. Below that temperature a broad maximum near 30 K is observed, which may be fit approximately to the 1D Heisenberg antiferromagnetic model with $|J|/k_B \approx 25$ K and the assumption that only ca. 20% of the possible spins participate in the susceptibility.[55]

2.3.2. With SO_2CF_3 Groups

The ET salt of the bis(trifluoromethanesulfon)imide, $N(SO_2CF_3)_2^-$, anion was prepared because this anion possesses features that are similar to those found in other ET superconductors: the NR_2^- group contains the same bent geometry as the dicyanamide anion in κ-$(ET)_2Cu[N(CN)_2]X$ (X = Br, Cl), and CF_3 groups are present in the κ-$(ET)_2M(CF_3)_4$(solvent) (M = Cu, Ag, Au) salts (see below). Crystals of $(ET)_2N(SO_2CF_3)_2$ were grown from TCE or THF solutions containing $Li[N(SO_2CF_3)_2]$ as the electrolyte.[56,57] This salt crystallizes in a layered motif with a β''-type packing: the ET molecules are canted with respect to the stacking axis and form nearly coplanar arrays along the interstack direction. The short (<3.60 Å) S···S contacts occur between the edges of ET molecules in adjacent stacks, forming ribbons along the a-axis. The anions are disordered with the two superimposed orientations related by an inversion center. The room-temperature ESR line width ranges from 27 to 38 G, depending on sample orientation, and decreases with temperature. The relative spin susceptibility decreases with temperature down to 150 K, indicating weak semiconducting behavior ($E_a = 18.7$ meV), but below this temperature becomes nearly constant at 35% of the room temperature value, indicating a weakly metallic low-temperature state. The resistivity measurements, which indicate that this salt is metallic over this entire temperature range, are reconciled by the fact that the cooling rates in the ESR and resistivity measurements are considerably different.

A second phase of $(ET)_2N(SO_2CF_3)_2$ forms when $PPN[N(SO_2CF_3)_2]$ is used as the supporting electrolyte. This phase has a much sharper (7 G) ESR line width and a δ-type packing motif of the ET molecules.[162]

The bis(trifluoromethanesulfonyl)methanide anion, $CH(SO_2CF_3)_2^-$, bears much similarity to its $N(SO_2CF_3)_2^-$ counterpart, and the $(ET)_2CH(SO_2CF_3)_2$ salt is characterized as an ordered superstructure of the $(ET)_2N(SO_2CF_3)_2$ structure. Although the $(ET)_2CH(SO_2CF_3)_2$ salt contains two crystallographically nonequivalent donor layers, the ET molecules in each pack in a β''-motif. The ET molecules in the two layers possess slightly different charges (approximately +0.56 and +0.42), which has been attributed to the orientation of the ordered $CH(SO_2CF_3)_2^-$ anions with respect to the ET layers. The room-temperature ESR line width of this salt is about 10−12 G, which decreases to less than 1 G at low temperature. While the spin susceptibility is nearly constant above 110 K, it decreases rapidly below this temperature, indicating a metal-to-insulator transition. Resistivity measurements confirm this conclusion.

Two ET salts with the tris(trifluoromethanesulfonyl)methide, $C(SO_2CF_3)_3^-$, have been reported.[57] The 2:1 $(ET)_2C(SO_2CF_3)_3$ salt has two nonequivalent donor layers that possess significantly different packing motifs. One layer packs in a dimerized β'-motif, while the other packs in a θ-motif. The room-temperature ESR line width of this salt is about 30 G. A sharp drop in both the line width and the spin susceptibility occurs between 180 and 240 K, indicating the presence of a metal-to-insulator transition. The rapid increase in the resistivity below 240 K confirms this conclusion.

A 1:1 $(ET)C(SO_2CF_3)_3$ salt with isolated dimers of the radical cation has been reported, but no physical characterization is presented. It is expected to be a poor conductor.[57]

2.4. Phenolate Anions

A number of phenols have been studied as components of charge-transfer salts because these mol-

ecules can act as both weak electron acceptors in the formation of charge-transfer complexes and as Brønsted acids in the formation of proton-transfer salts.

Black platelike crystals of α′-$(ET)_2$HCNAL (H_2-CNAL is cyanilic acid, 2,5-dicyano-3,6,dihydroxy-*p*-benzoquinone) were grown by diffusing together solutions containing neutral ET and H_2CNAL.[58] During the crystallization process the acidic oxidant H_2CNAL is deprotonated forming the $HCNAL^-$ monoanion. The crystal structure, which is characterized by stacks of twisted ET dimers, is typical of the α′-packing motif.[141] On the basis of bond-length analyses, the degree of charge transfer from the ET molecules is from +0.49 to +0.52, depending on the method used.[135,163] The optical absorption spectra contain bands resulting from intramolecular ET transitions (10 000−11 000 and 16 000−17 000 cm^{-1}) and an electronic charge-transfer band (5000−6000 cm^{-1}) indicative of highly conductive segregated materials. Although the band electronic structure calculations indicate that this material could be metallic, experimentally, this complex exhibits semiconducting behavior with a room-temperature conductivity between 0.3 and 0.8 S cm^{-1} and an activation energy of 0.15 eV. The magnetic susceptibility, which can be described by a one-dimensional $S = 1/2$ antiferromagnetic Heisenberg chain model with $J/k_B = -52$ K, defines this salt as a Mott insulator. The ESR line width, which is 4 G at room temperature, increases gradually to about 8 G at 100 K and then more rapidly to 17 G at 50 K.

Platelike crystals of $(ET)_4$(TNBP) were grown by electrooxidation of ET in an electrolyte solution containing tetrabutylammonium 3,3′,5,5′-tetranitrobiphenyl-4,4′-diolate (TNBP).[59] The crystal structure of this layered salt is characterized by tetramers of ET which are arranged in a β''_{432}-type motif.[74] This structural motif appears to be stabilized through hydrogen-bonding interactions between the ethylene groups of ET and the oxygen atoms of the anion. An analysis of the bond lengths of the two crystallographically independent ET molecules indicate that they both have a degree of charge transfer of approximately +1/2.[135,163] Solid-state $^{13}C-CP/MAS$ NMR has been used to confirm the dianionic nature of the TNBP anion in this salt, leading to the formalism $(ET^{+0.5})_4(TNBP^{2-})$.[164] Band electronic structure calculations indicate the presence of a wide (0.94 eV) conduction band and a density of states at the Fermi level comparable to salts such as κ-$(ET)_2Cu(NCS)_2$. $(ET)_4$(TNBP) is metallic down to 3 K with a room-temperature conductivity of 50−80 S cm^{-1} within the conducting plane. The optical spectrum contains absorptions at 3000 (electronic transition among partially charged or charge separated ET molecules), 10 000−11 000 (intramolecular $ET^{+\bullet}$ transition), and 17 000 cm^{-1} (HOMO to LUMO transition of $ET^{+\bullet}$) which are consistent with the highly conductive nature of this complex. Absorption bands at 20 000 and 30 000 are ascribable to intramolecular transitions of the anion. The ESR line width, which is 28−34 G at room temperature, decreases to near 10 G at 5 K. The weakly temperature-dependent magnetic susceptibility indicates semimetallic behavior, while the room-temperature value suggests strong electron correlation.

A second phase of ET with the TNBP anion was obtained as a black powder and identified as $(ET)_2$-(HTNBP).[59] This phase was in minority when electrocrystallization occurred in the presence of $[N(C_4H_9)_4]_2$(TNBP) but became the majority phase in the presence of Na_2(TNBP)/18-crown-6. The optical spectra of this salt is quite similar to that of $(ET)_4$-(TNBP), indicating a partial charge-transfer state. A compressed powder sample of $(ET)_2$(HTNBP) has a room-temperature conductivity of 0.2 S cm^{-1} and with decreasing temperature exhibits activated behavior. It is suggested that this material is $(ET^{+0.5})_2(HTNBP^-)$ rather than $(ET^+)_2(HTNBP^{2-})$, although confirmation through solid-state $^{13}C-CP/MAS$ NMR has been ambiguous potentially due to disorder of the anion.[164] The crystal structure of this complex is yet to be determined.

Black platelike crystals of $(ET)_2$(PIC)(THF) (PIC = picrate, $C_6H_2N_3O_7^-$) were grown by electrocrystallization.[61,165] The two-dimensional crystal structure of this complex is characterized by ET radical cations arranged in an α″-type packing motif.[141] This salt is a semiconductor with a room-temperature conductivity of 0.3 S cm^{-1} and an activation energy of 57 meV. The optical spectra contain strong bands at 3000 (electronic transition between partially charged ET molecules) and 10 000 cm^{-1}. The high room-temperature susceptibility (8.7×10^{-4} emu/mol) suggests that this material is a Mott insulator, while the variable-temperature magnetic properties of this salt can be expressed by an alternating chain model with dominating exchange constant, $|J|/k_B = 143$ K, and an alternation parameter, $\alpha = 0.419$, where $\alpha = J'/J$.

Electrooxidation of ET in the presence of $[N(C_2H_5)_4]$-(HTNR) (H_2TNR = trinitroresorcinol or styphnic acid, $C_6H_3N_3O_8$) resulted in the formation of black platelets of the $(ET)_2$(HTNR) salt.[61,165] Similar to $(ET)_2$(PIC)-(THF), the crystal structure of $(ET)_2$(HTNR) possesses an α″-type packing motif.[141] The room-temperature conductivity of this salt is 0.1 S cm^{-1}, and semiconducting behavior is observed with an activation energy of 93 meV. A second phase in which ET crystallizes with the HTNR anion has more recently been reported.[166] The crystal structure of this $(ET)_2$-(HTNR)(H_2TNR) salt incorporates a neutral H_2TNR molecule in the anionic layer. Charge localization within the ET layer is responsible for the observed semiconducting behavior.

2.5. Organometallic Anions

2.5.1. Tetrakis(trifluoromethyl)metallates, $M(CF_3)_4^-$

Four phases of crystals form when ET is crystallized with tetrakis(trifluoromethyl)metallate, $M(CF_3)_4^-$ (M = Cu, Ag, Au), anions. Three of these phases contain cocrystallized trihaloethane solvent molecules, making this a highly tunable class of materials. Although these phases often grow simultaneously in the electrocrystallization cell, they can be identified by their morphology and via ESR spectroscopy. Superconductivity has been observed in the κ_L- and

κ_H-phases. A fairly complete review of these materials has been published.[62]

2.5.1.1. $(ET)_2M(CF_3)_4$ (M = Cu, Ag and Au). The three isostructural $(ET)_2M(CF_3)_4$ (M = Cu, Ag and Au) salts typically crystallize in a rod-type morphology with a layered structural motif, although sometimes a chunky hexagon morphology has been observed. Although the crystal structure of the Ag salt has been published,[63] only the unit cells of the Cu and Au analogues have been reported because of severe twinning.[62] Within the ET layers, the electron-donor molecules pack in a θ-type arrangement with the dihedral angle between molecules on adjacent stacks being approximately 120°. As is the case with most θ-type ET salts with a related packing arrangement,[78] these salts exhibit semiconductive behavior with an activation energy of about 0.2 eV. This phase has a distinct ESR line width in the range of 35−40 G at room temperature. A study of the ESR spectra of $(ET)_2Cu(CF_3)_4$ as a function of temperature indicates the presence of an uncharacterized phase transition below 70 K.[167] The nonsolvated $(ET)_2Cu(CF_3)_4$ phase can be formed by heating the solvated κ-phases above 340 K.[167]

2.5.1.2. κ_L-$(ET)_2M(CF_3)_4$(1,1,2-trihaloethane) Salts. These superconducting salts can typically be identified by their hexagonal plate-type morphology. Fifteen isostructural κ_L-$(ET)_2M(CF_3)_4$(1,1,2-trihaloethane) (M = Cu, Ag and Au) salts have been crystallized through modification of the organometallic anion and cocrystallized solvent molecule. The subscript, L, has been used to designate the lower-T_c phase.

A full crystal structure determination has only been reported for the κ_L-$(ET)_2M(CF_3)_4$(TCE) (M = Cu and Ag, TCE = 1,1,2-trichloroethane)[65] salts with the other κ_L-salts inferred to be isostructural from unit cell determinations. Although these salts crystallize in the same orthorhombic space group, *Pnma*, as κ-$(ET)_2[N(CN)_2]Br$,[168] the interlayer dimension (crystallographic *b*-axis) is about 8 Å longer in the $M(CF_3)_4^-$ salts. The anion layers, which also contain the cocrystallized solvent molecules, are the thickest known (~8.3 Å) for any molecular based superconductor. The crystallographic mirror plane bisects the anion's C−M−C angle rather than pass through one of the molecular mirror planes. For steric reasons, adjacent CF_3 groups cannot be related by mirror symmetry, and thus the anions are crystallographically disordered. Positioned on the same mirror plane, the cocrystallized TCE solvent molecule is also disordered. An isosceles triangle is formed by the chlorine atoms, with one lying on the mirror plane and the other two being related by it. The packing of the ET molecules within the electron-donor layers has a typical κ-type arrangement: the molecules are arranged in face-to-face dimers which are rotated about 90° with respect to a neighboring pair. The ethylene groups are ordered in an eclipsed manner at 120 K.

Superconductivity was first discovered in the κ_L-$(ET)_2M(CF_3)_4$(TCE) salts, which have superconducting transition temperatures of 4.0 (M = Cu),[64] 2.6 (M = Ag),[169] and 2.1 K (M = Au).[66] Subsequently, superconductivity was discovered in 12 additional salts through replacement of the TCE solvent molecule with 1,1,2-tribromoethane, 1-bromo-1,2-dichloroethane, 1,2-dibromo-1-chloroethane, and 2-bromo-1,1-dichloroethane.[62] It is anticipated that additional superconducting salts would be formed through the use of 1,1-dibromo-2-chloroethane, but this solvent is not currently available. Although a large number of similar solvents have been investigated, including fluoro and iodo derivatives, only the 1,1,2-trihaloethane solvents in which the halogen is chlorine or bromine yielded solvated superconducting salts.[170]

The pressure derivative of T_c, dT_c/dp, for κ_L-$(ET)_2Cu(CF_3)_4$(TCE) has been determined to be −2.5 K/kbar,[64] with a similar value obtained for the Ag analogue.[169] These values are typical of other cation−radical superconductors, most notably κ-$(ET)_2Cu(NCS)_2$ (dT_c/dp = −3 K/kbar)[171] and κ-$(ET)_2Cu[N(CN)_2]Br$ (dT_c/dp = −2.4 K/kbar).[172]

Typical of κ-type structures, the room-temperature ESR line width of the κ_L-$(ET)_2M(CF_3)_4$(1,1,2-trihaloethane) salts are between 50 and 70 G,[167,169] and upon rotation around the layer normal, the orientation with the minimum line width corresponds to that of the maximum *g*-value. The temperature dependence of the ESR spectra of the Cu salt shows that the line width first increases to 86 G near 100 K and then decreases to 49 G at 10 K. This behavior is a common feature of κ-type salts and parallels the maximum in resistivity that also occurs between 100 and 150 K.[173]

Electronic structure calculations have been performed for the κ_L-$(ET)_2Cu(CF_3)_4$(TCE) salt.[174] It was shown that the Fermi surface could be described by overlapping circles centered at Γ, and this salt was expected to have two-dimensional metallic properties similar to κ-$(ET)_2Cu[N(CN)_2]X$ (X = Cl and Br).[168,175]

The infrared optical properties of κ_L-$(ET)_2Cu(CF_3)_4$-(TCE) have been reported.[176] These results are very similar to those reported for the higher-T_c κ-$(ET)_2Cu[N(CN)_2]Br$ salt;[177] however, the $Cu(CF_3)_4^-$ salt was found to be less two-dimensional and the effects of crystallographic disorder were visible in its spectra.

The thermodynamic properties of κ_L-$(ET)_2Cu(CF_3)_4$-(TCE) have been investigated.[178] From ac susceptibility measurements the anisotropy ratio of the critical fields, $B_{||}^*/B_{\perp}^* \approx 72$, was found to be very large, indicating that the extremely thick anion layers result in a highly two-dimensional system. The strong frequency dependence of B^* indicates that the pinning centers are extremely weak. Specific heat measurements confirm bulk superconductivity in this salt, with the linear coefficient ($\gamma \approx 50$ mJ/mol K^2) a factor of 9 greater than expected from a free-electron picture.

An initial attempt was made to correlate the structural properties of eight κ_L-$(ET)_2M(CF_3)_4$(1,1,2-trihaloethane) salts with their superconducting transition temperature.[179] From these preliminary results it was suggested that the superconducting transition temperature increased approximately linearly with the ratio of the *b* (interlayer) to *c* (intralayer) unit cell lengths. Thus, higher superconducting transition temperatures would be achieved by expanding the

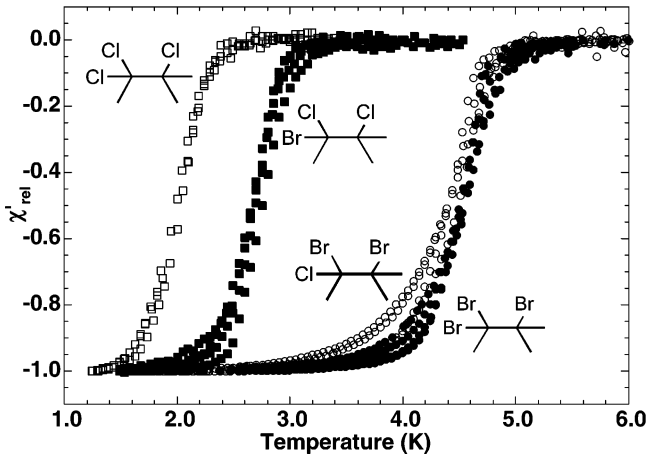

Figure 6. Real part of the volume ac susceptibility χ' (corrected for demagnetization) for four crystals each of κ_L-(BEDT-TTF)$_2$Ag(CF$_3$)$_4$(solvent) (solvent = TCE, 1-bromo-1,2-dichloroethane, 1,2-dibromo-1-chloroethane, and 1,1,2-tribromoethane).

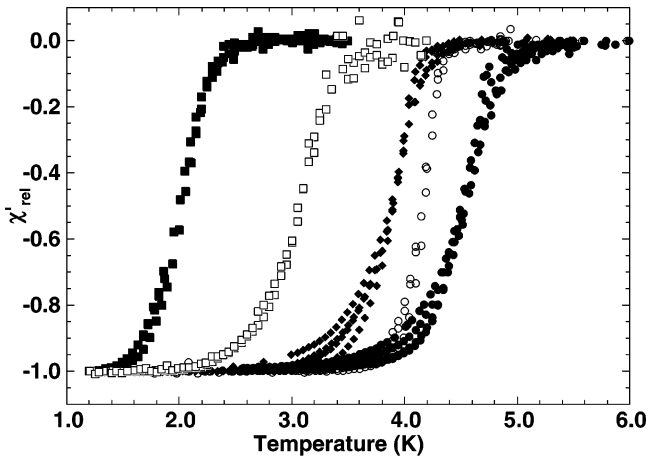

Figure 7. Superconducting transition temperature in κ_L-(BEDT-TTF)$_2$Ag(CF$_3$)$_4$(solvent) salts through the use of mixed solvents. Illustrated are the normalized ac susceptibility data as a function of temperature for several single crystals each grown from the following solvents and mixtures: 100% TCE (■), 75% TCE/25% TBE (□), 50% TCE/50% TBE (◆), 25% TCE/75% TBE (○), and 100% TBE (●).

interlayer dimension. A similar conclusion was obtained through a more quantitative comparison of the six κ_L-(ET)$_2$M(CF$_3$)$_4$(solvent) (M = Cu, Ag, and Au; solvent = 1-bromo-1,2-dichloroethane, 2-bromo-1,1-dichloroethane) salts: these two solvent molecules are nominally the same size, but the location of the bromine atom in the latter tends to force the conducting layers further apart, resulting in an increased T_c.[62] The general trend of increasing T_c in the κ_L-(ET)$_2$Ag(CF$_3$)$_4$(1,1,2-trihaloethane) salts with increasing amounts of bromine (0, 1, 2, and 3) in the cocrystallized solvent molecule is illustrated in Figure 6.[79]

An additional degree of tunability can be achieved in the κ_L-(ET)$_2$M(CF$_3$)$_4$(solvent) salts through the use of mixed solvents.[62] As illustrated in Figure 7, for the case where the solvent is a mixture of TCE and 1,1,2-tribromoethane, the superconducting transition temperature can be tuned in the range of 2.4−4.8 K. The presence of a superconducting state in the presence

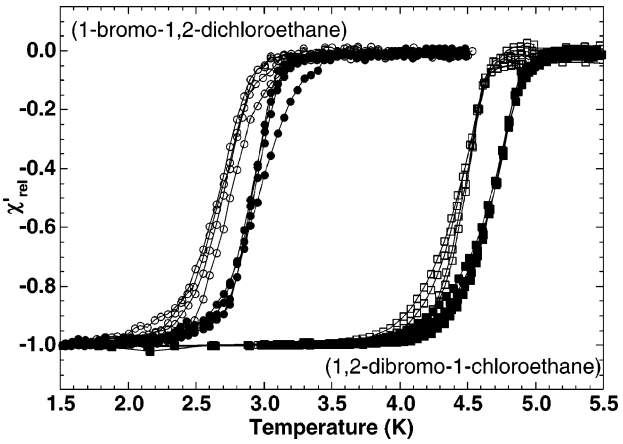

Figure 8. Normalized real part of the ac susceptibility χ' (corrected for demagnetization) for eight crystals of κ_L-(BEDT-TTF)$_2$Ag(CF$_3$)$_4$(solvent), where solvent = 1-bromo-1,2-dichloroethane (circles) and 1,2-dibromo-1-chloroethane (squares), four with isotopes of natural abundance (empty symbols) and four with deuterium labeling (filled symbols) of the eight hydrogen atoms.

of disorder within the anion layer is in contrast to what has been observed in the β-(ET)$_2$X (X = I_3^-, IBr_2^-, and AuI_2^-) system.[180] It is somewhat surprising that relatively sharp superconducting transitions are observed even in the presence of this additional disorder. This has been explained by the fact that there are no short contacts between the hydrogen atoms of the ET molecules and the cocrystallized solvent molecules, thus somewhat shielding the conducting layers from the disorder in the anion layers.

The effect of isotopic substitution on T_c has been reported for the κ_L-(ET)$_2$Ag(CF$_3$)$_4$(1-bromo-1,2-dichloroethane)[110,119] and κ_L-(ET)$_2$Ag(CF$_3$)$_4$(1,1,2-tribromoethane) salts.[181] Upon deuteration of the ethylene groups of ET, the linearly extrapolated superconducting transition temperature increases from 2.90 to 3.11 K ($\Delta T_c = +0.21 \pm 0.06$ K) and from 4.55 to 4.91 K ($\Delta T_c = +0.36 \pm 0.13$ K), respectively. As shown in Figure 8, an intermediate shift in T_c from 4.59 to 4.87 K ($\Delta T_c = +0.28 \pm 0.03$ K) is observed for the κ_L-(ET)$_2$Ag(CF$_3$)$_4$(1,2-dibromo-1-chloroethane) salt.[182] From these results it may appear that ΔT_c increases slightly with T_c for this series of salts. The magnitude of these 'inverse' isotope effects are similar to those observed in the β''-(ET)$_2$SF$_5$CH$_2$CF$_2$SO$_3$ ($\Delta T_c = +0.27 \pm 0.05$ K)[109,110] and κ-(ET)$_2$Cu(SCN)$_2$ ($\Delta T_c = +0.30 \pm 0.07$ K) salts.[116]

All the κ_L-(ET)$_2$M(CF$_3$)$_4$(1,1,2-trihaloethane) salts have been found to gradually lose the cocrystallized solvent under ambient conditions, which results in formation of the corresponding (ET)$_2$M(CF$_3$)$_4$ phase and a decreased superconducting fraction. This irreversible decomposition has been studied most extensively for the κ_L-(ET)$_2$Cu(CF$_3$)$_4$(2-bromo-1,1-dichloroethane) salt, in which the superconducting fraction was found to decrease about 37% after 55 days under ambient conditions.[170] While this solvent loss can be essentially eliminated by storing the crystals at dry ice temperatures, ESR studies have indicated that this process is accelerated at increased temperatures.[167]

2.5.1.3. $\kappa_{L'}$-$(ET)_2Cu(CF_3)_4$(DBCE) (DBCE = 1,2-Dibromo-1-chloroethane). Polymorphism has been reported in the κ_L-$(ET)_2Cu(CF_3)_4$(DBCE) system.[67] During the crystallographic investigation of the orthorhombic κ_L-$(ET)_2M(CF_3)_4$(1,1,2-trihaloethane) system, a few platelike crystals were observed to have slanted edges. A complete structural characterization revealed that this phase belongs to the monoclinic space group *C*2/*c*. The primary difference between the two structures is that adjacent ET layers in the κ_L-phase are tilted in opposite directions, while in the $\kappa_{L'}$-phase these layers are tilted in the same direction.

A single crystal of $\kappa_{L'}$-$(ET)_2Cu(CF_3)_4$(DBCE) has been characterized by ESR spectroscopy.[129] The ESR line widths observed for different crystal orientations (45−58 G) at room temperature are slightly sharper than, but overlap with, those observed for the κ_L-phases. Uncharacteristic of κ-phase ET salts, the orientation with the maximum *g*-value does not correspond to the minimum line width. With decreasing temperature, both the line width and *g*-value decrease monotonically, indicative of a metallic state.

Under the crystallization conditions employed, the $\kappa_{L'}$-phase is quite rare and the physical properties have not been well characterized. Preliminary ac susceptibility measurements indicate that this phase is probably also a superconductor with T_c comparable to the κ_L-phase.[67]

2.5.1.4. κ_H-$(ET)_2M(CF_3)_4$(1,1,2-trihaloethane) Salts. The κ_H-phase salts typically grow as a minority phase and, to date, have been reported for six compositions.[179] The subscript 'H' refers to the higher-T_c phase of a given stoichiometry: the T_c values of the κ_H-phases range from 7.2 to 11.1 K. Superconductivity was first discovered in the κ_H-$(ET)_2M(CF_3)_4$(TCE) salts, which have superconducting transition temperatures of 9.2 (M = Cu),[173] 9.4 and 11.1 (M = Ag),[169] and 10.5 K (M = Au).[66] It was noted that the two superconducting κ_H-phases were observed in the ac susceptibility, rf penetration, and dc magnetization studies of the Ag salt, but these phases could not be physically separated. Subsequently, superconductivity was discovered in three other κ_H-$(ET)_2Ag(CF_3)_4$(1,1,2-trihaloethane) salts.[179] It is anticipated that the κ_H-phase should exist for each of the various compositions which correspond to the κ_L-phase, but many of these have not yet been prepared.

This phase typically grows as poorly diffracting striated black needles, and thus the crystal structure of this phase has not yet been determined. The κ designation has been assigned as a result of preliminary X-ray data (persistent axial lengths of 9 and 13 Å in indexing attempts) as well as similarities of the physical properties (see below). The X-ray diffraction experiments also hint at a possible doubling of the *b*-axis of the unit cell.[170] It was conjectured that this could be a result of the loss of a mirror plane perpendicular to the longest unit cell axis, which could result in an ordered anion layer and thus a higher T_c. An EDAX characterization revealed that the κ_H-phase has the same 2:1:1 (donor:anion:solvent) ratio as the κ_L-phase.

The room-temperature resistivity of κ_H-$(ET)_2Ag(CF_3)_4$(TCE) has been reported to be about 2 orders of magnitude lower than that for the corresponding κ_L-salt.[169] Both salts show a maximum in resistivity near 100 K, with the maximum for the κ_H-phase being slightly lower in temperature than the κ_L-phase. Similar behavior was reported for the Cu analogues.[173] A similar resistivity profile has been observed for the κ-$(ET)_2Cu(NCS)_2$ superconductor.[111,183]

The pressure derivative of T_c of the κ_H-$(ET)_2M(CF_3)_4$(TCE) (M = Cu, Ag, and Au) salts have been determined to be between −2 and −3 K/kbar,[66,169,173] which is typical of κ-phase ET superconductors.[171,172]

The room-temperature ESR line widths of the κ_H-phase salts are 5−7 G,[167,169] considerably sharper than other κ-phase salts of ET. Typical of κ-phase salts, however, an angular-dependent study revealed that the orientation with the minimum line width corresponds to that of the maximum *g*-value. The variable-temperature ESR study of the κ_H-phase was complicated by the presence of small amounts of the nonsolvated $(ET)_2M(CF_3)_4$ phase. The solvent can be irreversibly removed from the κ_H-$(ET)_2M(CF_3)_4$(1,1,2-trihaloethane) salts, resulting in formation of the $(ET)_2M(CF_3)_4$ phase. This process is much more rapid than in the κ_L-salts and can be accelerated by heating.

2.5.2. ET Salts Containing Derivatives of the $M(CF_3)_4^-$ Anion

ET salts containing derivatives of the $M(CF_3)_4^-$ anion have been prepared in a search for new superconductors and in order to better understand the structural features which are important to superconductivity. By replacing one of the trifluoromethyl groups of the $Ag(CF_3)_4^-$ anion with Cl^-, the κ_L-$(ET)_2Ag(CF_3)_3Cl$(1,1,2-trichloroethane) salt was crystallized.[62] Although isomorphous to the κ_L-$(ET)_2Ag(CF_3)_4$(1,1,2-trichloroethane) salt, each of the unit cell lengths is contracted as a result of the smaller $Ag(CF_3)_3Cl^-$ anion. The chlorine atom was found to be disordered over two of the trifluoromethyl sites. This additional disorder suppressed the superconducting transition from 2.4 K to below 1.4 K.

The $(ET)_2Ag(CF_3)_2(CN)_2$ salt is isomorphous to the nonsolvated $(ET)_2Ag(CF_3)_4$ phase described above.[62] The cyano groups in the *trans*-$Ag(CF_3)_2(CN)_2^-$ salt extend further from the metal atom than the trifluoromethyl groups, resulting in a small expansion along the *c*-axis. As expected by analogy with the nonsolvated $(ET)_2M(CF_3)_4$ salts, no indication of superconductivity was observed in this salt.

Attempts to grow ET crystals with the closely related $Cu(CF_2H)_4^-$ anion failed to produce good-quality crystals, perhaps indicating the importance of the F···H interactions in the crystal growth process. The platelike crystals that were grown with ET and $Cu(CF_2CF_3)_4^-$ were not structurally characterized. The observations that they are nonsuperconducting above 1.2 K and have an ESR line width between 38 and 46 G suggest that they are similar in structure to the nonsolvated $(ET)_2M(CF_3)_4$ salts.[62]

2.5.3. Other Organometallic Anions

The $(ET)Au(C_6Cl_5)_4$ salt was formed through a novel electrochemical synthesis and crystallization

Table 2. Crystallographic Data for (Donor)$_n$X$_m$ Salts with Organic and Organometallic Anions for Donor Molecules Other than ET (at room temperature unless indicated otherwise)

compound	space group	a (Å)	b (Å)	c (Å)	α (°)	β (°)	γ (°)	unit cell vol. (Å^3)	Z	ref
κ-(BETS)$_2$C(CN)$_3$	$C2/c$	35.086	8.475	11.583	90	91.10	90	3444	4	187
κ_L-(BETS)$_2$Ag(CF$_3$)$_4$(TCE)[a]	$Pnma$	13.155	39.333	8.648	90	90	90	4474.6	4	62
(BETS)$_2$CF$_3$SO$_3$	$P2_1/c$	34.972	8.332	11.732	90	99.68	90	3370	4	188
(BEDO-TTF)[C(CN)$_3$]$_{0.4}$(H$_2$O)$_{0.3}$	$P\bar{1}$	4.0307	5.342	17.225	93.47	102.85	98.59	335.8	1	189
(BEDO-TTF)$_5${C[C(CN)$_2$]$_3$}(BzN)$_2$[b]	$P\bar{1}$	10.286	10.855	19.224	107.22	91.77	91.76	1047.3	1	189
α″-(BEDO-TTF)$_5${C$_3$[C(CN)$_2$]$_3$}(BzN)$_{0.2}$[b,c]	$P2_1/c$	17.075	4.085	20.462	90	96.46	90	1481	0.8	190
(BEDO-TTF)$_6$(HCDAH)[c,d]	$P2_1/c$	16.820	4.086	20.243	90	99.45	90	1372.4	0.67	191, 192
(BEDO-TTF)$_4$[C(NCN)$_3$](H$_2$O)$_3$	$P\bar{1}$	11.963	14.102	17.083	81.27	70.21	77.04	2633.4	2	193
(BEDO-TTF)$_4${C$_2$H$_5$OC[C(CN)$_2$]$_2$}	$P\bar{1}$	8.093	10.657	20.401	103.85	98.75	98.42	1670.3	2	194
(BEDO-TTF)$_5${NCCH$_2$C[C(CN)$_2$]$_2$}$_2$(BzN)$_2$[b]	$P\bar{1}$	7.262	14.972	19.732	79.88	82.84	87.38	2094.9	1	194
(BEDO-TTF)$_4$[C$_6$(CN)$_8$](THF)$_2$[e]	$P2_1/n$	23.105	12.001	30.707	90	102.13	90	8324	4	194
(BEDO-TTF)$_2$(C$_4$O$_4$)$_{0.5}$(H$_2$O)$_3$	$P\bar{1}$	4.097	10.752	16.517	79.74	87.35	82.01	708.9	1	189
(BEDO-TTF)TNBP[f]	$C2/c$	15.220	11.118	16.426	90	109.96	90	2613	4	189
κ-(BEDO-TTF)$_2$CF$_3$SO$_3$	$Pnma$	7.955	34.396	10.427	90	90	90	2853.0	4	195
(BEDO-TTF)$_2$CF$_3$SO$_3$(C$_4$H$_8$O)$_{0.5}$	$C2/c$	23.885	7.195	35.235	90	101.45	90	5934	8	195
(TMTSF)$_2$CF$_3$SO$_3$	$P\bar{1}$	7.333	7.781	13.799	83.26	85.72	71.18	739.5	1	196
(TMTTF)$_2$(C$_6$H$_2$N$_3$O$_8$)	$P2_1/n$	12.634	14.343	18.550	90	105.95	90	3232	4	61
(TMTTF)$_2$(HCNAL)[g]	$C2/m$	21.691	9.675	7.547	90	103.86	90	1537.5	2	197, 198
(TMTTF)$_2$CF$_3$SO$_3$	$P\bar{1}$	8.598	12.995	13.081	75.36	87.35	82.30	1401.2	2	199
(TTF)(4-oxo-tetramethylpiperidinsulfate)	$P\bar{1}$	7.948	10.884	12.132	79.52	77.22	73.98	975.5	2	200
(TTF)(CF$_3$SO$_3$)(H$_2$O)$_{0.5}$	$P2_1/c$	21.530	7.954	15.846	90	107.21	90	2592	8	199
(TTF)$_2$[TTF(CO$_2$H)$_2$(CO$_2$)$_2$]	$P\bar{1}$	8.143	8.203	10.519	85.04	82.87	84.00	691.5	1	201
(TTF)$_2$[C$_6$(CN)$_8$](CH$_3$CN)	$P\bar{1}$	8.319	8.917	21.891	91.74	91.64	101.13	1592	2	202
(TTF)$_2$(HCDAH)(CH$_3$CN)[d]	$P\bar{1}$	8.258	9.572	10.070	89.89	70.76	80.76	740.7	2	191
(TTF)(CA)$_{0.5}$(H$_4$CA)$_{0.5}$[h]	$C2/m$	13.279	13.589	9.249	90	118.69	90	1464.0	4	203
(TTF)$_3$[C$_5$(COOCH$_3$)$_5$]$_2$	Cc	16.017	14.307	25.091	90	92.11	90	5746	4	204
(OMTTF)$_3$(HCNAL)$_2$[g]	$C2/m$	15.566	13.946	13.527	90	102.813	90	2863.4	2	205
(TTFPh$_2$)$_2$[Au(C$_6$F$_5$)$_2$]	$P\bar{1}$	7.481	10.111	15.639	77.00	80.16	73.18	1096.2[i]	1	206
[Pd(dddt)$_2$]$_2$CF$_3$SO$_3$	$P\bar{1}$	6.521	8.354	16.113	87.12	85.51	67.94	811	1	207
(TTM-TTP)[C(CN)$_3$]	$C2/c$	23.94	5.881	21.00	90	118.7	90	2529	4	208
(DIDTPY)[C$_3$(CN)$_5$](THF)[e]	$P2_1/c$	13.545	7.868	23.791	90	103.44	90	2465.8	4	209
(TTT){CH$_3$OC[C(CN)$_2$]$_2$}	$P2_1/n$	12.351	23.632	7.603	90	101.48	90	2174.9	4	49
(TTT){C$_2$H$_5$OC[C(CN)$_2$]$_2$}(THF)$_{0.25}$[e]	$P\bar{1}$	7.573	14.909	23.061	74.42	88.64	83.51	2491.3	4	210
(TTT){C$_2$H$_5$OC[C(CN)$_2$]$_2$}$_2$	$P\bar{1}$	7.814	8.649	14.448	105.06	91.61	116.51	823.0	1	210
(TTT){C$_3$H$_7$OC[C(CN)$_2$]$_2$}(THF)$_{0.5}$[e]	$P\bar{1}$	11.166	11.969	12.060	59.91	73.67	84.16	1336.8	2	210
(TTT){C$_3$H$_7$OC[C(CN)$_2$]$_2$}$_2$	$P\bar{1}$	7.915	8.736	14.680	74.50	75.25	64.59	872.0	1	210
(TTT)$_3${C$_3$H$_7$OC[C(CN)$_2$]$_2$}$_2$	$P\bar{1}$	10.357	12.243	14.085	74.74	69.26	73.11	1573	1	210
(TTT){C$_4$H$_9$OC[C(CN)$_2$]$_2$}	$C2/c$	20.971	21.949	14.078	90	128.7	90	5057	8	210

[a] TCE = 1,1,2-Trichloroethane. [b] BzN = Benzonitrile. [c] Donor molecule subcell. [d] HCDAH = Hexacyanodiazahexadienediide. [e] THF = Tetrahydrofuran. [f] TNBP = 3,3′,5,5′-Tetranitrobiphenyl-4,4′-diol(ate). [g] HCNAL, CNAL = Mono- and dideprotonated anion of H$_2$CNAL (2,5-dicyano-3,6-dihydroxy-1,4-benzoquinone = cyananilic acid). [h] CA = Dideprotonated anion of H$_2$CA (2,5-dichloro-3,6-dihydroxy-1,4-benzoquinone = chloranilic acid) and H$_4$CA = dihydrochloranilic acid (reduced form of H$_2$CA). [i] Unit cell at 178 K.

procedure.[68] The Au(C$_6$Cl$_5$)$_4^-$ anion had not previously been prepared, yet when ET was electrochemically oxidized in an electrolyte solution of [N(C$_4$H$_9$)$_4$][Au(C$_6$Cl$_5$)$_2$], the Au(C$_6$Cl$_5$)$_4^-$ anion formed and crystallized as a 1:1 salt with ET. In this salt the ET$^+$ cations are completely surrounded by the pentachlorophenyl rings of the anions, providing a unique opportunity to study a highly isolated ET monocation in the solid state. The ν_2 and ν_3 modes of ET$^+$ in the Raman spectrum of (ET)Au(C$_6$Cl$_5$)$_4$ were observed at 1455 and 1425 cm^{-1}, respectively, in perfect agreement with the +1 oxidation state. The peak-to-peak ESR line width, which is between 2.8 and 3.5 G at room temperature (depending on sample orientation), is even narrow in comparison to other ET^{+1} salts such as (ET)(Re$_6$Se$_5$Cl$_9$)[(CH$_3$)$_2$NCOH]$_2$ (3.7−4.3 G),[184] (ET)Cu[N(CN)$_2$]$_2$ (8−10 G),[185] and (ET)Ag$_4$(CN)$_5$ (12−14 G).[186] This extremely sharp line width is consistent with highly isolated spins within the lattice. Similar attempts to crystallize the (ET)Au(C$_6$F$_5$)$_4$ salt were unsuccessful.

3. Salts of Other Electron-Donor Radical Cations

This section is grouped by electron-donor molecule, approximately in decreasing order of number of salts reported. We start with the homologues of ET, followed by the TMTXF (X = S, Se) molecules, TTF, the remaining TTF derivatives, and finally some miscellaneous other donor molecules. Basic crystallographic data are given in Table 2. In some cases the unit cell parameters were transformed from those in the literature in order to facilitate comparisons or to present them in a standard setting.

3.1. BETS, Bis(ethylenedithio)tetraselenafulvalene

The BETS electron-donor molecule is a derivative of ET in which the inner sulfur atoms have been replaced with selenium. The larger atomic orbitals of the selenium atoms in the BETS salts lead to more isotropic electronic structures and more stable molecular metals than their ET counterparts. The charge-transfer salts of BETS exhibit a wide variety of interesting physical properties, including a molec-

ular antiferromagnetic metal, a conductor with an antiferromagnetic metal state at ambient pressure, and an antiferromagnetic superconductor. Unprecedented superconductor-to-insulator and superconductor-to-metal transitions have also been observed.[211] Although the most interesting materials in this family are those with the general composition $(BETS)_2Fe_xGa_{1-x}Cl_{4-y}Br_y$, a few examples of BETS salts with organic anions have been reported.

3.1.1. Polycyano Anions

The tricyanomethanide [also known as cyanoform, $C(CN)_3^-$] anion has been crystallized with BETS to form the κ-$(BETS)_2C(CN)_3$ salt.[212,213] The electron-donor layer of this salt, unlike the ET derivative,[48] is characterized by dimers of BETS arranged in an approximately orthogonal manner. While this κ-type packing motif has led to many superconductors in the ET family, this salt is metallic ($\rho_{RT} \approx 50$ Ω cm) to 1.3 K without a transition to a superconducting state. At room temperature disorder is found in both the $[C(CN)_3]^-$ anions and the ethylene groups of BETS. A first-order phase transition has been observed at 260 K, which is a result of an approximately 20° rotation of the $[C(CN)_3]^-$ anions.[187] The anions are still disordered at 50 K, but at this temperature the ethylene groups order in a staggered fashion. This anion disorder has been suggested as a possible reason for the lack of superconductivity.

Electronic band structure calculations predict a Fermi surface very similar to that observed in the superconducting κ-$(MDT\text{-}TTF)_2AuI_2$ (MDT-TTF = methylenedithiotetrathiafulvalene) and κ-$(ET)_2X$ salts[214,215] consisting of a series of superposing ellipses. The first-order phase transition, which mostly affects the anion layer, has minimal effects on the Fermi surface.[187] Shubnikov-de Haas and de Haas-van Alphen oscillations have been observed in κ-$(BETS)_2C(CN)_3$ in magnetic fields up to 25 T and under pressures to 9 kbar.[187,216,217] For the field perpendicular to the highly conducting planes, the Fourier spectrum of these oscillations exhibit four prominent peaks at $F_\gamma = 230$ T, $F_\alpha = 950$ T, $F_\beta - F_\alpha \approx 3400$ T, and $F_\beta = 4380$ T, where the classical orbit on the cylinder is α and the magnetic breakdown orbit is β. The corresponding cyclotron masses are $m_\alpha = 1.7m_0$, $m_{\beta-\alpha} = 1.5m_0$, and $m_\beta = 3.3m_0$, which are smaller than those values typical of ET salts because of the lower density of states at the Fermi level.[218] At tilted fields, an additional low frequency, F_λ, has been observed.[187] The origin of the low-frequency orbits F_γ and F_λ is still controversial.[187,213] No sharp transformations have been observed under pressure with only gradual changes in the main oscillations and a diminishing of the combination frequencies.[187]

3.1.2. $M(CF_3)_4^-$ Anions

Crystals of κ_L-$(BETS)_2Ag(CF_3)_4(TCE)$ have been found to be isomorphous to the ET analogue.[62] The replacement of the inner sulfur atoms of ET by selenium results in a volume increase of about 3.5%, mostly due to the 3% expansion of the interlayer dimension. No superconductivity has been observed in the BETS salt to temperatures as low as 1.2 K. This has been attributed to either the disorder in one of the ethylene groups or a broadening of the electronic bandwidth and concomitant decrease in the density of states at the Fermi level in the selenium salt. The broad ESR line width has rendered this technique inapplicable for phase identification of various phases in the $BETS/M(CF_3)_4$ system. To date, only the M = Ag system has been explored.

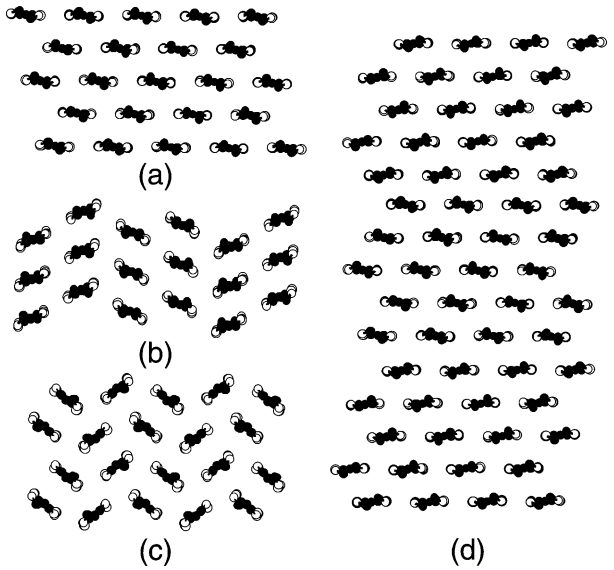

Figure 9. Four donor packing motifs found in BEDO-TTF salts with organic anions: (a) β''- or $(BEDO\text{-}TTF)_{2.4}I_3$-type as observed, e.g., in $(BEDO\text{-}TTF)_4(C_4N_6)(H_2O)_3$;[193] (b) α″-type as observed in $(BEDO\text{-}TTF)_5(HCP)(PhCN)_{0.2}$;[189] (c) κ-type as observed in $(BEDO\text{-}TTF)_2CF_3SO_3$.[195] (d) The BEDO-TTF molecules in the $(BEDO\text{-}TTF)_5(DHCP)(THF)$ structure pack in a modified β''-type structure in which the stacking direction reverses every fifth molecule.[194]

3.1.3. Sulfonate Anions

Only one BETS salt with a sulfonate anion has been reported. The κ-$(BETS)_2CF_3SO_3$ salt has two different types of cation layers, but no further structural details have been described.[188] The room-temperature resistivity is 0.06 S cm^{-1}, and a metal-to-insulator transition occurs near 80 K. The band electronic structure is similar to κ-phase ET salts[215] and consists of overlapping ovals centered at Γ, suggesting two-dimensional metallic character at room temperature.

3.2. BEDO−TTF, Bis(ethylenedioxo)tetrathiafulvalene

Next to ET, the BEDO-TTF electron-donor molecule has been used most extensively for the formation of cation radical salts with organic anions. These salts also form layered structures, which seem to be templated by intermolecular C−H···O (in addition to S···S) interactions. BEDO-TTF salts prefer to pack in what has been termed the 'I$_3$ type' motif (after the $(BEDO\text{-}TTF)_{2.4}I_3$ structure,[219] see Figure 9), which is often preferred because of intermolecular C−H···O contacts. This packing type results in 2D band electronic structures which are often metallic to low temperature. There is less structural diversity in this

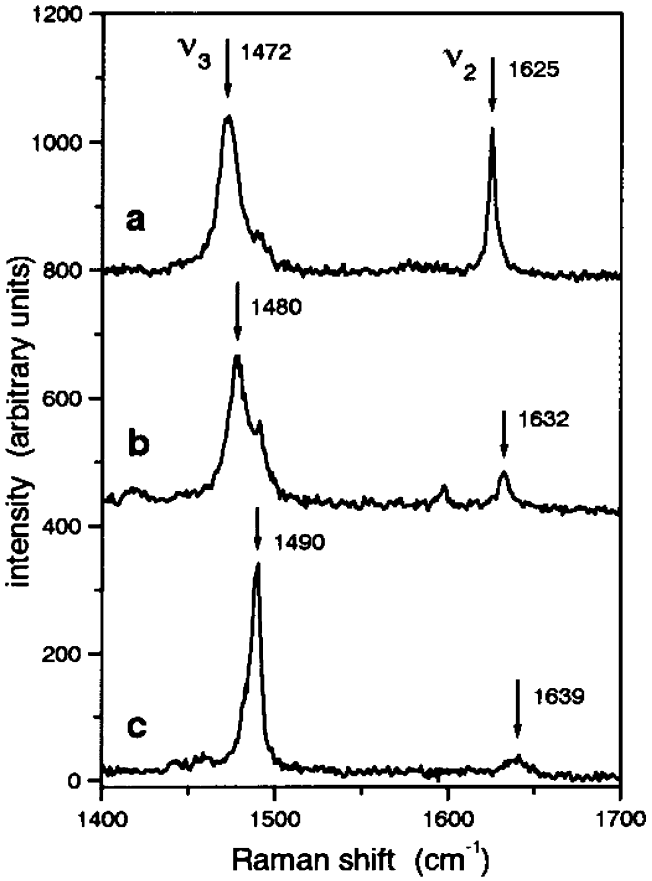

Figure 10. The ν_3 and ν_2 bands of the BEDO-TTF molecule are sensitive to the degree of charge transfer. Illustrated are the Raman spectra of (a) $(BEDO\text{-}TTF)_2Cl(H_2O)_3$ ($\rho = 0.5$), (b) $(BEDO\text{-}TTF)_5(HCTMM)(Ph\text{-}CN)_2$ ($\rho = 0.4$), and (c) $(BEDO\text{-}TTF)_2(HCDAH)$ ($\rho = 0.33$). (Reprinted with permission from ref 221. Copyright 2000 American Chemical Society.)

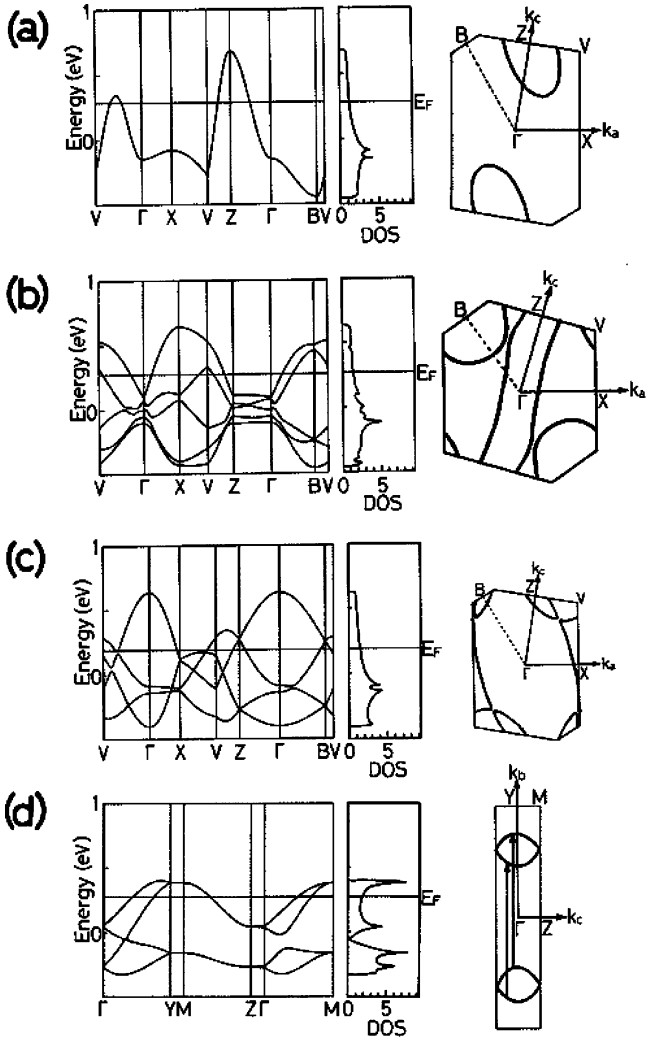

Figure 11. Calculated band electronic structures, density of states [given in states (total)/(eV molecule of BEDO-TTF)], and corresponding Fermi surfaces of (a) $(BEDO\text{-}TTF)_{10}[C(CN)_3]_4(H_2O)_3$, (b) $(BEDO\text{-}TTF)_5(HCTMM)(PhCN)_2$, (c) $(BEDO\text{-}TTF)_4(C_4O_4)(H_2O)_6$, and (d) $(BEDO\text{-}TTF)_5(HCP)(PhCN)_{0.2}$. The nesting vector is represented by the arrows in d. (Reprinted with permission from ref 189. Copyright 1996 American Chemical Society.)

family of salts (as compared to the ET family), and while four packing motifs of the BEDO-TTF molecule have been reported with organic anions, three of them are closely related. Because the packing is dominated by the BEDO-TTF layer, the anion layers in these salts are often disordered, resulting in ambiguous conclusions about the stoichiometry and donor−anion interactions. BEDO-TTF salts can be classified into three groups based on the type of anion: (1) polycyano-based, (2) oxo-based, and (3) amphiphilic. The amphiphilic anions are discussed in the thin-film section (section 5).

3.2.1. Polycyano Anions

Black platelike crystals of $(BEDO\text{-}TTF)_5(HCTMM)(PhCN)_2$ (HCTMM = hexacyanotrimethylenemethanediide, $C[C(CN)_2]_3^{2-}$) have been prepared by electrocrystallization in benzonitrile (PhCN).[189,190,220] The X-ray crystal structure reveals that the BEDO-TTF molecules, which are packed in layers parallel to the *ac*-plane, form nearly uniform stacks along the $a + 2c$ direction in which the molecular planes are canted about 30° with respect to the stacking axis. This donor packing motif is similar to that observed in $(BEDO\text{-}TTF)_{2.4}I_3$,[219] see Figure 9a. The positions of the anion and cocrystallized solvent molecules could not be determined due to severe disorder within the anion layer; thus, the stoichiometry was determined from the crystal density and elemental analysis. The charge on the BEDO-TTF electron-donor molecule has been assigned as +0.40, based on the stoichiometry, anion charge, and Raman spectroscopy (see Figure 10).[221,222] This salt exhibits metallic behavior, which is isotropic within the conducting plane, down to the lowest temperature measured (5 K). As shown in Figure 11b, the band electronic structure, which consists of closed pockets centered around *B* and open surfaces along the c^* direction, supports the 2D nature of this material. The spin susceptibility of this salt, as derived from ESR spectroscopy, drops gradually with cooling; however, about one-third of the spins remain at temperatures as low as 4.2 K.[190]

When the HCTMM anion is crystallized with BEDO-TTF in TCE (TCE = 1,1,2-trichloroethane), black needles of the $(BEDO\text{-}TTF)_4(HCTMM)(TCE)_2$ salt form.[189,220] The crystal structure of this derivative has not been reported, and the stoichiometry, which is slightly different than the PhCN solvate, has been

determined solely by elemental analysis. Because the charge of the anion remains −2, this change in stoichiometry results in a change in the charge on BEDO-TTF from +0.4 to +0.5. Similar to other highly conducting BEDO-TTF salts, the powder electronic spectrum of $(BEDO\text{-}TTF)_4(HCTMM)(TCE)_2$ shows a band around 2.3×10^3 cm^{-1}, which arises from an intermolecular charge-transfer transition. In contrast to the PhCN derivative, the TCE derivative exhibits a metal-to-insulator transition at 235 K.

A crude crystal structure has been reported for black needles of the tricyanomethanide salt, $(BEDO\text{-}TTF)_{10}[C(CN)_3]_4(H_2O)_3$, in which the positions of the anions and cocrystallized solvent molecules could not be ascertained.[189] However, the BEDO-TTF molecules were found to pack in the common $(BEDO\text{-}TTF)_{2.4}I_3$ motif,[219] with the molecular planes tilted 60.6° with respect to the stacking axis and the intermolecular separation along the stack being 3.51 Å. The stoichiometry of these crystals was determined by density measurements, elemental analysis, and Raman spectroscopy, from which the charge on the BEDO-TTF molecules was determined to be +0.4.[221,222] It was suggested that the anions were randomly disordered in layers between the BEDO-TTF molecules. Conductivity measurements on single crystals showed metallic behavior down to 1.3 K. As shown in Figure 11a, the Fermi surface is elliptical and elongated approximately along the stacking direction.[189]

In an analogous manner, black needlelike crystals of $(BEDO\text{-}TTF)_5(HCP)(PhCN)_{0.2}$ (HCP = tri(dicyanomethylene)cyclopropanediide, $C_3[C(CN)_2]_3^{2-}$) were prepared,[189,190] the stoichiometry of which was determined by a combination of elemental analysis, experimental density, and X-ray characterization. Superlattice reflections indicate that a (a, $5b$, c) supercell is present, but the superstructure could not be solved; thus, an averaged partial structure was reported. One crystallographically independent electron-donor molecule was present per small unit cell. Each donor layer has a repetition of AA′BB′ stacks in which the molecular planes within the A (or B) and A′ (or B′) stacks are parallel to each other while the molecular planes within A (or A′) and B (or B′) stacks are canted about 60° with respect to each other, leading to a corrugated herringbone-type network, see Figure 9b. This packing motif has been designated α″ in the ET salts and is illustrated in the α″-$(ET)_2CsHg(SCN)_4$ structure.[160] This packing of the electron-donor molecules is unique among BEDO-TTF salts. Considerable ambiguity is present in the anion layer: the position of the HCP^{2-} anion is uncertain, and the location of the cocrystallized solvent molecule has not been identified. To balance the HCP^{2-} anion, the calculated charge on the BEDO-TTF molecules is +0.4. This degree of charge transfer has been confirmed by Raman spectroscopy.[221,222] Band electronic structure calculations (Figure 11d) indicate that the four HOMO bands are much more dispersive along b^* than c^*. Nesting of the Fermi surfaces has been used to explain the single-crystal conductivity measurements which indicated that this salt is a semiconductor with an activation energy of 0.05−0.10 eV depending on the direction within the conducting plane.

More recently, a BEDO-TTF salt of $HCDAH^{2-}$ (HCDAH = hexacyanodiazahexadiene, $N_2[C_2(CN)_3]_2^{2-}$) has been shown to crystallize as black prisms with the same donor molecule packing type as the HCP^{2-} salt (see above) and an approximate stoichiometry of $(BEDO\text{-}TTF)_6(HCDAH)$.[191,192] The room-temperature resistivity is in the range 0.06−9.6 Ω cm. The stoichiometry of this salt has been confirmed by Raman spectroscopy (see Figure 10), which has shown that the degree of charge transfer is 1/3.[221,222]

The stoichiometry of the brownish-green powder obtained when BEDO-TTF is oxidized electrochemically in the presence of tetrabutylammonium 1,1,2,3,3-pentacyanopropenide has been determined by elemental analysis to be $(BEDO\text{-}TTF)_8[C_3(CN)_5]_4(H_2O)$.[189] No X-ray structural characterization of the salt has been reported. Assuming a charge of −1 on the anion, the BEDO-TTF electron-donor molecules are assigned a charge of +0.5. Conductivity measurements on a compressed pellet indicate that this salt is metallic down to 16 K, at which point a transition to an insulating state occurs.

Black, elongated plates of $(BEDO\text{-}TTF)_4(C_4N_6)(H_2O)_3$ ($C_4N_6^{2-}$ = *N*,*N*′,*N*″-tricyanoguanidinate) have been found to contain layers of crystallographically equivalent $BEDO\text{-}TTF^{+0.5}$ cations[193] which pack in the common $(BEDO\text{-}TTF)_{2.4}I_3$ motif,[219] see Figure 9a. This complex has a room-temperature conductivity of 11.5 S cm^{-1} and exhibits metallic behavior down to 8 K, where a metal to insulator transition occurs. The ESR line width decreases nearly linearly from 52.2 G at room temperature to 7.8 G at 4 K, while the spin susceptibility is nearly constant down to 50 K, consistent with the Pauli paramagnetism expected for a metallic sample.

Four BEDO-TTF salts with alkoxy tetracyanoallyl *R*O-TCA^- (TCA = tetracyanoallyl, *R* = Me (−CH_3), Et (−CH_2CH_3), *n*-Pr (−$CH_2CH_2CH_3$) and *n*-Bu (−$CH_2CH_2CH_2CH_3$) anions have been reported.[194] As determined by elemental analysis, the stoichiometry of these salts varies: $(BEDO\text{-}TTF)_9(MeO\text{-}TCA)_4(H_2O)_5$, $(BEDO\text{-}TTF)_2(EtO\text{-}TCA)$, $(BEDO\text{-}TTF)_2(n\text{-}PrO\text{-}TCA)$, and $(BEDO\text{-}TTF)_5(MeO\text{-}TCA)_2(THF)_{0.5}$. It is noted that a preliminary report indicated that the stoichiometry of the EtO-TCA^- salt was $(BEDO\text{-}TTF)_2(EtO\text{-}TCA)(H_2O)_{0.75}$,[49] but it appears that further analysis has led to the conclusion that this salt is not solvated. On the basis of stoichiometry, the average formal charge on the BEDO-TTF electron-donor molecules range from +0.4 to +0.5. The room-temperature conductivity of these salts range from 7 to 100 S cm^{-1} with metallic behavior observed for all but the *n*-PrO-TCA salt. The conductivity measurements for the *n*-PrO-TCA and BuO-TCA salts were measured on compressed pellets where grain boundaries can significantly affect the measured resistance, and it is thus possible the *n*-PrO-TCA salt could show metallic behavior if measured on a single crystal. The EtO-TCA salt has a metal-to-insulator transition near 150 K but reverts to a metallic state below 40 K. The only crystallographically characterized salt in this series is $(BEDO\text{-}TTF)_2(EtO\text{-}TCA)$, which has been found to

possess the common (BEDO-TTF)$_{2.4}$I$_3$-type structure.

The cyanomethyltetracyanoallyl anion (hereafter referred to as CM-TCA), in which the alkoxy substituent (*R*O−) of the *R*O-TCA$^-$ anion has been replaced with −CH$_2$CN, has also been crystallized with BEDO-TTF to form black platelike crystals of (BEDO-TTF)$_5$(CM-TCA)$_2$(acetonitrile)$_2$.[194] This phase possesses a (BEDO-TTF)$_{2.4}$I$_3$-type structure and exhibits metallic properties with a room-temperature conductivity of 50 S cm^{-1}.

A similar result was found for the (BEDO-TTF)$_5$(DHCP)(THF)$_2$ [DHCP = 2-dicyanomethyl-1,1,3,4,5,5-hexacyanopentadienediide, C$_6$(CN)$_8^{2-}$, THF = tetrahydrofuran] salt which possesses the same formal charge of +0.4 on the BEDO-TTF molecules[194] because DHCP is a dianion. The DHCP salt has a unique packing of the BEDO-TTF molecules which can be described as a derivative of the (BEDO-TTF)$_{2.4}$I$_3$ structural type in which the stacking direction reverses for every fifth BEDO-TTF molecule within a stack, see Figure 9d. This salt has a room-temperature conductivity of 100 S cm^{-1} [202] and is metallic to 8 K below which temperature a slight increase in the resistivity is observed which has been attributed to the weak localization of 2D conduction electrons resulting from disorder.[52] The optical absorption spectra show three bands with the band at 2700−3000 cm^{-1} attributed to the partial charge-transfer state and the presence of segregated BEDO-TTF molecules in the solid state.[52]

3.2.2. Oxo Anions

Two BEDO-TTF salts with the triflate (CF$_3$SO$_3^-$) anion have been reported.[195] The kinetically favored phase appears to be κ-(BEDO-TTF)$_2$CF$_3$SO$_3$, which crystallizes as regular black plates in a packing motif that is referred to as 'κ' in the ET family. This salt is the lone example of this packing motif among BEDO-TTF salts. The crystal structure is characterized by one crystallographically unique BEDO-TTF molecule per unit cell which packs as orthogonal dimers (see Figure 9c) that are separated by layers containing ordered anions. This phase is isomorphous with one of the triflate salts of ET, i.e., κ-(ET)$_2$CF$_3$SO$_3$.[36] The majority phase is the thermodynamically favored tetrahydrofuran-solvated salt, (BEDO-TTF)$_2$CF$_3$SO$_3$(THF)$_{0.5}$, which grows with irregular shape. The poor quality of these crystals has prevented a full structural determination, and thus only a unit cell has been reported. Although both salts have a room-temperature conductivity of about 100 S cm^{-1}, the κ-phase salt shows a gradual monotonic decrease in conductivity upon cooling while the solvated phase possesses a more rapid decrease near 250 K which may be the result of a metal to insulator transition. The room-temperature ESR line width of the κ-phase is about 60 G, while for the solvated derivative it is about 40 G. For both phases the ESR line widths decrease monotonically with decreasing temperature, which is in contrast to that observed for the ET-based κ-(ET)$_2$Cu[N(CN)$_2$]Br,[223] κ-(ET)$_2$Cu(NCS)$_2$,[224,225] and κ-(ET)$_2$CF$_3$SO$_3$[36] salts. The calculated transfer integrals, band electronic structure, and Fermi surface of the κ-salt agree with 2D interactions typically of this packing motif.

When the squarate anion (squarate, hereafter abbreviated as SQA, is C$_4$O$_4^{2-}$) is electrocrystallized with BEDO-TTF, black needles of composition (BEDO-TTF)$_4$(SQA)(H$_2$O)$_6$ were formed.[189] The stoichiometry was determined by a combination of elemental analysis, density measurement, and X-ray structural characterization. The structural characterization was complicated by a supercell whose corresponding reflections were too weak for a definite structure determination. It is clear that the BEDO-TTF molecules pack in layers along the *ac*-plane in a pattern typical of (BEDO-TTF)$_{2.4}$I$_3$ motif,[219] with *c* being the stacking axis. Adjacent molecules in the *a*−2*c* direction are nearly coplanar. The terminal hydrogen atoms of the BEDO-TTF molecules fit into the hollow sites in the anion layer.[192] Assuming the SQA anion has charge of −2, the BEDO-TTF molecules are expected to have an average oxidation state of +0.5, which has been confirmed by Raman spectroscopy.[221,222] The HOMO calculated for the BEDO-TTF molecules in this structure has the same symmetry as the electron-donor molecules in most ET salts. While the maximum coefficients for both donor systems reside on the inner sulfur atoms, the coefficients on the oxygen atoms are notably smaller than those found on the outer sulfur atoms in ET salts. As illustrated in Figure 11c, the 2D structure of this salt is seen in the band electronic structure, which shows electron-like pockets centered around the *B* and *Z* points and a hole-like pocket centered around *X*. This salt has metallic conductivity down to at least 1.4 K.

Elemental analysis has been used to determine the stoichiometry of the dark green needles obtained when BEDO-TTF is electrocrystallized in the presence of tetrabutylammonium picrate (PIC).[189] No structural characterization of the (BEDO-TTF)$_6$(PIC)$_3$(TCE) salt has been reported. Assuming a charge of −1 on the picrate anion, a charge of +0.5 is assigned to the BEDO-TTF electron-donor molecules, which has been confirmed by Raman analysis.[221] Single-crystal conductivity measurements on this salt indicate that it is metallic down to at least 1.4 K.

A salt of composition (BEDO-TTF$^{0.4+}$)$_3$(TNBP^{2-})$_{0.2}$(HTNBP^{1-})$_{0.8}$(H$_2$O)$_2$ (H$_2$TNBP = 3,3′,5,5′-tetranitrobiphenyl-4,4′-diol) has been obtained as a brown powder.[164] This material has a room-temperature conductivity of 30 S cm^{-1} and exhibits metallic behavior. The presence of both the dianion TNBP^{2-} and the monoanion HTNBP^{1-} has been confirmed by the ^{13}C−CP/MAS NMR spectrum, which indicates the presence of both neutral and ionic phenol groups in the H$_n$TNBP molecule. On the basis of Raman spectroscopy, the charge on the BEDO-TTF molecule has been estimated as +0.4.[221] It is noted that the fully protonated H$_2$TNBP species forms the (BEDO-TTF)(TNBP) charge-transfer salt,[189] the discussion of which is beyond the scope of this review.

3.3. TMTSF, Tetramethyltetraselenafulvalene

3.3.1. Polycyano Anions

Eleven salts have been reported in which the TMTSF (tetramethyltetraselenafulvalene) radical cat-

ion has been crystallized with polycyano organic anions.[226] Some of their crystal structures were determined, but basic crystallographic data are not reported. Each of these materials exhibits semiconductive behavior. The (TMTSF)X (X = tetracyano-2-azapropenide or TCAP$^-$, and the tetracyanoallyl (TCA) derivatives hydroxyethyl-TCA$^-$, EtO-TCA$^-$, Me-TCA$^-$, MeNH-TCA$^-$, and NH_2-TCA$^-$) salts, which have a 1:1 stoichiometry, lack an optical absorption band around 4000 cm^{-1}. The stoichiometry of the PCA$^-$ (pentacyanoallyl) and EtO-TCA$^-$ salts has not yet been determined but is expected not to be 1:1 because of the presence of the optical band near 4000 cm^{-1}, which indicates a mixed valence state. These latter two materials have only been obtained as powders with the former possessing a room-temperature resistivity of 14 Ω cm. Single, needlelike crystals of $(TMTSF)_3(TCA)_2$ have been found to have a trimerized TMTSF structure (the anion positions have not been determined), which leads to a relatively high room-temperature resistivity of 1.9×10^4 Ω cm. In addition to the needlelike crystals of (TMTSF)(HE-TCA) (HE-TCA = hydroxyethoxy-TCA), a blocklike phase has been crystallized with the composition $(TMTSF)_4(HE\text{-}TCA)_3$. The structure of this first example of a TMTSF salt with a 4:3 stoichiometry is characterized by segregated columns of TMTSF electron-donor molecules and disordered HE-TCA$^-$ anions. The TMTSF columns have both twisted and ring-over-bond overlap patterns, reminiscent of the δ-type packing in ET salts. The $(TMTSF)_4$HCTMM salt possesses a novel layered structure in which three of the TMTSF molecules, with a charge of +2/3, construct a column within the electron-donor layers, and the fourth TMTSF molecule lies nearly orthogonal to the column and has a charge of +1. The fractional oxidation state of the molecules within the column leads to a fairly low resistivity (7.3 Ω cm) and the presence of an optical absorption near 4000 cm^{-1}.

The TMTSF complex with the DHCP^{2-} anion [DHCP = 2-dicyanomethyl-1,1,3,4,5,5-hexacyanopentadienediide, $C_6(CN)_8^{2-}$] has been reported without much structural detail.[52] Brown platelike crystals of this material exhibit low conductivity ($\sigma_{RT} = 10^{-5}$ S cm^{-1}). Optical absorption bands are observed at 8800 and 14 900 cm^{-1}; the former is ascribed to the transition between the donor cation radical molecules within segregated columns. The lack of a band in the 3400−4100 cm^{-1} region is consistent with the lack of partially oxidized TMTSF molecules and the resulting poor conductivity. Attempts to grow crystals of TMTSF with HCDAH^{2-} (hexacyanodiazahexadiene, $N_2[C_2(CN)_3]_2^{2-}$) have so far been unsuccessful.[191]

3.3.2. Phenolate Anions

Black platelike crystals of $(TMTSF)_2$(TNBP) (H_2-TNBP = 3,3′,5,5′-tetranitro-4,4′-biphenyldiol) were grown by electrocrystallization.[165] Structurally, this salt is characterized by one-dimensional columns of TMTSF which are separated by the TNBP^{2-} anions (basic crystallographic data are missing from the report). A calculation of the overlap integrals indicates that a weak dimerization is present in the TMTSF columns. A strong absorption band at 9−11 $\times 10^3$ cm^{-1} is assigned to an electronic transition between fully ionized molecules, but a shoulder at 3.5×10^3 cm^{-1} suggests the presence of some fractionally charged TMTSF molecules. Thus, it has been speculated that the charge on the TMTSF is slightly less than +1 and the anion layer contains a mixture of the TNBP^{2-} dianion and the HTNBP$^-$ monoanion. Support for this assumption is given by the ^{13}C−CP/MAS NMR spectra, which indicate the presence of both neutral and ionic phenol groups.[164] Thus, a more exact chemical formula for this salt is given by $(TMTSF^{(1-x/2)+})_2(TNBP^{2-})_{1-x}(HTNBP^{1-})_x$ ($0 < x < 1$). $(TMTSF)_2$(TNBP) exhibits semiconductive behavior with a room-temperature conductivity of $\sigma_{RT} = 3 \times 10^{-3}$ S cm^{-1} and an activation energy of 170 meV. This crystalline phase can be identified by its room-temperature ESR line width of 40 G, which is much narrower than most other $TMTSF_2X$ salts. Two additional types of black crystals in the TMTSF/TNBP system have been identified by their morphologies: blocky and needlelike.[164] The blocky crystals have a room-temperature conductivity of 1×10^{-5} S cm^{-1}, while the needles have a room-temperature conductivity of less than 10^{-8} S cm^{-1}. Additional details about these phases are not available.

3.3.3. Sulfonate Anions

The $(TMTSF)_2CF_3SO_3$ salt is isomorphous to the $(TMTSF)_2X$ (X = NO_3^-, ClO_4^-, PF_6^-, etc.) series of salts but possesses an expanded unit cell due to the larger size of the anion.[196,227] The anion is disordered over two conformations in which the $-CF_3$ and $-SO_3$ groups are interchanged. No physical properties have been reported for this salt.

3.4. TMTTF, Tetramethyltetrathiafulvalene

3.4.1. Phenolate Anions

Thin black needlelike crystals of $(TMTTF)_2$-$(C_6H_2N_3O_8)$ ($C_6H_2N_3O_8$ = trinitroresorcinate, commonly called styphnate) were grown through electrochemical methods.[61,228] The crystal structure is characterized as one-dimensional stacks of TMTTF molecules which are surrounded by four chains of trinitroresorcinate anions. The three crystallographically independent TMTTF molecules that reside in the structure pack in an A−B−A−C pattern. An analysis of the calculated HOMO levels of these electron-donor molecules suggests an approximate charge distribution of C^+, $A^{+1/3}$, and $B^{+1/3}$. This salt possesses a room-temperature conductivity of 2×10^{-3} S cm^{-1} and two semiconductive regimes with activation energies of 0.12 (280−400 K) and 0.094 eV (200−280 K).[166] Electronic band structure calculations confirm that this salt is a one-dimensional semiconductor. A sharp decrease in the conductivity near 280 K has been attributed to a structural change, although a crystal structure determination at 110 K reveals a structure very similar to that observed at room temperature, and no clear reason for this discontinuity has been presented. However, the calculated energy gap decreases by 18% between room temperature and 110 K, which is consistent with the observed 21% decrease in activation energy.

While only a black powder of $(TMTTF)_2(TNBP)$ (H_2-TNBP = 3,3′,5,5′-tetranitro-4,4′-biphenyldiol) could be obtained through electrochemical methods, black rodlike single crystals of this salt were obtained through gradual oxidation of TMTTF in acetonitrile by H_2O_2 (6 days) or air (30 days) in the presence of H_2TNBP.[165] Structurally, $(TMTTF)_2(TNBP)$ is quite similar to the analogous TMTSF salt (see above) as far as it is possible to discern in the absence of crystallographic detail. An analysis of calculated overlap integrals indicates a stronger dimerization in the TMTTF salt, which explains the lower conductivity (1×10^{-7} S cm^{-1}) and higher activation energy (250 meV). A strong absorption band in the $9-11 \times 10^3$ cm^{-1} region is assigned to an electronic transition between fully ionized molecules, and no bands are observed below 5000 cm^{-1}, which would result from partially oxidized TMTTF molecules.

Black platelike crystals of $(TMTTF)_2HCNAL$ (H_2-CNAL is 2,5-dicyano-3,6-dihydroxy-1,4-benzoquinone or cyananilic acid) were obtained by diffusion of TMTTF and H_2CNAL from opposite arms of an H-tube.[198] As identified by the X-ray crystal structure analysis, this salt contains the anion formed by the mono-deprotonation of H_2CNAL. The crystal structure of this salt is characterized by segregated stacks of dimerized TMTTF molecules which have been assigned an ionicity of +0.4 and +0.6 based on a bond-length analysis,[197] which is in agreement with the observed stoichiometry. Semiconductive behavior is observed in $(TMTTF)_2HCNAL$ with a room-temperature resistivity of 31 Ω cm and an activation energy of 52 meV. An optical absorption near 5000 cm^{-1} has been assigned to a charge-transfer transition between the neutral state and the cation radical state within the dimeric TMTTF unit. The temperature dependence of the static magnetic susceptibility possesses a broad maximum near 270 K which is a result of the one-dimensional antiferromagnetic $S = 1/2$ interactions. Various other electron-donor molecules have been examined with the $HCNAL^{1-}$ anion but have not been characterized.[229]

3.4.2. Sulfonate Anions

The soluble precursor compound $(TMTTF)CF_3SO_3$ has been prepared by a novel chemical oxidation procedure through the use of (diacetoxyiodo)benzene in the presence of triflic acid.[199] Single crystals of the partially oxidized $(TMTTF)_2CF_3SO_3$ salt were subsequently prepared through reaction of the precursor 1:1 complex and neutral TMTTF. The crystal structure[199] of $(TMTTF)_2CF_3SO_3$ is comprised of layers of $TMTTF^{+0.5}$ cation radicals arranged in a packing motif similar to that observed in the β-$(ET)_2X$ salts.[74] The $CF_3SO_3^-$ anions are disordered at room temperature.[199]

The (TMTTF)(tosylate) salt has been prepared through chemical oxidation by adding equimolar amounts of (hydroxytosyloxyiodo)benzene and *p*-toluenesulfonic acid to a solution of TMTTF.[155] The electronic absorption spectra were characteristic of stoichiometric radical cation salts of TMTTF, but no additional physical characterization was reported.

3.4.3. Polycyano Anions

A poorly characterized TMTTF complex with the $DHCP^{2-}$ anion has been reported.[52] The insulating material ($\sigma_{RT} = 10^{-7}$ S cm^{-1}) forms as black platelike crystals. Optical absorption bands at 11 500 and 17 200 cm^{-1} have been observed, where the former is ascribed to the transition between the donor cation radical molecules within segregated columns. The lack of a band in the 3400−4100 cm^{-1} region is consistent with the lack of partially oxidized TMTTF molecules and the resulting poor conductivity. Attempts to grow crystals of TMTTF with $HCDAH^{2-}$ (HCDAH = hexacyanodiazahexadiene, $N_2[C_2(CN)_3]_2^{2-}$) have so far yielded uncharacterized powders.[191]

3.5. TTF, Tetrathiafulvalene

3.5.1. Sulfonate Anions

A black powder of (TTF)(tsfa) (tsfa = TEMPO−$NHSO_3^-$, TEMPO = 2,2,6,6-tetramethylpiperidinyl-*N*-oxy) was obtained by combining acetone solutions of $(TTF)_3(BF_4)_2$ and (PPh_4)(tsfa).[154] Transparent platelike single crystals of (TTF)(tsfa) were obtained by allowing these combined solutions to stand in a refrigerator for an extended period of time.[153] The crystal structure is characterized by centrosymmetric TTF dimer units which are separated by the sulfamate groups of two tsfa anions. No contacts between TTF dimers are present. Magnetic measurements indicate that this salt follows Curie−Weiss behavior with $C = 0.360$ emu K mol^{-1} and $\theta = -0.52$ K, suggesting the presence of a radical spin on the TEMPO component and the absence of spin on the TTF site. This picture is consistent with the high experimental resistivity (> 10^6 Ω cm). The ESR line width is 11.5 G at room temperature, while the *g*-value (2.0076) is close to that observed for the PPh_4^+ salt, suggesting that the ESR signal is mainly from the anion.[153] The related (TTF)(TEMPO−OSO_3) salt was obtained by a similar procedure but not further characterized.[154]

While attempting to crystallize an organic, magnetic, conducting salt of TTF with the 2,2,6,6-tetramethylpiperidinyloxy-4-hydroxy-4-sulfonate anion by a metathesis reaction between $(TTF)_3(BF_4)_2$ and the PPh_4^+ salt of this sulfonate anion, the (TTF)(4-oxo-2,2,6,6-tetramethylpiperidin-1-sulfate) salt formed.[200] The crystal structure of this salt consists of planar, dimerized TTF cations arranged in a stair-like stack. No physical properties have been reported.

A powder sample of (TTF)(tosylate) has been grown by electrocrystallization.[230] The room-temperature conductivity of a compressed pellet was reported to be about 1 S cm^{-1}, although a more recent result indicates that the conductivity is vastly lower (2×10^{-6} S cm^{-1}).[231] Since these salts were not fully characterized, it is possible that two different phases are responsible for this discrepancy. A salt of the same composition has been prepared through chemical oxidation by adding equimolar amounts of (hydroxytosyloxyiodo)benzene and *p*-toluenesulfonic acid to a solution of TTF, although again no additional characterization has been reported.[155]

A novel chemical oxidation procedure in which TTF is oxidized by (diacetoxyiodo)benzene in the presence of triflic acid has been used to prepare $(TTF)CF_3SO_3(H_2O)_{0.5}$.[199] Although the crystal structure of this salt has been determined, its physical properties have not been reported. This salt is highly soluble in solvents such as acetonitrile and dichloromethane, making it a suitable precursor for metathesis reactions for the crystallization of TTF with various other anions.

Crystals of $(TTF)(OSO_2OMe)$ were prepared by electrocrystallization.[232] When crystals were grown galvanostatically, single crystals were obtained with a room-temperature conductivity of 8.2 S cm^{-1}, although more recent results indicate that this conductivity may be as high as 59 S cm^{-1}.[231] Potentiostatic growth resulted in a polycrystalline material which gave a compressed pellet conductivity of 5.1×10^{-8} S cm^{-1}.

3.5.2. Carboxylate Anions

A novel salt, $(TTF)_2[TTF(CO_2H)_2(CO_2)_2]$, in which both the cation and anion possess the TTF framework has recently been prepared by electrocrystallization.[201] Because $TTF(CO_2H)_2(CO_2)_2^{2-}$ is a dianion, the oxidation state of TTF in this salt is +1, consistent with a bond-length analysis.[233] The crystal structure is constructed of columns consisting of alternating dimerized $(TTF^+)_2$ and $TTF(CO_2H)_2(CO_2)_2^{2-}$ units. The integrated stacking of this salt leads to semiconducting properties ($E_a = 0.10$ eV) with a low room-temperature conductivity of 10^{-5} S cm^{-1}. An optical absorption band is observed at $\lambda = 750$ nm which is attributed to the $(TTF^+)_2$ dimer. A salt of composition $(TTF)_3[TTF(CO_2H)_2(CO_2)_2]$ has been obtained as a dark brown powder in some electrocrystallization experiments. The fact that this material has an optical absorption at $\lambda = 2500$ nm, indicating a mixed valence state, suggests that it may have an increased conductivity, but no further characterization has been reported.

Black, needlelike single crystals of (TTF)(acetate)$_{0.7}$, (TTF)(maleate)$_x$, and (TTF)(fumarate)$_{0.25}$ have been grown by electrocrystallization.[230] The room-temperature conductivities of these complexes are 3, 0.02, and 0.002 S cm^{-1}, respectively. No additional characterization of these salts has been reported. More recently, TTF salts of hydrogenfumarate ($HO_2CCH{=}CHCO_2^-$) and hydrogenoxalate ($HO_2CCO_2^-$) have also been grown by electrocrystallization, but no stoichiometry, structural analysis, or physical properties have been reported.[73]

3.5.3. Polycyano Anions

Black, blocky crystals of $(TTF)_2(DHCP)(CH_3CN)$ were prepared by the metathesis method whereby acetonitrile solutions of $(TTF)_3(BF_4)_2$ and (TEA)(DHCP) were combined.[52,202] The crystal structure contains two crystallographically independent TTF^+ molecules (A and B). Dimers of the TTF^+ (A) cations form columns, which are separated from TTF^+ (B) cations by neutral acetonitrile solvent molecules. Parallel to the long molecular axis of TTF^+ (A), the segregated TTF^+ (A) stacks are separated by a bis(dicyanomethyl)methylide group of the anion. The remainder of the anion forms alternating *ADDA* (*A* = DHCP, *D* = TTF) stacks with TTF^+ (B). Consistent with the crystal structure, this salt is an electrical insulator with a room-temperature conductivity of 10^{-7} S cm^{-1}. Optical bands are observed at 12 300 and 19 200 cm^{-1}; the former band is attributed to an optical transition between the donor cation radicals within the segregated columns. The lack of an absorption band in the 3400−4100 cm^{-1} region, associated with segregated columns of partially oxidized TTF molecules, is consistent with the insulating state of this salt.

Black blocky crystals of $(TTF)_2(HCDAH)(CH_3CN)$ were prepared by electrocrystallization.[191] The crystal structure is two-dimensional in nature with $(TTF^{\bullet+})_2(CH_3CN)$ layers alternating with $HCDAH^{2-}$ layers. A bond-length analysis indicates that the oxidation state of the TTF molecules is +1. The $TTF^{\bullet+}$ molecules are dimerized and isolated by disordered solvent molecules. Although no physical properties were reported, based on the oxidation state of TTF and the crystal packing, it is anticipated that this salt is nonmetallic.

The $(TTF)_2(HCP)$ salt was prepared as a black microcrystalline powder by the metathesis reaction of $(TBA)_2(HCP)$ or (TBA)(HCP) with (TTF)Cl.[234] A compressed pellet of this material had a resistivity of 1 Ω cm. No further characterization has been reported.

3.5.4. Squarate and Phenolate Anions

Thin, long black needles of $(TTF)_7(SQA)_4$ were grown by electrocrystallization, but their quality was not sufficient for structural determination by single-crystal X-ray diffraction.[235] On the basis of electrochemical evidence, this material is believed to contain $TTF^{\bullet+}$ and $SQA^{\bullet-}$ radicals along with neutral TTF molecules. The complex ESR signal is probably a result of a superposition of the resonances of the $TTF^{\bullet+}$ and $SQA^{\bullet-}$ radicals. The UV−vis−NIR spectra of this salt have an absorption at 800 nm (attributed to charge transfer between $TTF^{\bullet+}$ molecules) and a broad band extending into the near-IR ($\lambda = 1000$ nm) (attributed to charge transfer between partially oxidized TTF molecules). The conductivity, determined by impedance spectroscopy, indicated semiconducting behavior with an activation energy of 0.64 eV and a room-temperature conductivity of 8000 Ω cm. This semiconductive behavior was confirmed by infrared spectroscopy, which also indicates that the TTF molecules are arranged in stacks.

Black crystals of $(TTF)(CA)_{0.5}(_{red}H_4CA)_{0.5}$ (H_2CA = chloranilic acid, $_{red}H_4CA$ = reduced form of H_2CA) were grown from an acetonitrile solution containing TTF and chloranilic acid.[203] During the crystallization process a proton-coupled electron transfer occurs which results in the formation of chloranilate dianions and neutral hydrogenated chloranilic acid. In the crystal structure these molecular units form alternating hydrogen-bound chains which link together dimerized TTF^{+1} cations. The physical properties of this salt have not been reported, but based on the crystal structure and oxidation state of TTF, it is anticipated that this material would be a poor electrical conductor.

Microcrystalline samples of several TTF complexes with oxonol dyes have been prepared by electrocrystallization.[236] The stoichiometry of the crystallites is not well known, and there are probable defects from unknown oxidation products. While the solution EPR spectrum of these complexes shows the expected isotropic quintet signal of $TTF^{\bullet+}$, the solid-state EPR spectrum is broadened by the high concentration of radicals. The room-temperature conductivities of these materials range from 7.6×10^{-5} to 9.8×10^{-4} S cm^{-1}. The dc conductance dominates the dielectric response, and semiconducting behavior has been observed with an activation energy of 0.19 eV.[237]

3.5.5. Cyclopentadienide Anions

Black platelets of $(TTF)_3(PMC)_2$ were prepared by reaction of TTF with Ag(PMC) [PMC = pentakis(methoxycarbonyl)cyclopentadieniide] in hot acetonitrile.[204] Three crystallographically unique TTF molecules are present in the crystal structure. On the basis of a bond-length analysis, molecules **A** and **B** are fully ionic (TTF^{+1}) while **C** is nearly neutral. The crystal structure is characterized by weakly alternating stacks of $(TTF)_2^{+1}$ (**AC**) cationic dimers and TTF^{+1} (**B**) cations. These TTF columns form two-dimensional layers. In adjacent layers, the TTF stacking axes are orthogonal, forming a square grid. Single-crystal conductivity measurements, carried out along the two in-plane stacking axes as well as perpendicular to these planes, indicate semiconductive behavior. The room-temperature conductivity ranges from 1.5×10^{-5} (in plane) to 4.1×10^{-7} S cm^{-1} (perpendicular to planes). Within the conducting planes, the conductivity anisotropy is 3.5. Weak triplet exciton signals are observed in the ESR spectra, consistent with the presence of neighboring localized $TTF^{\bullet+}$ radicals within the stack.

3.5.6. Tetraazafulvalenediide Anions

A fine reddish brown powder of $(TTF)_3(TCTAF)(CH_2Cl_2)$ (TCTAF = tetracyano-1,1′,3,3′-tetraazafulvalene) was obtained by electrocrystallization.[238] A brown powder sample of $(TTF)_3(TBTAF)(CHCl_3)$ (TBTAF = tetrabromo-1,1′,3,3′-tetraazafulvalene) was obtained by combination of chloroform solutions of TTF and TBTAF. Although the formal charge on the TTF molecules in these salts would be estimated at +0.67 from the stoichiometry, the optical spectrum indicates that the salt may consist of two $TTF^{\bullet+}$ cations and one neutral TTF molecule per unit cell. Both salts are semiconductors: $(TTF)_3(TCTAF)(CH_2Cl_2)$ has a room-temperature resistivity of 230 Ω cm and an activation energy of 0.18 eV, while similar values are reported for $(TTF)_3(TBTAF)(CHCl_3)$ (ρ_{RT} = 1200 Ω cm, E_a = 0.08 eV). Although these conductivity measurements were performed on compressed powders, it was believed that the semiconductive behavior is intrinsic to the sample and not a result of intergrain transport. The room-temperature ESR line width for the TCTAF salt is 12 G, while for the TBTAF analogue it is 13 G. For both salts the ESR line width is nearly constant down to 133 K, and the signal intensity is Curie paramagnetic in nature.

3.5.7. Organometallic Anions

Black needles of $(TTF)[Au(C_6F_5)Cl]$ and $(TTF)[Au(C_6F_3H_2)_2Cl_2]$ salts have been prepared by the electrocrystallization technique.[206] The room-temperature conductivity of both materials, measured on compacted pellets, is on the order of 10^{-6} S cm^{-1}. The ESR line width of $(TTF)[Au(C_6F_5)Cl]$ decreases from 10 G at room temperature to 6 G at 77 K, while for $(TTF)[Au(C_6F_3H_2)_2Cl_2]$ only the room-temperature line width (10 G) has been reported. Black prisms of $(TTF)_2Au(C_6F_5)_2$ have also been grow by electrocrystallization and found to have a room-temperature conductivity of 3 S cm^{-1}, although no further characterization was reported.[239]

3.6. OMTTF, Octamethylenetetrathiafulvalene

Diffusion of solutions of H_2CNAL and OMTTF in an H-tube yielded black platelike single crystals of $(OMTTF)_3(HCNAL)_2$.[205] These results indicate that under these conditions the cyananilic acid was monodeprotonated as the OMTTF was oxidized. The crystal structure consists of OMTTF trimers in which the central molecule is nearly planar while the outer molecules are warped by about 10° at the central C=C bond. On the basis of a bond-length analysis, the OMTTF molecules appear to be oxidized to the +1 state, although the ionicity has been suggested to be +2/3 based on the stoichiometry. Raman spectroscopy supports the ionic nature of OMTTF. The anions are arranged in hydrogen-bonded uniform chains in which the molecular planes of adjacent anions are normal to each other. In agreement with the structural features, a very low conductivity of 3×10^{-8} S cm^{-1} was measured.

Attempts to grow crystals of OMTTF with $HCDAH^{2-}$ (HCDAH = hexacyanodiazahexadiene, $N_2[C_2(CN)_3]_2^{2-}$) have so far yielded uncharacterized powders.[191]

3.7. $TTFPh_2$, 3,4′-Diphenyltetrathiafulvalene

Dark brown or black needlelike crystals of $(TTFPh_2)_2[Au(C_6F_5)_2]$ have been prepared by electrocrystallization.[206,239] The crystal structure of this salt is characterized by stacks of $TTFPh_2$ radical cations. The two crystallographically unique $TTFPh_2$ molecules, which alternate within the stack, are not parallel to each other, and their bond lengths are sufficiently different to suggest that their partial charges are not the same. This complex has a room-temperature conductivity of 1.5 S cm^{-1} and exhibits semiconductive behavior with an activation energy of 0.13 eV down to 200 K. Below this temperature the activation energy gradually decreases to 12 meV at 77 K. The room-temperature ESR line width is 30 G, which decreases to 20 G at 77 K.

Black microcrystals of $(TTFPh_2)[Au(C_6F_5)_2]$ have been reported to have a ESR line width at room temperature of 5 G and a powder conductivity of 1.5×10^{-6} S cm^{-1}.[206] Two $TTFPh_2$ salts with organoaurate(III) anions have been prepared.[206] $(TTFPh_2)_{2.5}[Au(C_6F_5)_2Cl_2]$ has a compressed powder conductivity of 2×10^{-4} S cm^{-1} and an ESR line width which decreases from 7 G at room temperature to 1 G at

77 K. The $(TTFPh_2)[Au(C_6F_5)_2I_2]$ salt is about an order of magnitude more conductive (1×10^{-3} S cm^{-1}) and has a room-temperature ESR line width of 5 G.

3.8. EDT–TTF, Ethylenedithiotetrathiafulvalene

3.8.1. Oxy Anions

Single crystals of the molecular conductor $(EDT\text{-}TTF)_3(HSQA)(H_2SQA)$ (H_2SQA = squaric acid) have been prepared.[240] The crystal structure (no crystallographic detail given) is characterized by one-dimensional stacks of EDT-TTF molecules which are arranged as alternating dimer and monomer units. Similar bond lengths in both the dimer and monomer units indicate that the oxidation state is similar in all EDT-TTF molecules. Band electronic structure calculations indicate that this salt possesses a two-dimensional Fermi surface. The room-temperature resistivity is 5 Ω cm. Semiconducting properties have been observed in both electrical conductivity (E_a = 740 K) and thermopower measurements.

3.8.2. Polycyano Anions

Black platelike crystals of a complex of EDT-TTF with $DHCP^{2-}$ [DHCP = 2-dicyanomethyl-1,1,3,4,5,5-hexacyanopentadienediide, $C_6(CN)_8^{2-}$] have been prepared by electrocrystallization.[52,202] These crystals have a high room-temperature conductivity of 100 S cm^{-1},[202] and an optical band near 3900 cm^{-1} which has been attributed to partially oxidized EDT-TTF molecules arranged in a segregated manner.[52] An optical absorption at 13 900 cm^{-1} is ascribed to an intramolecular transition. No structural or stoichiometric information is known.

3.9. EDTMe–TTF, Ethylenedithio-methyl-tetrathiafulvalene

Single crystals of $(EDTMe\text{-}TTF)_2(SQA)(H_2SQA)_2$ have been prepared.[241] In this structure (no crystallographic detail given) the electron-donor molecules form two-leg-ladder columns which are separated from each other by hydrogen-bonded anionic trimers consisting of one squarate dianion and two neutral squaric acid molecules. The magnetic susceptibility of this complex exhibits Curie–Weiss behavior (C = 0.77 emu K mol^{-1}, $\theta = -90$ K) down to 120 K. A broad maximum in the susceptibility is present around 80 K. Over the temperature region 50–120 K the susceptibility can be fit to a Heisenberg antiferromagnetic spin ladder model (with exchange constants $J_c/k_B = -30$ K along the leg and $J_b/k_B = -170$ K along the rung of the ladder). Electrically this material is a semiconductor with a room-temperature conductivity of 10^{-4} S cm^{-1} and an activation energy of 340 K. An unusual time-dependent increase in room-temperature conductivity has been suggested to be a result of a solid-state chemical reaction initiated by the applied electrical current.

3.10. EDO–TTF, Ethylenedioxytetrathiafulvalene

Poor quality black needles of an EDO-TTF complex with $HSQA^-$ have been prepared through galvanostatic electrocrystallization.[241] The crystal structure of this salt is not known, but it is metallic to 50 K and possesses a room-temperature conductivity of 20 S cm^{-1}. Below the MI transition an activation energy (E_a/k_B) of 10 K is observed.

A powder sample of a radical cation salt of EDO-TTF with the $CF_3SO_3^-$ anion has been prepared by anodic oxidation.[242] No structural or physical characterization has yet been reported.

3.11. TMT–TTF, Tetrakis(thiomethyl)tetrathiafulvalene

The $(TMT\text{-}TTF)CF_3SO_3$ salt has been prepared by a novel chemical oxidation procedure through the use of (diacetoxyiodo)benzene in the presence of triflic acid.[199] The UV–vis–NIR and IR spectra of this salt have been reported but not discussed. This salt is highly soluble in solvents such as acetonitrile and dichloromethane, rendering it a possible precursor for nonstoichiometric materials. To this end, a nonstoichiometric $(TMT\text{-}TTF)_xCF_3SO_3$ salt has been reported but not characterized.

3.12. Nucleobase-Functionalized TTF Derivatives

A novel salt containing a nucleobase-functionalized derivative, (2′,3′,5′-tri-*tert*-butyldimethylsiloxyladenosine-8-yl)-tetrathiafulvalene, and the $HCNAL^-$ (cyanilic acid) monoanion had been prepared as a powder.[243] The electronic spectra of this complex show intramolecular transitions in the 18 000–25 000 cm^{-1} region, indicating complete charge transfer. Also, on the basis of infrared data, an alternating stacking motif has been proposed.

3.13. Various Other TTF-Derived Electron Donors with $DHCP^{2-}$

Charge-transfer salts containing the $DHCP^{2-}$ anion [2-dicyanomethyl-1,1,3,4,5,5-hexacyanopentadienediide, $C_6(CN)_8^{2-}$] with several additional fulvalene-based electron-donor molecules have been prepared by electrocrystallization.[52,202] Two crystalline phases formed with the BMDT-TTF [BMDT-TTF = bis(methylenedithio)tetrathiafulvalene] electron-donor molecule. The electrically insulating BMDT-TTF complex forms as brown plates, while a brown wool-like material has semiconducting properties (σ_{RT} = 0.5 S cm^{-1}, E_a = 25 meV).[202] The insulating complex has an optical intramolecular absorption at 11 300 cm^{-1}, while the semiconducting salt exhibits bands at 3800 (indicative of segregated electron-donor molecules in a partially oxidized state) and 8400 cm^{-1} (indicating a degree of charge-transfer greater than +0.5).[52] The BPDT-TTF [BPDT-TTF = bis(propylenedithio)tetrathiafulvalene] analog[52] grows as black plates with a room-temperature conductivity of 3×10^{-3} S cm^{-1} and an activation energy of 70 meV. For this salt optical bands have been reported at 3600, 13 700, and 17 400 cm^{-1}, consistent with a partially oxidized electron-donor molecule and a conducting system.[52] Similar to the BPDT-TTF salt, the BVDT-TTF [BVDT-TTF = bis(vinylenedithio)tetrathiafulvalene] derivative, which crystallizes as brown needles, has a room-temperature conductivity of about 100 S cm^{-1}[202] and optical absorptions at 3200, 10 700, and

16 400 cm^{-1}. Semiconducting black needles of the BOPDT-TTF [BOPDT-TTF = bis[oxybis(methylenethio)]tetrathiafulvalene] derivative have a room-temperature conductivity of 1 S cm^{-1},[202] an activation energy of 50 meV, and optical bands at 4000, 14 300, and 16 800 cm^{-1}.[52] Insulating salts of $DHCP^{2-}$ were formed with the HMTTF and TMB electron-donor molecules. These salts, which exhibited optical bands at 10 300 and 15 900 (HMTTF) and 8000 and 14 000 cm^{-1} (TMB), lacked a band in the 3400−4100 cm^{-1} region, consistent with their poor conductivity.[52]

4. Non-TTF Radical Cations

4.1. Oxidized $Pd(dddt)_2$ Cations

Monoanionic $M(dddt)_2^-$ (M = Ni, Pd, and Au; $dddt^{2-}$ = 5,6-dihydro-1,4-dithiin-2,3-dithiolate) complexes were first synthesized and studied in the mid-1980s because of their similarity to $M(dmit)_2^-$ (dmit = 1,3-dithiole-2-thione-4,5-dithiolate).[244−246] In contrast to the latter, which upon oxidation primarily form $M(dmit)_2^{\delta-}$ (δ < 1), the dddt complexes have much lower oxidation potentials and readily oxidize to the neutral form and even to partially oxidized cations, $M(dddt)_2^{+\delta}$.[247,248] Thus, these constitutional analogues of the ET electron-donor molecule, with the metal center replacing the central C=C moiety, can readily act as electron donors and form salts with a variety of anions with a range of electrical properties (the one salt with an organic anion is described below). Some $M(dddt)_2$ salts are isostructural with the corresponding ET salts, with the difference in conducting properties attributed to the electronic structures of the electron-donor molecules. For further reading on this class of electron-donor complexes, see the review article by Yagubskii.[249]

Thin platelike crystals of the $[Pd(dddt)_2]_2CF_3SO_3$ salt were prepared by electrocrystallization from an electrolyte solution of $(TBA)CF_3SO_3$ and neutral $Pd(dddt)_2$.[207] The crystal structure of this salt is composed of layers of strongly dimerized $[Pd(dddt)_2]^{+0.5}$ radical cations separated by $CF_3SO_3^-$ anions which are disordered about a center of symmetry. If the dimerization is disregarded, the packing motif is similar to that termed β-type in the ET salts.[74] The room-temperature conductivity of this complex is about 1 S cm^{-1}, which decreases upon cooling.

4.2. TTM-TTP, 2,5-Bis[4,5-bis(methylthio)-1,3-dithiol-2-ylidene]-2−1,3,4,6-tetrathiapentalene

Single crystals of $(TTM\text{-}TTP)[C(CN)_3]$ were obtained by electrocrystallization.[208] The crystal structure is characterized by uniform stacks of tilted TTM-TTP molecules in which the tilt direction of the stacks alternates along the *c*-axis. This complex has a fairly high room-temperature conductivity (σ_{RT} = 140−500 S cm^{-1}) and is metallic to 70 K. The thermoelectric power is about −8 μV K^{-1} at room temperature and is nearly constant within the metallic regime but falls rapidly below the metal−insulator transition. Static magnetic measurements indicate a nearly constant susceptibility, while the ESR spin susceptibility gradually decreases from room temperature to the metal−insulator transition, below which point a rapid Curie-like increase is observed.[250]

4.3. DIDTPY, 2,7-Diiodo-1,6-dithiapyrene

The electrocrystallization technique was used to prepare single crystals of the $(DIDTPY)[C_3(CN)_5](THF)$ (THF = tetrahydrofuran) charge-transfer salt.[209] The crystal structure is characterized by segregated stacks of dimerized $DIDTPY^{\bullet+}$ radical cations in which the intradimer and interdimer distances are 3.28 and 3.59 Å, respectively. It is proposed that the dimeric structure is a result of intermolecular I···CN interaction. The optical absorption bands at 7800 and 17 500 cm^{-1} have been attributed to the inter- and intramolecular charge-transfer transitions of $DIDTPY^{\bullet+}$, respectively. No further physical characterization has been reported.

4.4. TTT, Tetrathiatetracene

Eight cation−radical salts of TTT with various substituted tetracyanoallyl, RO-TCA^- (R = Me, Et, Pr, and Bu), anions have been prepared by electrocrystallization.[49,210,251] These salts can be classified into three groups depending on their stoichiometries. A 3:2 salt $[(TTT)_3(PrO\text{-}TCA)_2]$, four 1:1 salts [(TTT)(MeO-TCA), (TTT)(EtO-TCA)$(THF)_{0.25}$, (TTT)(PrO-TCA)$(THF)_{0.25}$, and (TTT)(BuO-TCA)], and two 1:2 salts [$(TTT)(EtO\text{-}TCA)_2$ and $(TTT)(PrO\text{-}TCA)_2$] have been obtained (THF = tetrahydrofuran). The average oxidation states of the TTT molecules are thus +2/3, +1, and +2. These materials are all semiconducting with the room-temperature electrical resistivity of these three classes being 10^4-10^6, 10^6, and 10^3 Ω cm, respectively. Each class has a characteristic optical absorption. The 1:2 salts exhibit a band around 20 000 cm^{-1} which has been assigned to the TTT^{+2} cation. The 1:1 salts have a band in the 7000 cm^{-1} region originating from an intermolecular transition of isolated TTT^+. The 3:2 salts have additional absorptions around 14 000 and 3500 cm^{-1} resulting from neutral TTT and charge transfer from neutral TTT to TTT^+, respectively. On the basis of a bond-length analysis, the 3:2 salts contain both neutral TTT to TTT^+. Structurally, the 1:1 salts contain stacks of dimerized TTT^+ cations. The 1:2 salts possess mixed stacks consisting of alternating TTT^{+2} dications and RO-TCA^- anions, while the 3:2 salts are characterized by stacks of TTT^+ cations and neutral TTT molecules.

The powder optical absorption spectra of TTT(acetate) has been reported and compared to the solution spectrum.[252]

5. Thin Films

5.1. Langmuir−Blodgett Films

Metallic behavior has been observed in thin films composed of BEDO-TTF and behenic acid ($C_{21}H_{43}COOH$) which were fabricated through the Langmuir−Blodgett (LB) technique.[253] The room-temperature conductivity was as high as 40 S cm^{-1}, and metallic conductivity persisted down to 14 K. The infrared spectrum of the film showed the presence

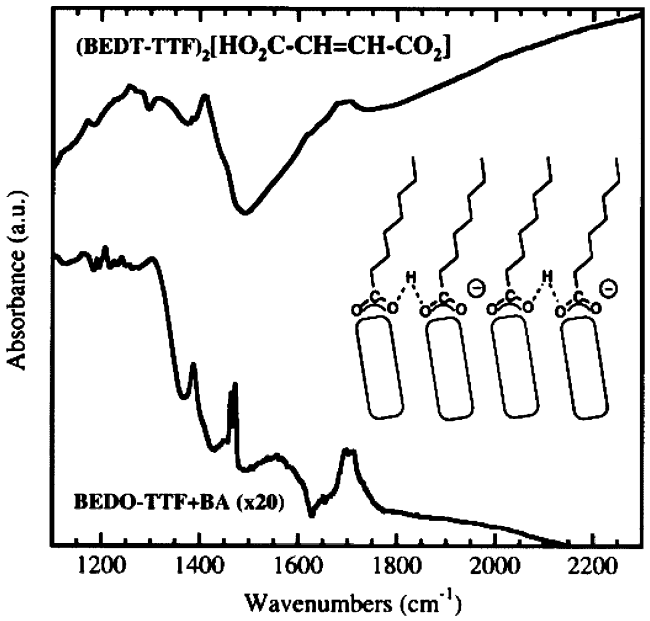

Figure 12. Infrared spectra of a thin film of BEDO-TTF with behenic acid as compared to a powder sample of $(ET)_2$-$[HO_2C-CH=CH-CO_2]$. The peaks at 1705 (C=O) and 1390 cm^{-1} (C−O) correspond to the hydrogen-bonding carboxylate group of $C_{21}H_{43}COO\cdots H\cdots OOCC_{21}H_{43}$. (inset) Expected molecular organization. (Reprinted with permission from ref 255. Copyright 2001 American Chemical Society.)

of a broad charge-transfer band and a series of vibronic bands which indicate the formation of mixed valence dimer states of BEDO-TTF. The degree of charge transfer has been estimated as $\rho = +0.5$. As illustrated in Figure 12, based on the infrared spectra, the anion has not been positively identified but is suggested to be a hydrogen-bound dimer of behenic acid and its conjugate base.[254,255] X-ray diffraction has indicated that the double-layer thickness is about 66 Å, consistent with a 24 Å layer of behenic acid separated by a 9 Å layer of BEDO-TTF. The observed pressure vs area (Π/A) isotherms can be explained by a bilayer model in which the BEDO-TTF molecules occupy the lower layer while the behenic acid comprises the upper layer.[256] These films have been investigated by ESR spectroscopy.[257] Above 50 K the spin susceptibility is nearly constant, indicating Pauli susceptibility and metallic behavior. Below this temperature a Curie-like susceptibility is observed which has been attributed to localization of electrons resulting from disorder. The room-temperature ESR line width of about 50 G remains nearly constant down to 150 K, at which point it decreases linearly with temperature to 20 G at 10 K. The tilt angle of the long molecular axis of the BEDO-TTF molecules from the normal has been determined to be about 30° based on an analysis of the *g*-values.

Closely related LB films have been prepared through the use of behenic acid and the bis(ethylenedioxy)diselenadithiafulvalene (BEDO−STF) electron-donor molecule.[254] An X-ray diffraction profile of films with 11 LB layers indicates a layer periodicity of 67 Å. Infrared vibronic modes around 2400 and 1300 cm^{-1} indicate the presence of a partial charge-transfer state. The room-temperature conductivity of a nine-layer film was 19 S cm^{-1}. Attempts to grow similar films with the 4,5-ethylenedioxy-4′,5′-ethylenedithio-tetrathiafulvalene (EOET-TTF) electron-donor molecule resulted in poorer quality films with a weaker charge-transfer band, suggesting the importance of the oxygen atoms in the electron-donor molecules for film growth. Fifteen-layer films with an EOET/behenic acid ratio of 2:1 possessed a room-temperature conductivity of 1 S cm^{-1}, while those with a 1:1 ratio lacked a charge-transfer band in the infrared and were assumed to be insulating.[256]

In a similar manner, LB films were prepared in which BEDO-TTF was combined with stearic acid ($C_{17}H_{35}COOH$), octadecyl phosphonic acid ($C_{18}H_{37}PO_3H_2$), and dicetyl phosphate $[(C_{16}H_{33})_2PO_4^-]$.[258,259] The films which incorporated stearic acid had an improved conductivity of 80 S cm^{-1} at room temperature and remained metallic down to 100 K.[260] The exposure of these films to ultraviolet radiation results in a 10^5-fold decrease in conductivity due to the loss of long-range order.[261] An analysis of 21-layer films indicates a logarithmic decrease of the dc conductivity and a negative transverse magnetoresistance at low temperature which has been interpreted as a weak localization of a two-dimensional electronic system as a result of random potentials resulting from disorder within the BEDO-TTF layers.[262] Analysis of the infrared spectra of these films indicated that the anionic species in these films is the stearate anion ($C_{17}H_{35}COO^-$). A detailed study of the formation of this conducting LB films has been described.[255] Small islands containing mixed valence BEDO-TTF initially form on the water surface which grow into a homogeneous film as the surface area is decreased. The charge-transfer interaction between BEDO-TTF and the aliphatic carboxylate anions apparently promotes film formation, and thus the pH of the subphase has dramatic effects on the growth process. A lamellar X-ray diffraction profile has been obtained on a 15-layer film, indicating a stacking periodicity of 58 Å.[262] Similar experiments in which the acid was replaced with an alcohol (docosanol or octadecanol), which is not susceptible to dissociation, resulted in the formation of insulating films.[258,259]

Conducting EDT-TTF Langmuir−Blodgett films have been prepared with octadecanesulfonate (OS) and stearic acid (SA).[263] The best films were prepared when the SA:OS ratio was between 1 and 2. X-ray diffraction profiles of the films indicated a lattice spacing of 46 Å, indicating that the alkyl chains are inclined more than 30° from the surface normal. Infrared analysis of films of various SA/OS compositions indicate that no charge transfer occurs between SA and EDT-TTF but that OS induces charge transfer with the formation of a mixed valence state. Twenty-one-layer films with a SA:OS ratio of 1.0 have a room-temperature conductivity of 2.6×10^{-2} S cm^{-1} and exhibit semiconducting behavior with an activation energy of 54 meV.

5.2. Thin Films on Solid Substrates

Thin films of TTF with mandelate, tartrate, camphorate, and adipate anions have been electrodeposited onto an indium tin oxide coated glass.[264] Appli-

cation of a potential across the length of a sample resulted in a change in the visible absorption spectrum for salts of the former three anions which lack a center of symmetry. Such materials have potential as solid-state electrooptic devices.

6. Concluding Remarks

Fifty years have passed since the initial discovery of high conductivity in an organic perylene bromide complex.[1] The first metallic-like conductivity in a completely organic compound occurred 30 years ago with the discovery of TTF-TCNQ.[2,3] Twenty-five years ago, the first completely organic radical cation salts which were prepared by electrocrystallization of TTF in the presence of anions such as maleate, fumarate, and tosylate were reported.[230] A series of more than 20 superconducting ET salts which contained the organometallic $M(CF_3)_4^-$ anions were discovered a decade ago,[64] while even more recently the first completely organic superconductor β''-$(ET)_2SF_5CH_2CF_2SO_3$ was discovered.[39] Clearly, progress is being made in this area because of the vast potential for tailoring crystal structures through the fine-tuning of both organic anions and electron-donor molecules. Today over 100 completely organic cation radical salts are known with a wide range of electrical (ranging from insulating to superconducting) and magnetic properties. Progress is also being made as these salts are being deposited as conducting thin films which will be a prerequisite for many applications. Thus, as chemists learn to control solid-state properties through the engineering of crystal structures via molecular design, the future appears bright for the continuing development and occasional scientific breakthough in the field of organic conductors and superconductors.

7. Acknowledgments

Work at Argonne National Laboratory is supported by the Office of Basic Energy Sciences, Division of Materials Sciences of the U.S. Department of Energy under contract W-31-109-ENG-38. The authors also thank their current and former co-workers and numerous collaborators for their contributions to the original work underlying this review article. Among them, but by no means the only ones, are Aravinda M. Kini, H. Hau Wang, Brian H. Ward, and Jack M. Williams in the former category and the groups of James S. Brooks, Gary L. Gard, Michael Lang, Janice L. Musfeldt, Dieter Naumann, James S. Schilling, John Singleton, M.-H. ('Mike') Whangbo, Jochen Wosnitza, and Fulin Zuo among the latter. We are grateful to the anonymous reviewers of this article for suggesting a number of useful improvements over the original version. Michael Sternberg took the authors' portraits.

8. References

(1) Akamatu, H.; Inokuchi, H.; Matsunaga, Y. *Nature (London)* **1954**, *173*, 168.
(2) Coleman, L. B.; Cohen, M. J.; Sandman, D. J.; Yamagishi, F. G.; Garito, A. F.; Heeger, A. J. *Solid State Commun.* **1973**, *12*, 1125.
(3) Ferraris, J.; Cowan, D. O.; Walatka, V., Jr.; Perlstein, J. H. *J. Am. Chem. Soc.* **1973**, *95*, 948.
(4) Little, W. A. *Phys. Rev.* **1964**, *134*, A1416.
(5) Greene, R. L.; Grant, P. M.; Suter, L. J. *Phys. Rev. Lett.* **1975**, *34*, 577−579.
(6) Jérome, D.; Mazaud, A.; Ribault, M.; Bechgaard, K. *J. Phys. Lett. (Orsay, Fr.)* **1980**, *41*, L95.
(7) Hebard, A. F.; Rosseinsky, M. J.; Haddon, R. C.; Murphy, D. W.; Glarum, S. H.; Palstra, T. T. M.; Ramirez, A. P.; Kortan, A. R. *Nature (London)* **1991**, *350*, 600.
(8) Williams, J. M.; Ferraro, J. R.; Thorn, R. J.; Carlson, K. D.; Geiser, U.; Wang, H. H.; Kini, A. M.; Whangbo, M.-H. *Organic Superconductors (Including Fullerenes): Synthesis, Structure, Properties and Theory*; Prentice Hall: New Jersey, 1992.
(9) Ishiguro, T.; Yamaji, K.; Saito, G. *Organic Superconductors*; Fulde, P., Ed.; Springer-Verlag: Berlin, Heidelberg, New York, 1998.
(10) Williams, J. M.; Beno, M. A.; Wang, H. H.; Leung, P. C. W.; Emge, T. J.; Geiser, U.; Carlson, K. D. *Acc. Chem. Res.* **1985**, *18*, 261.
(11) Bulaevskii, L. N. *Adv. Phys.* **1988**, *37*, 443.
(12) *The Physics and Chemistry of Organic Superconductors*; Saito, G., Kagoshima, S., Eds.; Springer-Verlag: Berlin, Heidelberg, 1990.
(13) Bryce, M. R. *Chem. Soc. Rev.* **1991**, *20*, 355.
(14) Jérome, D. *Science (Washington, D.C.)* **1991**, *252*, 1509.
(15) Williams, J. M.; Schultz, A. J.; Geiser, U.; Carlson, K. D.; Kini, A. M.; Wang, H. H.; Kwok, W.-K.; Whangbo, M.-H.; Schirber, J. E. *Science (Washington, D.C.)* **1991**, *252*, 1501.
(16) Ishiguro, T.; Nogami, Y. In *Selected Topics in Superconductivity*; Gupta, L. C., Multani, M. S., Ed.; World Scientific Publishing Co. Pte. Ltd.: Singapore, 1993; Vol. 1, p 81.
(17) Wosnitza, J. *Int. J. Mod. Phys. B* **1993**, *7*, 2707.
(18) Graja, A. *Condens. Matter News* **1994**, *3*, 14.
(19) Mori, H. *Int. J. Mod. Phys. B* **1994**, *8*, 1.
(20) Lang, M. *Supercond. Rev.* **1996**, *2*, 1.
(21) Kobayashi, H. *Curr. Opin. Solid State Mater. Sci.* **1997**, *2*, 440.
(22) Saito, G. In *Organic Molecular Solids: Properties and Applications*; Jones, W., Ed.; CRC Press: Boca Raton, FL, 1997; p 309.
(23) Brandow, B. *Phys. Rep.* **1998**, *296*, 1.
(24) Bryce, M. R.; Moore, A. J.; Batsanov, A. S.; Howard, J. A. K.; Robertson, N.; Perepichka, I. F. In *Supramolecular Engineering of Synthetic Metallic Materials—Conductors and Magnets*; Veciana, J., Rovira, C., Amabilino, D. B., Eds.; Kluwer Academic Publishers: Dordrecht, Boston, London, 1999; Vol. 518, p 437.
(25) Wosnitza, J. *Curr. Opin. Solid State Mater. Sci.* **2001**, *5*, 131.
(26) Jérome, D.; Schulz, H. J. *Adv. Phys.* **2002**, *51*, 293.
(27) Torrance, J. B. *Ann. N.Y. Acad. Sci.* **1978**, *313*, 210.
(28) Torrance, J. B. *Acc. Chem. Res.* **1979**, *12*, 79.
(29) Wudl, F. *Acc. Chem. Res.* **1984**, *17*, 227.
(30) Cassoux, P.; Valade, L.; Kobayashi, H.; Kobayashi, A.; Clark, R. A.; Underhill, A. E. *Coord. Chem. Rev.* **1991**, *110*, 115.
(31) Hünig, S.; Erk, P. *Adv. Mater.* **1991**, *3*, 225.
(32) Olk, R.-M.; Olk, B.; Dietzsch, W.; Kirmse, R.; Hoyer, E. *Coord. Chem. Rev.* **1992**, *117*, 99.
(33) Canadell, E. *Coord. Chem. Rev.* **1999**, *185*−*186*, 629.
(34) Giffard, M.; Riou, A.; Mabon, G.; Mercier, N.; Molinié, P.; Nguyen, T. P. *J. Mater. Chem.* **1999**, *9*, 851.
(35) Chasseau, D.; Watkin, D.; Rosseinsky, M. J.; Kurmoo, M.; Talham, D. R.; Day, P. *Synth. Met.* **1988**, *24*, 117.
(36) Fettouhi, M.; Ouahab, L.; Gómez-Garcia, C.; Ducasse, L.; Dalhaes, P. *Synth. Met.* **1995**, *70*, 1131.
(37) Jia, C.; Zhang, D.; Xu, W.; Zhu, D. *Synth. Met.* **2004**, *140*, 9.
(38) Ward, B. H.; Schlueter, J. A.; Geiser, U.; Wang, H.-H.; Morales, E.; Parakka, J. P.; Thomas, S. Y.; Williams, J. M.; Nixon, P. G.; Winter, R. W.; Gard, G. L.; Koo, H.-J.; Whangbo, M.-H. *Chem. Mater.* **2000**, *12*, 343.
(39) Geiser, U.; Schlueter, J. A.; Wang, H. H.; Kini, A. M.; Williams, J. M.; Sche, P. P.; Zakowicz, H. I.; Vanzile, M. L.; Dudek, J. D.; Nixon, P. G.; Winter, R. W.; Gard, G. L.; Ren, J.; Whangbo, M.-H. *J. Am. Chem. Soc.* **1996**, *118*, 9996.
(40) Wang, H. H.; Geiser, U.; Schlueter, J. A.; Ward, B. H.; Parakka, J. P.; Kini, A. M.; O'Malley, J. L.; Thomas, S. Y.; Morales, E.; Dudek, J. D.; Williams, J. M.; Gard, G. L. *Synth. Met.* **1999**, *102*, 1666.
(41) Schlueter, J. A.; Ward, B. H.; Geiser, U.; Wang, H. H.; Kini, A. M.; Parakka, J. P.; Morales, E.; Koo, H.-J.; Whangbo, M.-H.; Winter, R. W.; Mohtasham, J.; Gard, G. L. *J. Mater. Chem.* **2001**, *11*, 2008.
(42) Schlueter, J. A.; Ward, B. H.; Geiser, U.; Kini, A. M.; Wang, H. H.; Hata, A. N.; Mohtasham, J.; Winter, R. W.; Gard, G. L. *Mol. Cryst. Liq. Cryst.* **2002**, *130*, 129.
(43) Geiser, U.; Schlueter, J. A.; Kini, A. M.; Wang, H. H.; Ward, B. H.; Whited, M. A.; Mohtasham, J.; Gard, G. L. Poster presented at the annual meeting of the American Crystallographic Association, San Antonio, TX, May 25−30, 2002.
(44) Liu, Z.; Yu, W. T.; Fang, Q.; Jiang, M. J.; Zhang, D. Q.; Xu, C. Y.; Zhu, D. B. *Synth. Met.* **2003**, *135*, 699.

(45) Geiser, U.; Schlueter, J. A.; Kini, A. M.; Wang, H. H.; Ward, B. H.; Whited, M. A.; Mohtasham, J.; Gard, G. L. *Synth. Met.* **2003**, *133−134*, 401.
(46) Akutsu, H.; Yamada, J.-i.; Nakatsuji, S. *Chem. Lett.* **2003**, *32*, 1118.
(47) Geiser, U.; Wang, H. H.; Schlueter, J. A.; Kini, A. M.; O'Malley, J. L. Unpublished results.
(48) Beno, M. A.; Wang, H. H.; Soderholm, L.; Carlson, K. D.; Hall, L. N.; Nuñez, L.; Rummens, H.; Anderson, B.; Schlueter, J. A.; Williams, J. M.; Whangbo, M.-H.; Evain, M. *Inorg. Chem.* **1989**, *28*, 150.
(49) Yamochi, H.; Tada, C.; Sekizaki, S.; Saito, G. *Mol. Cryst. Liq. Cryst.* **1996**, *284*, 379.
(50) Yamochi, H.; Tsuji, T.; Saito, G.; Suzuki, T.; Miyashi, T.; Kabuto, C. *Synth. Met.* **1988**, *27*, A479.
(51) Watson, W. H.; Kini, A. M.; Beno, M. A.; Montgomery, L. K.; Wang, H. H.; Carlson, K. D.; Gates, B. D.; Tytko, S. F.; DeRose, J.; Cariss, C.; Rohl, C. A.; Williams, J. M. *Synth. Met.* **1989**, *33*, 1.
(52) Saito, G.; Sekizaki, S.; Konsha, A.; Yamochi, H.; Matsumoto, K.; Kusunoki, M.; Sakaguchi, K.-i. *J. Mater. Chem.* **2001**, *11*, 364.
(53) Bu, X.; Coppens, P.; Lederle, B.; Naughton, M. J. *Acta Crystallogr.* **1992**, *C48*, 1560.
(54) Geiser, U.; Kini, A. M.; Schlueter, J. A. Unpublished results.
(55) Sekizaki, S.; Matsukawa, N.; Yamochi, H.; Saito, G. *Synth. Met.* **2003**, *133*, 455.
(56) Wang, H. H.; Geiser, U.; Kelly, M. E.; Vanzile, M. L.; Skulan, A. J.; Williams, J. M.; Schlueter, J. A.; Kini, A. M.; Sirchio, S. A.; Montgomery, L. K. *Mol. Cryst. Liq. Cryst.* **1996**, *284*, 427.
(57) Schlueter, J. A.; Geiser, U.; Wang, H. H.; Kini, A. M.; Ward, B. H.; Parakka, J. P.; Daugherty, R. G.; Kelly, M. E.; Nixon, P. G.; Gard, G. L.; Montgomery, L. K.; Koo, H.-J.; Whangbo, M.-H. *J. Solid State Chem.* **2002**, *168*, 524.
(58) Zaman, M. B.; Toyoda, J.; Morita, Y.; Nakamura, S.; Yamochi, H.; Saito, G.; Nishimura, K.; Yoneyama, N.; Enoki, T.; Nakasuji, K. *J. Mater. Chem.* **2001**, *11*, 2211.
(59) Nishimura, K.; Kondo, T.; Drozdova, O. O.; Yamochi, H.; Saito, G. *J. Mater. Chem.* **2000**, *10*, 911.
(60) Aso, Y.; Yui, K.; Ishida, H.; Otsubo, T.; Ogura, F.; Kawamoto, A.; Tanaka, J. *Chem. Lett.* **1988**, 1069.
(61) Abashev, G. G.; Kazheva, O. N.; Dyachenko, O. A.; Gritsenko, V. V.; Tenishev, A. G.; Nishimura, K.; Saito, G. *Mendeleev Commun.* **2001**, 125.
(62) Schlueter, J. A.; Geiser, U.; Kini, A. M.; Wang, H. H.; Williams, J. M.; Naumann, D.; Roy, T.; Hoge, B.; Eujen, R. *Coord. Chem. Rev.* **1999**, *190*, 781.
(63) Geiser, U.; Schlueter, J. A.; Dudek, J. D.; Williams, J. M.; Naumann, D.; Roy, T. *Acta Crystallogr.* **1995**, *C51*, 1779.
(64) Schlueter, J. A.; Geiser, U.; Williams, J. M.; Wang, H. H.; Kwok, W.-K.; Fendrich, J. A.; Carlson, K. D.; Achenbach, C. A.; Dudek, J. D.; Naumann, D.; Roy, T.; Schirber, J. E.; Bayless, W. R. *J. Chem. Soc., Chem. Commun.* **1994**, 1599.
(65) Geiser, U.; Schlueter, J. A.; Williams, J. M.; Naumann, D.; Roy, T. *Acta Crystallogr.* **1995**, *B51*, 789.
(66) Schlueter, J. A.; Williams, J. M.; Geiser, U.; Dudek, J. D.; Sirchio, S. A.; Kelly, M. E.; Gregar, J. S.; Kwok, W. K.; Fendrich, J. A.; Schirber, J. E.; Bayless, W. R.; Naumann, D.; Roy, T. *J. Chem. Soc., Chem. Commun.* **1995**, 1311.
(67) Geiser, U.; Schlueter, J. A.; Williams, J. M.; Kini, A. M.; Dudek, J. D.; Kelly, M. E.; Naumann, D.; Roy, T. *Synth. Met.* **1997**, *85*, 1465.
(68) Schlueter, J. A.; Geiser, U.; Wang, H. H.; VanZile, M. L.; Fox, S. B.; Williams, J. M.; Laguna, A.; Laguna, M.; Naumann, D.; Roy, T. *Inorg. Chem.* **1997**, *36*, 4265.
(69) Williams, J. M.; Wang, H. H.; Emge, T. J.; Geiser, U.; Beno, M. A.; Leung, P. C. W.; Carlson, K. D.; Thorn, R. J.; Schultz, A. J.; Whangbo, M.-H. In *Progress in Inorganic Chemistry;* Lippard, S. J., Ed.; John Wiley & Sons: New York, 1987; Vol. 35, p 51.
(70) Mori, T.; Inokuchi, H. *Chem. Lett.* **1987**, 1657.
(71) Rosseinsky, M. J.; Kurmoo, M.; Talham, D. R.; Day, P.; Chasseau, D.; Watkin, D. *J. Chem. Soc., Chem. Commun.* **1988**, 88.
(72) Lobkovskaya, R. M.; Shibaeva, R. P.; Laukhina, E. É.; Zvarykina, A. V. *Zh. Strukt. Khim.* **1990**, *31*, 3 (Engl. Transl. *J. Struct. Chem.* **1990**, *31*, 687).
(73) Giffard, M.; Mabon, G.; Mercier, N.; Molinié, P.; Nguyen, T. P.; Riou, A.; Vautrin, M. *Synth. Met.* **1999**, *102*, 1766.
(74) Mori, T. *Bull. Chem. Soc. Jpn.* **1998**, *71*, 2509.
(75) Kreuer, K. D. *J. Membr. Sci.* **2001**, *185*, 29.
(76) Olah, G., A.; Prakash, G. K. S.; Sommer, J. *Superacids*; John Wiley & Sons: New York, 1985.
(77) Marsden, I. R.; Obertelli, S. D.; Allan, M. L.; Friend, R. H.; Kurmoo, M.; Rosseinsky, M. J.; Day, P. *Synth. Met.* **1991**, *42*, 2151.
(78) Mori, T.; Mori, H.; Tanaka, S. *Bull. Chem. Soc. Jpn.* **1999**, *72*, 179.
(79) Schlueter, J. A.; Geiser, U.; Williams, J. M.; Dudek, J. D.; Kelly, M. E.; Flynn, J. P.; Wilson, R. R.; Zakowicz, H. I.; Sche, P. P.; Naumann, D.; Roy, T.; Nixon, P. G.; Winter, R. W.; Gard, G. L. *Synth. Met.* **1997**, *85*, 1453.
(80) Koo, H.-J.; Whangbo, M.-H.; Dong, J.; Olejniczak, I.; Musfeldt, J. L.; Schlueter, J. A.; Geiser, U. *Solid State Commun.* **1999**, *112*, 403.
(81) Su, X.; Zuo, F.; Schlueter, J. A.; Williams, J. M.; Nixon, P. G.; Winter, R. W.; Gard, G. L. *Phys. Rev. B: Condens. Matter* **1999**, *59*, 4376.
(82) Su, X.; Zuo, F.; Schlueter, J. A.; Williams, J. M. *J. Appl. Phys.* **1999**, *85*, 5353.
(83) Zuo, F.; Zhang, P.; Su, X.; Brooks, J. S.; Schlueter, J. A.; Mohtasham, J.; Winter, R. W.; Gard, G. L. *J. Low Temp. Phys.* **1999**, *117*, 1711.
(84) Sadewasser, S.; Looney, C.; Schilling, J. S.; Schlueter, J. A.; Williams, J. M.; Nixon, P. G.; Winter, R. W.; Gard, G. L. *Solid State Commun.* **1997**, *104*, 571.
(85) Hagel, J.; Wosnitza, J.; Pfleiderer, C.; Schlueter, J. A.; Geiser, U.; Mohtasham, J.; Winter, R. W.; Gard, G. L. *Synth. Met.* **2003**, *137*, 1267.
(86) Wanka, S.; Hagel, J.; Beckmann, D.; Wosnitza, J.; Schlueter, J. A.; Williams, J. M.; Nixon, P. G.; Winter, R. W.; Gard, G. L. *Phys. Rev. B: Condens. Matter* **1998**, *57*, 3084.
(87) Prozorov, R.; Giannetta, R. W.; Schlueter, J.; Kini, A. M.; Mohtasham, J.; Winter, R. W.; Gard, G. L. *Phys. Rev. B: Condens. Matter* **2001**, *63*, 052506.
(88) Beckmann, D.; Wanka, S.; Wosnitza, J.; Schlueter, J. A.; Williams, J. M.; Nixon, P. G.; Winter, R. W.; Gard, G. L.; Ren, J.; Whangbo, M.-H. *Eur. Phys. J. B* **1998**, *1*, 295.
(89) Wosnitza, J.; Goll, G.; Beckmann, D.; Wanka, S.; Schlueter, J. A.; Williams, J. M.; Nixon, P. G.; Winter, R. W.; Gard, G. L. *Physica B (Amsterdam)* **1998**, *246*, 104.
(90) Symington, J. A.; Singleton, J.; Clayton, N.; Schlueter, J.; Kurmoo, M.; Day, P. *Physica B (Amsterdam)* **2001**, *294*, 439.
(91) Symington, J. A.; Singleton, J.; Harrison, N.; Clayton, N.; Schlueter, J.; Kurmoo, M.; Day, P. *Synth. Met.* **2001**, *120*, 867.
(92) Wosnitza, J.; Wanka, S.; Qualls, J. S.; Brooks, J. S.; Mielke, C. H.; Harrison, N.; Schlueter, J. A.; Williams, J. M.; Nixon, P. G.; Winter, R. W.; Gard, G. L. *Synth. Met.* **1999**, *103*, 2000.
(93) Brooks, J. S.; Balicas, L.; Storr, K.; Ward, B. H.; Uji, S.; Terashima, T.; Terakura, C.; Winter, R. W.; Mohtasham, J.; Gard, G. L.; Papavassiliou, G. C.; Tokumoto, M. *Mol. Cryst. Liq. Cryst.* **2002**, *380*, 109.
(94) Hayes, W.; Nam, M.-S.; Symington, J. A.; Blundell, S. J.; Ardavan, A.; Singleton, J. *Synth. Met.* **2001**, *120*, 989.
(95) Edwards, R. S.; Symington, J. A.; Rzepniewski, E.; Ardavan, A.; Singleton, J.; Schlueter, J. A. *Synth. Met.* **2001**, *120*, 1033.
(96) Schrama, J. M.; Singleton, J.; Edwards, R. S.; Ardavan, A.; Rzepniewski, E.; Harris, R.; Goy, P.; Gross, M.; Schlueter, J.; Kurmoo, M.; Day, P. *J. Phys.: Condens. Matter* **2001**, *13*, 2235.
(97) Wosnitza, J.; Wanka, S.; Hagel, J.; Balthes, E.; Harrison, N.; Schlueter, J. A.; Kini, A. M.; Geiser, U.; Mothasham, J.; Winter, R. W.; Gard, G. L. *Phys. Rev. B: Condens. Matter* **2000**, *61*, 7383.
(98) Hagel, J.; Wanka, S.; Wosnitza, J.; Balthes, E.; Schlueter, J. A.; Kini, A. M.; Geiser, U.; Mohtasham, J.; Winter, R. W.; Gard, G. L. *Synth. Met.* **2001**, *120*, 813.
(99) Nam, M.-S.; Ardavan, A.; Symington, J. A.; Singleton, J.; Harrison, N.; Mielke, C. H.; Schlueter, J. A.; Winter, R. W.; Gard, G. L. *Phys. Rev. Lett.* **2001**, *87*, 11701.
(100) Wosnitza, J.; Wanka, S.; Hagel, J.; Häussler, R.; von Löhneysen, H.; Schlueter, J. A.; Geiser, U.; Nixon, P. G.; Winter, R. W.; Gard, G. L. *Phys. Rev. B: Condens. Matter* **2000**, *62*, R11973.
(101) Wosnitza, J.; Hagel, J.; Meeson, P. J.; Bintley, D.; Schlueter, J. A.; Mothasham, J.; Winter, R. W.; Gard, G. L. *Phys. Rev. B: Condens. Matter* **2003**, *67*, 060504.
(102) Zuo, F.; Su, X.; Zhang, P.; Brooks, J. S.; Wosnitza, J.; Schlueter, J. A.; Williams, J. M.; Nixon, P. G.; Winter, R. W.; Gard, G. L. *Phys. Rev. B: Condens. Matter* **1999**, *60*, 6296.
(103) Wosnitza, J.; Wanka, S.; Hagel, J.; von Löhneysen, H.; Qualls, J. S.; Brooks, J. S.; Balthes, E.; Schlueter, J. A.; Geiser, U.; Mohtasham, J.; Winter, R. W.; Gard, G. L. *Phys. Rev. Lett.* **2001**, *86*, 508.
(104) Wosnitza, J.; Wanka, S.; Hagel, J.; Qualls, J. S.; Brooks, J. S.; Harrison, N.; Balthes, E.; Schweitzer, D.; Schlueter, J. A.; Geiser, U.; Mothasham, J.; Winter, R. W.; Gard, G. L. *Physica B (Amsterdam)* **2001**, *294*, 442.
(105) Hagel, J.; Wosnitza, J.; Pfleiderer, C.; Schlueter, J. A.; Mohtasham, J.; Gard, G. L. *Phys. Rev. B: Condens. Matter* **2003**, *68*, 104503.
(106) Wosnitza, J.; Hagel, J.; Qualls, J. S.; Brooks, J. S.; Balthes, E.; Schweitzer, D.; Schlueter, J. A.; Geiser, U.; Mohtasham, J.; Winter, R. W.; Gard, G. L. *Phys. Rev. B: Condens. Matter* **2002**, *65*, 180506.
(107) Wosnitza, J.; Hagel, J.; Schlueter, J. A.; Geiser, U.; Mohtasham, J.; Winter, R. W.; Gard, G. L. *Synth. Met.* **2003**, *137*, 1269.
(108) Müller, J.; Lang, M.; Steglich, F.; Schlueter, J. A.; Kini, A. M.; Geiser, U.; Mohtasham, J.; Winter, R. W.; Gard, G. L.; Sasaki, T.; Toyota, N. *Phys. Rev. B: Condens. Matter* **2000**, *61*, 11739.
(109) Schlueter, J. A.; Kini, A. M.; Ward, B. H.; Geiser, U.; Wang, H. H.; Mohtasham, J.; Winter, R. W.; Gard, G. L. *Physica C (Amsterdam)* **2001**, *351*, 261.
(110) Kini, A. M.; Schlueter, J. A.; Ward, B. H.; Geiser, U. W.; Wang, H. H. *Synth. Met.* **2001**, *120*, 713.

(111) Oshima, K.; Urayama, H.; Yamochi, H.; Saito, G. *Physica C (Amsterdam)* **1988**, *153*−*155*, 1148.
(112) Oshima, K.; Urayama, H.; Yamochi, H.; Saito, G. *Synth. Met.* **1988**, *27*, A473.
(113) Oshima, K.; Urayama, H.; Yamochi, H.; Saito, G. *J. Phys. Soc. Jpn.* **1988**, *57*, 730.
(114) Schweitzer, D.; Polychroniadis, K.; Klutz, T.; Keller, H. J.; Hennig, I.; Heinen, I.; Haeberlen, U.; Gogu, E.; Gärtner, S. *Synth. Met.* **1988**, *27*, A465.
(115) Ito, H.; Watanabe, M.; Nogami, Y.; Ishiguro, T.; Komatsu, T.; Saito, G.; Hosoito, N. *J. Phys. Soc. Jpn.* **1991**, *60*, 3230.
(116) Kini, A. M.; Carlson, K. D.; Wang, H. H.; Schlueter, J. A.; Dudek, J. D.; Sirchio, S. A.; Geiser, U.; Lykke, K. R.; Williams, J. M. *Physica C (Amsterdam)* **1996**, *264*, 81.
(117) Schirber, J. E.; Overmyer, D. L.; Carlson, K. D.; Williams, J. M.; Kini, A. M.; Wang, H. H.; Charlier, H. A.; Love, B. J.; Watkins, D. M.; Yaconi, G. A. *Phys. Rev. B: Condens. Matter* **1991**, *44*, 4666.
(118) Mori, H.; Hirabayashi, I.; Tanaka, S.; Mori, T.; Maruyama, Y.; Inokuchi, H. *Synth. Met.* **1993**, *56*, 2437.
(119) Schlueter, J. A.; Williams, J. M.; Kini, A. M.; Geiser, U.; Dudek, J. D.; Kelly, M. E.; Flynn, J. P.; Naumann, D.; Roy, T. *Physica C (Amsterdam)* **1996**, *265*, 163.
(120) Bardeen, J.; Cooper, L. N.; Schrieffer, J. R. *Phys. Rev.* **1957**, *106*, 162.
(121) Bardeen, J.; Cooper, L. N.; Schrieffer, J. R. *Phys. Rev.* **1957**, *108*, 1175.
(122) Kawamoto, A.; Taniguchi, H.; Kanoda, K. *J. Am. Chem. Soc.* **1998**, *120*, 10984.
(123) Dong, J.; Musfeldt, J. L.; Schlueter, J. A.; Williams, J. M.; Nixon, P. G.; Winter, R. W.; Gard, G. L. *Phys. Rev. B: Condens. Matter* **1999**, *60*, 4342.
(124) Dong, J.; Musfeldt, J. L.; Schlueter, J. A.; Williams, J. M.; Gard, G. L. *Synth. Met.* **1999**, *103*, 1892.
(125) Jacobsen, C. S.; Williams, J. M.; Wang, H. H. *Solid State Commun.* **1985**, *54*, 937.
(126) Jacobsen, C. S.; Tanner, D. B.; Williams, J. M.; Geiser, U.; Wang, H. H. *Phys. Rev. B: Condens. Matter* **1987**, *35*, 9605.
(127) Blundell, S. J.; House, A. A.; Singleton, J.; Kurmoo, M.; Pratt, F. L.; Pattenden, P. A.; Hayes, W.; Graham, A. W.; Day, P.; Perenboom, J. A. A. J. *Synth. Met.* **1997**, *85*, 1569.
(128) Wang, H. H.; VanZile, M. L.; Schlueter, J. A.; Geiser, U.; Kini, A. M.; Sche, P. P.; Koo, H.-J.; Whangbo, M.-H.; Nixon, P. G.; Winter, R. W.; Gard, G. L. *J. Phys. Chem. B* **1999**, *103*, 5493.
(129) Wang, H. H.; VanZile, M. L.; Geiser, U.; Schlueter, J. A.; Williams, J. M.; Kini, A. M.; Sche, P. P.; Nixon, P. G.; Winter, R. W.; Gard, G. L.; Naumann, D.; Roy, T. *Synth. Met.* **1997**, *85*, 1533.
(130) Chapman, A. C.; Rhodes, P.; Seymour, E. F. W. *Proc. Phys. Soc., Sect. B* **1957**, *70*, 345.
(131) Olejniczak, I.; Jones, B. R.; Zhu, Z.; Dong, J.; Musfeldt, J. L.; Schlueter, J. A.; Morales, E.; Geiser, U.; Nixon, P. G.; Winter, R. W.; Gard, G. L. *Chem. Mater.* **1999**, *11*, 3160.
(132) Jones, B. R.; Olejniczak, I.; Dong, J.; Pigos, J. M.; Zhu, Z. T.; Garlach, A. D.; Musfeldt, J. L.; Koo, H.-J.; Whangbo, M.-H.; Schlueter, J. A.; Ward, B. H.; Morales, E.; Kini, A. M.; Winter, R. W.; Mohtasham, J.; Gard, G. L. *Chem. Mater.* **2000**, *12*, 2490.
(133) Garlach, A. D.; Musfeldt, J. L.; Pigos, J. M.; Jones, B. R.; Olejniczak, I.; Graja, A.; Whangbo, M.-H.; Schlueter, J. A.; Geiser, U.; Winter, R. W.; Gard, G. L. *Chem. Mater.* **2002**, *14*, 2969.
(134) Olejniczak, I.; Jones, B. R.; Dong, J.; Pigos, J. M.; Zhu, Z.; Garlach, A. D.; Musfeldt, J. L.; Koo, H.-J.; Whangbo, M.-H.; Schlueter, J. A.; Ward, B. H.; Morales, E.; Kini, A. M.; Winter, R. W.; Mohtasham, J.; Gard, G. L. *Synth. Met.* **2001**, *120*, 785.
(135) Guionneau, P.; Kepert, C. J.; Bravic, G.; Chasseau, D.; Truter, M. R.; Kurmoo, M.; Day, P. *Synth. Met.* **1997**, *86*, 1973.
(136) Wang, H. H.; Ferraro, J. R.; Williams, J. M.; Geiser, U.; Schlueter, J. A. *J. Chem. Soc., Chem. Commun.* **1994**, 1893.
(137) Pigos, J. M.; Jones, B. R.; Zhu, Z.-T.; Musfeldt, J. L.; Homes, C. C.; Koo, H.-J.; Whangbo, M.-H.; Schlueter, J. A.; Ward, B. H.; Wang, H. H.; Geiser, U.; Mohtasham, J.; Winter, R. W.; Gard, G. L. *Chem. Mater.* **2001**, *13*, 1326.
(138) Geiser, U.; Ward, B. H.; Schlueter, J. A.; Morales, E. Unpublished results.
(139) Ward, B. H.; Rutel, I. B.; Brooks, J. S.; Schlueter, J. A.; Winter, R. W.; Gard, G. L. *J. Phys. Chem. B* **2001**, *105*, 1750.
(140) Rutel, I. B.; Zvyagin, S. A.; Brooks, J. S.; Krzystek, J.; Kuhns, P.; Reyes, A. P.; Jobiliong, E.; Ward, B. H.; Schlueter, J. A.; Winter, R. W.; Gard, G. L. *Phys. Rev. B: Condens. Matter* **2003**, *67*, 214417.
(141) Mori, T. *Bull. Chem. Soc. Jpn.* **1999**, *72*, 2011.
(142) Geiser, U.; Schlueter, J. A.; Kini, A. M.; Wang, H. H.; Ward, B. H.; Whited, M. A.; Morales, E.; Mohtasham, J.; Gard, G. L. Unpublished results.
(143) Mori, T.; Sakai, F.; Saito, G.; Inokuchi, H. *Chem. Lett.* **1987**, 927.
(144) Mori, H.; Kamiya, M.; Haemori, M.; Suzuki, H.; Tanaka, S.; Nishio, Y.; Kajita, K.; Moriyama, H. *J. Am. Chem. Soc.* **2002**, *124*, 1251.
(145) Mazaki, Y.; Awaga, K.; Kobayashi, K. *J. Chem. Soc., Chem. Commun.* **1992**, 1661.
(146) Nogami, T.; Ishida, T.; Yasui, M.; Iwasaki, F.; Takeda, N.; Ishikawa, M.; Kwakami, T.; Yamaguchi, K. *Bull. Chem. Soc. Jpn.* **1996**, *69*, 1841.
(147) Togashi, K.; Imachi, R.; Tomioka, K.; Tsuboi, H.; Ishida, T.; Nogami, T.; Takeda, N.; Ishikawa, M. *Bull. Chem. Soc. Jpn.* **1996**, *69*, 2821.
(148) Nakatsuji, S.; Takai, A.; Nishikawa, K.; Morimoto, Y.; Yasuoka, N.; Suzuki, K.; Enoki, T.; Anzai, H. *Chem. Commun.* **1997**, 275.
(149) Nakatsuji, S.; Takai, A.; Nishikawa, K.; Morimoto, Y.; Yasuoka, N.; Suzuki, K.; Enoki, T.; Anzai, H. *J. Mater. Chem.* **1999**, *9*, 1747.
(150) Aonuma, S.; Casellas, H.; Faulmann, C.; Garreau de Bonneval, B.; Malfant, I.; Lacroix, P. G.; Cassoux, P.; Hosokoshi, Y.; Inoue, K. *Synth. Met.* **2001**, *120*, 993.
(151) Aonuma, S.; Casellas, H.; Faulmann, C.; Garreau de Bonneval, B.; Malfant, I.; Cassoux, P.; Lacroix, P. G.; Hosokoshi, Y.; Inoue, K. *J. Mater. Chem.* **2001**, *11*, 337.
(152) Aonuma, S.; Casellas, H.; Garreau de Bonneval, B.; Faulmann, C.; Malfant, I.; Cassoux, P.; Hosokoshi, Y.; Inoue, K. *Mol. Cryst. Liq. Cryst.* **2002**, *380*, 263.
(153) Akutsu, H.; Yamada, J.-i.; Nakatsuji, S. *Chem. Lett.* **2001**, 208.
(154) Akutsu, H.; Yamada, J.; Nakatsuji, S. *Synth. Met.* **2001**, *120*, 871.
(155) Kreitsberga, Y. N.; Neiland, O. Y. *Zh. Org. Khim.* **1985**, *21*, 2009 (Engl. Transl. *Russ. J. Org. Chem.* **1985**, *21*, 1840).
(156) Kobayashi, A.; Kobayashi, H. *Mol. Cryst. Liq. Cryst.* **1997**, *296*, 181.
(157) Swietlik, R.; Kushch, L. A. *Synth. Met.* **1995**, *70*, 975.
(158) Sekizaki, S.; Yamochi, H.; Saito, G. *Synth. Met.* **2001**, *120*, 961.
(159) Kobayashi, H.; Kobayashi, A.; Sasaki, Y.; Saito, G.; Enoki, T.; Inokuchi, H. *J. Am. Chem. Soc.* **1983**, *105*, 297.
(160) Mori, H.; Tanaka, S.; Mori, T.; Maruyama, Y.; Inokuchi, H.; Saito, G. *Solid State Commun.* **1991**, *78*, 49.
(161) Middleton, W. J.; Little, E. L.; Coffman, D. D.; Engelhardt, V. A. *J. Am. Chem. Soc.* **1958**, *80*, 2795.
(162) Wang, H. H.; Kelly, M. E.; Patton, K.; Geiser, U.; Schlueter, J. A. Unpublished results.
(163) Saito, G.; Izukashi, H.; Shibata, M.; Yoshida, K.; Kushch, L. A.; Kondo, T.; Yamochi, H.; Drozdova, O. O.; Matsumoto, K.; Kusunoki, M.; Sakaguchi, K.-i.; Kojima, N.; Yagubskii, E. B. *J. Mater. Chem.* **2000**, *10*, 893.
(164) Nishimura, K.; Saito, G.; Takeda, S.; Drozdova, O. O. *Synth. Met.* **2003**, *133*−*134*, 437.
(165) Nishimura, K.; Saito, G.; Abashev, G. G.; Tenishev, A. G. *Synth. Met.* **2001**, *120*, 911.
(166) Kazheva, O. N.; Canadell, E.; Shilov, G. V.; Abashev, G. G.; Tenishev, A. G.; Dyachenko, O. A. *Physica E* **2002**, *13*, 1268.
(167) Wang, H. H.; Schlueter, J. A.; Geiser, U.; Williams, J. M.; Naumann, D.; Roy, T. *Inorg. Chem.* **1995**, *34*, 5552.
(168) Kini, A. M.; Geiser, U.; Wang, H. H.; Carlson, K. D.; Williams, J. M.; Kwok, W. K.; Vandervoort, K. G.; Thompson, J. E.; Stupka, D. L.; Jung, D.; Whangbo, M.-H. *Inorg. Chem.* **1990**, *29*, 2555.
(169) Schlueter, J. A.; Carlson, K. D.; Geiser, U.; Wang, H. H.; Williams, J. M.; Kwok, W.-K.; Fendrich, J. A.; Welp, U.; Keane, P. M.; Dudek, J. D.; Komosa, A. S.; Naumann, D.; Roy, T.; Schirber, J. E.; Bayless, W. R.; Dodrill, B. *Physica (Amsterdam)* **1994**, *C233*, 379.
(170) Schlueter, J. A.; Williams, J. M.; Geiser, U.; Dudek, J. D.; Kelly, M. E.; Sirchio, S. A.; Carlson, K. D.; Naumann, D.; Roy, T.; Campana, C. F. *Adv. Mater.* **1995**, *7*, 634.
(171) Schirber, J. E.; Venturini, E. L.; Kini, A. M.; Wang, H. H.; Whitworth, J. R.; Williams, J. M. *Physica C (Amsterdam)* **1988**, *152*, 157.
(172) Schirber, J. E.; Overmyer, D. L.; Williams, J. M.; Kini, A. M.; Wang, H. H. *Physica C (Amsterdam)* **1990**, *170*, 231.
(173) Schlueter, J. A.; Carlson, K. D.; Williams, J. M.; Geiser, U.; Wang, H. H.; Welp, U.; Kwok, W.-K.; Fendrich, J. A.; Dudek, J. D.; Achenbach, C. A.; Keane, P. M.; Komosa, A. S.; Naumann, D.; Roy, T.; Schirber, J. E.; Bayless, W. R. *Physica (Amsterdam)* **1994**, *C230*, 378.
(174) Geiser, U.; Schlueter, J. A.; Carlson, K. D.; Williams, J. M.; Wang, H. H.; Kwok, W.-K.; Welp, U.; Fendrich, J. A.; Dudek, J. D.; Achenbach, C. A.; Komosa, A. S.; Keane, P. M.; Naumann, D.; Roy, T.; Schirber, J. E.; Bayless, W. R.; Ren, J.; Whangbo, M.-H. *Synth. Met.* **1995**, *70*, 1105.
(175) Geiser, U.; Schultz, A. J.; Wang, H. H.; Watkins, D. M.; Stupka, D. L.; Williams, J. M.; Schirber, J. E.; Overmyer, D. L.; Jung, D.; Novoa, J. J.; Whangbo, M.-H. *Physica C (Amsterdam)* **1991**, *174*, 475.
(176) Eldridge, J. E.; Xie, Y.; Schlueter, J. A.; Williams, J. M.; Naumann, D.; Roy, T. *Solid State Commun.* **1996**, *99*, 335.
(177) Eldridge, J. E.; Kornelsen, K.; Wang, H. H.; Williams, J. M.; Strieby Crouch, A. V.; Watkins, D. M. *Solid State Commun.* **1991**, *79*, 583.
(178) Wosnitza, J.; Beckmann, D.; Wanka, S.; Schlueter, J. A.; Williams, J. M.; Naumann, D.; Roy, T. *Solid State Commun.* **1996**, *98*, 21.

(179) Schlueter, J. A.; Geiser, U.; Wang, H. H.; Kelly, M. E.; Dudek, J. D.; Williams, J. M.; Naumann, D.; Roy, T. *Mol. Cryst. Liq. Cryst.* **1996**, *284*, 195.
(180) Emge, T. J.; Wang, H. H.; Beno, M. A.; Leung, P. C. W.; Firestone, M. A.; Jenkins, H. C.; Carlson, K. D.; Williams, J. M.; Venturini, E. L.; Azevedo, L. J.; Schirber, J. E. *Inorg. Chem.* **1985**, *24*, 1736.
(181) Schlueter, J. A.; Williams, J. M.; Geiser, U.; Wang, H. H.; Kini, A. M.; Kelly, M. E.; Dudek, J. D.; Naumann, D.; Roy, T. *Mol. Cryst. Liq. Cryst.* **1996**, *285*, 43.
(182) Schlueter, J. A.; Kini, A. M.; Geiser, U. Unpublished results.
(183) Toyota, N.; Sasaki, T. *Solid State Commun.* **1990**, *74*, 361.
(184) Pénicaud, A.; Lenoir, C.; Batail, P.; Coulon, C.; Perrin, A. *Synth. Met.* **1989**, *32*, 25.
(185) Wang, H. H.; Geiser, U.; Williams, J. M.; Carlson, K. D.; Kini, A. M.; Mason, J. M.; Perry, J. T.; Charlier, H. A.; Strieby Crouch, A. V.; Heindl, J. E.; Lathrop, M. W.; Love, B. J.; Watkins, D. M.; Yaconi, G. A. *Chem. Mater.* **1992**, *4*, 247.
(186) Geiser, U.; Wang, H. H.; Williams, J. M.; Venturini, E. L.; Kwak, J. F.; Whangbo, M.-H. *Synth. Met.* **1987**, *19*, 599.
(187) Narymbetov, B. Z.; Canadell, E.; Togonidze, T.; Khasanov, S. S.; Zorina, L. V.; Shibayeva, R. P.; Kobayashi, H. *J. Mater. Chem.* **2001**, *11*, 332.
(188) Montgomery, L. K.; Bürgin, T.; Huffman, J. C.; Carlson, K. D.; Dudek, J. D.; Yaconi, G. A.; Megna, L. A.; Mobley, P. R.; Kwok, W. K.; Williams, J. M.; Schirber, J. E.; Overmyer, D. L.; Ren, J.; Rovira, C.; Whangbo, M.-H. *Synth. Met.* **1993**, *56*, 2090.
(189) Horiuchi, S.; Yamochi, H.; Saito, G.; Sakaguchi, K.-i.; Kusunoki, M. *J. Am. Chem. Soc.* **1996**, *118*, 8604.
(190) Yamochi, H.; Horiuchi, S.; Saito, G.; Kusunoki, M.; Sakaguchi, K.; Kikuchi, T.; Sato, S. *Synth. Met.* **1993**, *56*, 2096.
(191) Yamochi, H.; Tsutsumi, K.; Kawasaki, T.; Saito, G. *Mater. Res. Soc. Symp. Proc.* **1998**, *488*, 641.
(192) Yamochi, H.; Tsutsumi, K.; Kawasaki, T.; Saito, G. *Synth. Met.* **1999**, *103*, 2004.
(193) Ward, B. H.; Granroth, G. E.; Walden, J. B.; Abboud, K. A.; Meisel, M. W.; Rasmussen, P. G.; Talham, D. R. *J. Mater. Chem.* **1998**, *8*, 1373.
(194) Sekizaki, S.; Konsha, A.; Yamochi, H.; Saito, G. *Mol. Cryst. Liq. Cryst.* **2002**, *376*, 207.
(195) Fettouhi, M.; Ouahab, L.; Serhani, D.; Fabre, J.-M.; Ducasse, L.; Amiell, J.; Canet, R.; Delhaès, P. *J. Mater. Chem.* **1993**, *3*, 1101.
(196) Soling, H.; Rindorf, G.; Thorup, N. *Acta Crystallogr.* **1983**, *C39*, 490.
(197) Katayama, C.; Honda, M.; Kumagai, H.; Tanaka, J.; Saito, G.; Inokuchi, H. *Bull. Chem. Soc. Jpn.* **1985**, *58*, 2272.
(198) Zaman, M. B.; Morita, Y.; Toyoda, J.; Yamochi, H.; Saito, G.; Yoneyama, N.; Enoki, T.; Nakasuji, K. *Chem. Lett.* **1997**, 729.
(199) Giffard, M.; Mabon, G.; Leclair, E.; Mercier, N.; Allain, M.; Gorgues, A.; Molinié, P.; Neilands, O.; Krief, P.; Khodorkovsky, V. *J. Am. Chem. Soc.* **2001**, *123*, 3852.
(200) Akutsu, H.; Yamada, J.-i.; Nakatsuji, S. *Acta Crystallogr.* **2003**, *E59*, o1441.
(201) Mercier, N.; Giffard, M.; Pilet, G.; Allain, M.; Hudhomme, P.; Mabon, G.; Levillain, E.; Gorgues, A.; Riou, A. *Chem. Commun.* **2001**, 2722.
(202) Yamochi, H.; Konsha, A.; Saito, G.; Matsumoto, K.; Kusunoki, M.; Sakaguchi, K.-i. *Mol. Cryst. Liq. Cryst.* **2000**, *350*, 265.
(203) Kabir, M. K.; Tobita, H.; Matsuo, H.; Nagayoshi, K.; Yamada, K.; Adachi, K.; Sugiyama, Y.; Kitagawa, S.; Kawata, S. *Cryst. Growth Design* **2003**, *3*, 791.
(204) Jayanty, S.; Radhakrishnan, T. P. *J. Mater. Chem.* **1999**, *9*, 1707.
(205) Zaman, M. B.; Toyoda, J.; Morita, Y.; Nakamura, S.; Yamochi, H.; Saito, G.; Nakasuji, K. *Synth. Met.* **1999**, *102*, 1691.
(206) Cerrada, E.; Laguna, M.; Bartolomé, J.; Campo, J.; Orera, V.; Jones, P. G. *Synth. Met.* **1998**, *92*, 245.
(207) Gritsenko, V. V.; Dyachenko, O. A.; Kushch, L. A.; Yagubskii, É. B. *Synth. Met.* **1998**, *94*, 61.
(208) Mori, T.; Kawamoto, T.; Iida, K.; Yamaura, J.; Enoki, T.; Misaki, Y.; Yamabe, T.; Mori, H.; Tanaka, S. *Synth. Met.* **1999**, *103*, 1885.
(209) Morita, Y.; Miyazaki, E.; Yamochi, H.; Saito, G.; Nakasuji, K. *Synth. Met.* **2003**, *135*, 581.
(210) Sekizaki, S.; Tada, C.; Yamochi, H.; Saito, G. *J. Mater. Chem.* **2001**, *11*, 2293.
(211) Kobayashi, H.; Kobayashi, A.; Cassoux, P. *Chem. Soc. Rev.* **2000**, *29*, 325.
(212) Zorina, L. V.; Narymbetov, B. Z.; Khasanov, S. S.; Shibaeva, R. P.; Kushch, N. D.; Yagubskii, E. B.; Kobayashi, A.; Kobayashi, H. *Synth. Met.* **1999**, *102*, 1735.
(213) Narymbetov, B. Z.; Kushch, N. D.; Zorina, L. V.; Khasanov, S. S.; Shibaeva, R. P.; Togonidze, T. G.; Konalev, A. E.; Kartsovnik, M. V.; Buravov, L. I.; Yagubskii, E. B.; Canadell, E.; Kobayashi, A.; Kobayashi, H. *Eur. Phys. J. B* **1998**, *5*, 179.
(214) Kini, A. M.; Beno, M. A.; Son, D.; Wang, H. H.; Carlson, K. D.; Porter, L. C.; Welp, U.; Vogt, B. A.; Williams, J. M.; Jung, D.; Evain, M.; Whangbo, M.-H.; Overmyer, D. L.; Schirber, J. E. *Solid State Commun.* **1989**, *69*, 503.
(215) Jung, D.; Evain, M.; Novoa, J. J.; Whangbo, M.-H.; Beno, M. A.; Kini, A. M.; Schultz, A. J.; Williams, J. M.; Nigrey, P. J. *Inorg. Chem.* **1989**, *28*, 4516.
(216) Togonidze, T. G.; Kovalev, A. E.; Kartsovnik, M. V.; Canadell, E.; Kushch, N. D.; Yagubskii, E. B. *Synth. Met.* **1999**, *103*, 1969.
(217) Togonidze, T. G.; Kartsovnik, M. V.; Perenboom, J. A. A. J.; Kushch, N. D.; Kobayashi, H. *Physica B (Amsterdam)* **2001**, *294*, 435.
(218) Merino, J.; McKenzie, R. H. *Phys. Rev. B: Condens. Matter* **2000**, *62*, 2416.
(219) Wudl, F.; Yamochi, H.; Suzuki, T.; Isotalo, H.; Fite, C.; Kasmai, H.; Liou, K.; Srdanov, G.; Coppens, P.; Maly, K.; Frost-Jensen, A. *J. Am. Chem. Soc.* **1990**, *112*, 2461.
(220) Yamochi, H.; Nakamura, T.; Saito, G.; Kikuchi, T.; Sato, S.; Nozawa, K.; Kinoshita, M.; Sugano, T.; Wudl, F. *Synth. Met.* **1991**, *41*−*43*, 1741.
(221) Drozdova, O.; Yamochi, H.; Yakushi, K.; Uruichi, M.; Horiuchi, S.; Saito, G. *J. Am. Chem. Soc.* **2000**, *122*, 4436.
(222) Drozdova, O. O.; Yamochi, H.; Yakushi, K.; Uruichi, M.; Horiuchi, S.; Saito, G. *Synth. Met.* **2001**, *120*, 739.
(223) Wang, H. H.; Beno, M. A.; Carlson, K. D.; Geiser, U.; Kini, A. M.; Montgomery, L. K.; Thompson, J. E.; Williams, J. M. In *Organic Superconductivity*; Kresin, V., Little, W. A., Eds.; Plenum Press: New York, 1990; p 51.
(224) Wang, H. H.; Montgomery, L. K.; Kini, A. M.; Carlson, K. D.; Beno, M. A.; Geiser, U.; Cariss, C. S.; Williams, J. M.; Venturini, E. L. *Physica C (Amsterdam)* **1988**, *156*, 173.
(225) Urayama, H.; Yamochi, H.; Saito, G.; Sato, S.; Sugano, T.; Kinoshita, M.; Kawamoto, A.; Tanaka, J.; Inabe, T.; Mori, T.; Maruyama, Y.; Inokuchi, H.; Oshima, K. *Synth. Met.* **1988**, *27*, A393.
(226) Sekizaki, S.; Yamochi, H.; Saito, G. *Synth. Met.* **2003**, *135*, 631.
(227) Thorup, N.; Rindorf, G.; Soling, H.; Johannsen, I.; Mortensen, K.; Bechgaard, K. *J. Phys. (Les Ulis, Fr.), Colloque* **1983**, *6*, 1017.
(228) Abashev, G. G.; Gritsenko, V. V.; Kazheva, O. N.; Tenishev, A. G.; Canadell, E.; Dyachenko, O. A. *Z. Kristallogr.* **2001**, *216*, 623.
(229) Yamochi, H.; Nakamura, S.; Saito, G.; Zaman, M. B.; Toyoda, J.; Morita, Y.; Nakasuji, K.; Yamashita, Y. *Synth. Met.* **1999**, *102*, 1729.
(230) Kathirgamanathan, P.; Mucklejohn, S. A.; Rosseinsky, D. R. *J. Chem. Soc., Chem. Commun.* **1979**, 86.
(231) Rosseinsky, D. R.; Kathirgamanathan, P. *Mol. Cryst. Liq. Cryst.* **1982**, *86*, 43.
(232) Kathirgamanathan, P.; Rosseinsky, D. R. *J. Chem. Soc., Chem. Commun.* **1980**, 356.
(233) Teitelbaum, R. C.; Marks, T. J.; Johnson, C. K. *J. Am. Chem. Soc.* **1980**, *1980*, 9.
(234) Fukunaga, T.; Gordon, M. D.; Krusic, P. J. *J. Am. Chem. Soc.* **1976**, *98*, 611.
(235) Farnia, G.; Marcuzzi, F.; Meneghetti, M.; Sandona, G. *Adv. Mater.* **2000**, *12*, 1610.
(236) Grossel, M. C.; Edwards, D. J.; Hibbert, D. B.; El Nil, H. *Electrochim. Acta* **1989**, *34*, 425.
(237) Grossel, M. C.; Edwards, D. J.; Hill, R. M.; Dissado, L. A. *J. Mater. Chem.* **1992**, *2*, 423.
(238) Prasanna, S.; Radhakrishnan, T. P. *Synth. Met.* **1996**, *78*, 127.
(239) Cerrada, E.; Garin, J.; Gimeno, M. C.; Laguna, A.; Laguan, M.; Jones, P. G. *Spec. Publ.—R. Soc. Chem.* **1993**, *131*, 164.
(240) Miyazaki, A.; Yamaguchi, K.; Enoki, T.; Saito, G. *Synth. Met.* **1999**, *102*, 1676.
(241) Miyazaki, A.; Enoki, T. *Synth. Met.* **2001**, *120*, 939.
(242) Javidan, A.; Calas, M.; Gouasmia, A. K.; Fabre, J. M.; Ouahab, L.; Golhen, S. *Synth. Met.* **1997**, *86*, 1811.
(243) Morita, Y.; Maki, S.; Ohmoto, M.; Kitagawa, H.; Okubo, T.; Mitani, T.; Nakasuji, K. *Synth. Met.* **2003**, *135*, 541.
(244) Kato, R.; Kobayashi, H.; Kobayashi, A.; Sasaki, Y. *Bull. Chem. Soc. Jpn.* **1986**, *59*, 627.
(245) Schultz, A. J.; Wang, H. H.; Soderholm, L. C.; Sifter, T. L.; Williams, J. M.; Bechgaard, K.; Whangbo, M.-H. *Inorg. Chem.* **1987**, *26*, 3757.
(246) Vance, C. T.; Bereman, R. D.; Bordner, J.; Hatfield, W. E.; Helms, J. H. *Inorg. Chem.* **1985**, *24*, 2905.
(247) Nagapetyan, S. S.; Shklover, V. E.; Vetoshkina, L. V.; Kotov, A. I.; Ukhin, L. Y.; Struchkov, Y. T.; Yagubskii, E. B. *Mater. Sci.* **1988**, *14*, 5.
(248) Yagubskii, É. B.; Kotov, A. I.; Buravov, L. I.; Khomenko, A. G.; Shklover, V. E.; Nagapetyan, S. S.; Struchkov, Y. T.; Ukhin, L. Y.; Vetoshkina, L. V. *Izv. Akad. Nauk SSSR, Ser. Khim.* **1989**, *38*, 2158 (Engl. Transl. *Bull. Acad. Sci. USSR, Div. Chem. Sci.* **1989**, *38*, 1988).
(249) Yagubskii, E. B. *J. Solid State Chem.* **2002**, *168*, 464.
(250) Mori, T.; Katsuhara, M.; Hoshino, H.; Aragaki, M.; Kawamoto, T.; Misaki, Y.; Tanaka, K.; Mori, H.; Tanaka, S. *Synth. Met.* **2001**, *120*, 821.
(251) Sekizaki, S.; Yamochi, H.; Saito, G. *Synth. Met.* **1999**, *102*, 1711.
(252) Kamarás, K.; Gruner, G. *Solid State Commun.* **1979**, *30*, 277.

(253) Ohnuki, H.; Noda, T.; Izumi, M.; Imakubo, T.; Kato, R. *Phys. Rev. B: Condens. Matter* **1997**, *55*, R10225.
(254) Ohnuki, H.; Nagata, M.; Ishizaki, Y.; Imakubo, T.; Kobayashi, K.; Kato, R.; Izumi, M. *Synth. Met.* **1999**, *102*, 1699.
(255) Ohnuki, H.; Desbat, B.; Giffard, M.; Izumi, M.; Imakubo, T.; Mabon, G.; Delhaes, P. *J. Phys. Chem. B* **2001**, *105*, 4921.
(256) Ohnuki, H.; Noda, T.; Izumi, M.; Imakubo, T.; Kato, R. *Supramol. Sci.* **1997**, *4*, 413.
(257) Ohnuki, H.; Izumi, M.; Ishizaki, Y.; Nagata, M.; Imakubo, T.; Kato, R. *Thin Solid Films* **1998**, *327*−*329*, 458.
(258) Vignau, L.; Ohnuki, H.; Nagata, M.; Ishizaki, Y.; Imabuko, T.; Kato, R.; Izumi, M. *Mol. Cryst. Liq. Cryst.* **1998**, *322*, 99.
(259) Vignau, L.; Ohnuki, H.; Ishizaki, Y.; Kato, R.; Imakubo, T.; Izumi, M. *Synth. Met.* **1999**, *102*, 1723.
(260) Ohnuki, H.; Desbat, B.; Giffard, M.; Izumi, M.; Imakubo, T.; Mabon, G.; Delhaes, P. *Synth. Met.* **2001**, *120*, 889.
(261) Ishizaki, Y.; Ida, T.; Yartsev, V. M.; Ohnuki, H.; Imakubo, T.; Izumi, M. *Synth. Met.* **2003**, *137*, 925.
(262) Ishizaki, Y.; Izumi, M.; Ohnuki, H.; Kalita-Lipinska, K.; Imakubo, T.; Kobayashi, K. *Phys. Rev. B: Condens. Matter* **2001**, *63*, 134201.
(263) Ohnuki, H.; Suzuki, M.; Ishizaki, Y.; Imakubo, T.; Ida, T.; Izumi, M. *Synth. Met.* **2003**, *137*, 927.
(264) Abbott, A. P.; Jenkins, P. R.; Khan, N. S. *J. Chem. Soc., Chem. Commun.* **1994**, 1935.

CR0306844